Regionalization of Parameters of a Conceptual Rainfall-Runoff Model

Von der Fakultät Bau- und Umweltingenieurwissenschaften der Universität Stuttgart
zur Erlangung der Würde eines Doktors der
Ingenieurwissenschaften (Dr.-Ing.) genehmigte Abhandlung

Vorgelegt von

Yeshewatesfa Hundecha Hirpa

aus Addis Abeba, Äthiopien

Hauptberichter:	Prof. Dr. rer. nat. Dr.-Ing. András Bárdossy
Mitberichter:	Prof. Dr.-Ing. Axel Bronstert
Tag der müdlichen Prüfung:	26. November 2004

Institut für Wasserbau der Universität Stuttgart

Stuttgart 2005

Heft 142

Regionalization of Parameters of a Conceptual Rainfall-Runoff Model

von
Dr.-Ing.
Yeshewatesfa Hundecha Hirpa

Eigenverlag des Instituts für Wasserbau der Universität Stuttgart

D93 Regionalization of Parameters of a Conceptual Rainfall-Runoff Model

CIP-Titelaufnahme der Deutschen Bibliothek

Hundecha Hirpa, Yeshewatesfa:
Regionalization of Parameters of a Conceptual Rainfall-Runoff Model / von Yeshewatesfa Hundecha Hirpa. Institut für Wasserbau, Universität Stuttgart. – Stuttgart: Inst. für Wasserbau, 2005
(Mitteilungen / Institut für Wasserbau, Universität Stuttgart: H. 142)
Zugl.: Stuttgart, Univ., Diss., 2005
ISBN 3-933761-45-X
NE: Institut für Wasserbau <Stuttgart>: Mitteilungen

Herausgegeben 2005 vom Eigenverlag des Instituts für Wasserbau
Druck: Sprint-Digital-Druck GmbH, Stuttgart

Acknowledgement

I would like to express my gratitude to all those who helped me in one way or another in the course of my journey to complete this work.

My special thanks are due to Prof. András Bárdossy for giving me the opportunity to work in his team and helping me set up a direction for this work. Without him, this work wouldn't have been realised. His guidance and invaluable advices have greatly helped me finish this work with ease. Indeed, his experiences in the field and his multidisciplinary view have helped me take the proper route whenever I found myself at a crossroads in the course of my work.

I also owe a sincere gratitude to Prof. Axel Bronstert for his willingness to co-supervise my work and his invaluable comments and suggestions on the work.

Finally, I would like to extend my thanks to members of the Institut für Wasserbau for the exciting work environment I enjoyed while working at the institute.

Table of contents

List of Figures

List of Tables

Abstract

This work was aimed at developing a methodology for the regionalization of parameters of a conceptual continuous water balance rainfall-runoff model based on measurable physiographic and land use/land cover characteristics of a catchment. The motivation for this work lies in the need to address two problems that have drawn much attention in recent years. Firstly, traditional methods of estimating model parameters are based on calibrating the model against observed catchment responses, such as runoff from the catchment. In the absence of such observed catchment responses, estimation of the model parameters would not be straightforward and therefore there should be a way to estimate them from some attributes of the catchment. Secondly, assessment of the hydrologic impact of changes in land use/land cover attributes of a catchment will be possible only if the changes in these attributes are reflected in the model parameters. Therefore there is a need to relate the model parameters with the land use/land cover characteristics of a catchment.

Different attempts have been made so far to develop a scheme to relate model parameters with catchment attributes. Many of the works done generally involved first calibrating a model to a number of catchments without any reference to any of the catchment properties and then fitting an empirical relationship between the parameters of the calibrated model and the catchment attributes. This approach has, however, met with limited success so far mainly due to the fact that model calibration doesn't lead to a unique set of parameters when calibrated against observed catchment response. The parameters thus obtained are a single realisation among many other sets of parameters that would lead to a similar model performance. Therefore, the fitted empirical relationship between the parameters and the catchment properties tends to be rather random and the relationship would be weak.

This work was therefore devoted to developing a different methodology of establishing the relationship between model parameters and the catchment attributes. A modified version of a conceptual Rainfall-Runoff model, the HBV-IWS model, was calibrated for a number of gauged sub-catchments within the German part of the Rhine basin with the dual objective of reproducing the observed catchment responses based on daily observations of meteorological forcing data and catchment response data, and achieving a stronger relationship between the parameters and the catchment attributes. The catchment attributes were implicitly incorporated in the model setup by establishing a functional relationship between them and the model parameters a-priori and an automatic model calibration procedure was implemented to estimate the optimum regional relationship using a non-linear optimisation routine. The catchment attributes used for regionalizing the model parameters include a range of readily measurable physical catchment properties indexing land use and physiographic properties.

Since the model parameters are estimated based on readily measurable catchment attributes, estimation of model parameters corresponding to ungauged catchments is possible, rendering the scheme potentially suitable for modelling the runoff from such catchments. The results obtained from validation of the parameter estimation scheme in gauged subcatchments that were not used in deriving the regional relationship between the model parameters and the catchment descriptors suggest that the model performances in terms of different evaluation criteria in these subcatchments are comparable with that of the catchments used to derive the regional relationships.

The methodology was further implemented in the prediction of the hydrological consequence of land use changes, as land use was also considered for regionalization of the model parameters. The changes in the catchment reaction obtained for different land use change scenarios were consistent with the physical explanations that can be given about the effect of the scenarios on the runoff generation of a catchment and were supportive of the findings of many of the previous studies conducted on this issue using different approaches. The results indicate that there is an increase both in the long-term water yield and event based runoff from catchments due to urbanization, while they indicate a reduction in both attributes of the catchment response due to afforestation.

Kurzfassung

Diese Arbeit zielt darauf ab, eine Methode zur Regionalisierung der parameter in einem konzeptionellen Niederschlag-Abfluss-Modell zu entwickeln. Das untersuchte Modell berücksichtigt eine kontinuierliche Wasserbilanz und basiert auf physiographischen Eigenschaften sowie messbaren Landnutzungsdaten des jeweiligen Einzugsgebiets.

Motivation waren zwei Fragestellungen, die in den letzten Jahren wachsende Aufmerksamkeit auf sich zogen:
Traditionelle Methoden der Parameter schätzung basieren auf einer Kalibrierung des Modells mittels beobachteter Einzugsgebiets-Reaktionen auf jeweilige Niederschlags-ereignisse. Es sollte aber zum einen eine Möglichkeit geben, diese Parameter aus den Eigenschaften des Einzugsgebiets abzuschätzen, wenn keine Abfluss-Beobachtungen vorliegen. Zum anderen sind die Auswirkungen einer sich ändernden Landnutzung in einem Einzugsgebiet nur dann erfassbar, wenn die entsprechenden Größen auch in den Parametern des Modells berücksichtigt sind. Aus diesen zwei Punkten ergibt sich die Notwendigkeit, die Modellparameter mit den Landnutzungsdaten und anderen Einzugsgebietseigenschaften zu verbinden.

Bisher wurden verschiedene Ansätze entwickelt, um die Modell-Parameter mit den Charakteristika des Einzugsgebiets in Beziehung zu setzen. Viele der Arbeiten folgten dem Prinzip, zuerst ein Modell auf einige Einzugsgebiete zu kalibrieren und anschließend eine empirische Beziehung zwischen den Parametern des kalibrierten Models und den Eigenschaften der Einzugsgebiete anzupassen . Dieser Ansatz war bisher jedoch nur von begrenztem Erfolg. Dies liegt hauptsächlich daran, dass die Kalibrierung mit beobachteten Niederschlag-Abfluss-Ereignissen nicht zu einem eindeutigen Parameter-Satz führt. Die erzeugten Parameter sind also nur eine Realisation unter vielen anderen möglichen Parameter-Sätzen, die zu ähnlicher Modellgüte führen würden. Folglich ist die Beziehung zwischen den angepassten Modell-Parametern und den Charakteristika des Einzugsgebietes eher schwach.

Deshalb sollte in dieser Arbeit eine andere Methode entwickelt werden, um die Parameter des Modells mit den Kennwerten des Einzugsgebietes zu verbinden. Verwendet wurde das HBV-IWS Modell, eine modifizierte Version eines vorhandenen konzeptionellen Niederschlag-Abfluss-Modells. Die Kalibrierung wurde durchgeführt für einige mit Messpegeln bestückte Teileinzugsgebiete der deutschen Seite des Rhein-Einzugsgebiets. Dabei bestand eine doppelte Zielsetzung. Erstens sollte die Reaktion der Einzugsgebiete auf Niederschlags-ereignisse auf der Basis von täglichen Beobachtungen meteorologischer Daten vom Modell nachgebildet werden. Zweitens sollte ein stärkerer Zusammenhang erreicht werden zwischen den Modellparametern und den Kennwerten des Einzugsgebietes. Die Attribute der

Einzugsgebiete wurden dazu implizit in den Modellaufbau eingegliedert. Es wurde a priori ein funktionaler Zusammenhang zu den Modelparametern festgelegt und anschließend ein automatischer Ablauf zur Modellkalibrierung implementiert. Mit einer nicht-linearen Routine wurde dabei die optimale regionale Beziehung zwischen Einzugsgebietsdaten und Modellparametern berechnet. Die Kennwerte des Einzugsgebietes, welche für die Regionalisierung der Modell-Parameter genutzt werden, beinhalten direkt messbare physikalische Eigenschaften des Einzugsgebietes, welche die Landnutzung und die physiographischen Bedingungen charakterisieren.

Da ja die Abschätzung der Modellparameter nun auf direkt messbaren Einzugsgebiets-Kennwerten basiert, ist es möglich, diese Parameter auch für Einzugsgebiete ohne Pegel festzulegen. Dadurch kann es das System potentiell leisten, den Abfluss in solchen Einzugsgebieten ebenfalls zu modellieren. Dies wurde anhand von Teileinzugsgebieten mit Pegeln validiert, die nicht für die Kalibrierung verwendet wurden. Die Validierung lässt darauf schließen, dass die Anpassungsgüte des Modells in Bezug auf verschiedene Bewertungskriterien vergleichbar ist, ob es sich nun um die für das Modell neuen Einzugsgebiete handelt oder um jene, die verwendet wurden, um die regionalen Beziehungen herzuleiten.

Zusätzlich wurde diese Methode dazu eingesetzt, die Auswirkungen von veränderter Landnutzung auf die Abflussbildung vorherzusagen, da die Landnutzung in der Regionalisierung der Modellparameter berücksichtigt wird. Wenn auf ein Einzugsgebiet verschiedene Szenarien einer geänderten Landnutzung angesetzt werden, dann sind die Änderungen im simulierten Abfluss aus dem Einzugsgebiet konsistent mit der physikalischen Erklärung, wie sich die Landnutzung auf die Abflussbildung auswirkt. Die Ergebnisse stützen darüber hinaus die Befunde vieler anderer Untersuchungen dieses Problems, die mit unterschiedlichsten Ansätzen durchgeführt wurden. Bei zunehmender Urbanisierung zeigt sich gleichermaßen ein Einstieg im langzeitlichen Abfluss, wie im ereignisabhängigen Abfluss aus dem Einzugsgebiet. Als Antwort auf eine Aufforstung hingegen, reduzieren sich beide Größen.

1 Introduction

Proper management of the water resources of the globe entails skilful prediction of the amount and movement of water in its hydrologic cycle. One of the purposes this is required for is to be able to quantifying the availability and distribution of water for consumptive use and to make any necessary measures to budget its use in a safe and rational way. Not only are we interested in ensuring that we wouldn't run out of available water for consumption, but we may also need to predict the adverse effects of water that might result when some phase of the hydrologic cycle gets extreme or becomes persistent causing undesirable situations, such as flooding, and take measures that would mitigate the resulting consequences.

1.1 Modelling of the hydrologic cycle

Prediction of both the amount and movement of water in the different phases of the hydrologic cycle has traditionally been performed by implementing rainfall-runoff models. Such models are basically mathematical descriptions of the different components of the hydrologic cycle. They generally try to quantitatively explain the fate of a rainfall by apportioning it into a component returned to the atmosphere due to evapotranspiration, a part that percolates into a deeper zone of the ground to recharge the ground water, and a portion that turns into runoff. They further make a prediction on the time distribution of the resulting runoff.

Rainfall-runoff models have, of course, been under a continuous state of evolution. Models used in the earlier days didn't integrate the different phases of the hydrologic cycle. Instead, they implemented simplified mathematical relationships between precipitation and certain attributes of the final catchment reaction. Implementation of such a modelling practice dates back to the middle of the 19th century when the simplest one parameter Rational method (Mulvany, 1851) that predicts the peak runoff at the outlet of a catchment resulting from a given precipitation event was introduced. Because of its simplicity and minimum data requirement, it had enjoyed a wide application in the past, when hydrologists were in short of the computational power the current generation is enjoying, and are still in use to date to some extent (Hromadka and Whitley, 1994). However, the Rational method only predicts the magnitude of the peak runoff and it doesn't tell anything about the time distribution of the runoff resulting from precipitation. A further development in the rainfall-runoff models led to

the introduction of the time-area (Richards, 1944; Clark, 1945) and the unit hydrograph (Sherman, 1932) methods that are used to establish the time distribution of the ultimate runoff produced from a rainfall event.

The advent of computers had later brought up the introduction of computer-based models that try to integrate models of the different components of the hydrologic cycle. The pioneers to this class of models are Crawford and Linsley (1966) through the development of the Stanford watershed model, which falls in a class of conceptual models that idealize the processes taking place within the catchment by storage elements. A plethora of such class of models have been developed afterwards, some of which are presented in Singh (1995). Subsequently, another class of models that try to incorporate all the known physical principles to each of the catchment processes was introduced. Theoretical description of this class of models was first presented by Freeze and Harlan (1969) and was later put in practical application for the first time by Stephenson and Freeze (1974).

The current generation of rainfall-runoff models are classified into different categories based on different criteria. One categorization is based on the way the different components of the catchment processes are treated within the model. There are a group of models in which the modelling procedure is based on establishing a mathematical relationship between the input and the output variables using data analysis and fitting. Such models fall into a class of empirical models. The modelling approach in this class of models mainly relies on estimation of the catchment runoff from a range of predictor variables using multiple regression (Hirsch, 1982; Kletti and Stefan, 1997), or implementation of a soft computing approach such as artificial neural networks or fuzzy rules (Smith and Eli, 1995; Bárdossy, 1996; Minns and Hall, 1996; Haberlandt, et. al, 2001; Hundecha, et al. 2001). Another group of models try to model the components of the hydrologic cycle using simplified mathematical relationships, which are physically sound but are not based on precise description of the physical processes involved based on known physical laws. These models are referred to as conceptual models and there are dozens of such class of models that are widely used, such as the HBV model (Bergstrom, 1995), the IHACRES model (Jakeman et. al., 1990), and the VIC model (Wood, et. al., 1992). There is also another group of models, in which the different components of the catchment process are described by equations derived from known physical laws. These constitute what is known as a physically based model. Examples of this class of models are SHE (Abbott et al., 1986a,b) and IHDM (Beven et al., 1987).

Models can also be classified based on the spatial scale at which they treat the different processes. Models that treat the catchment as a single unit and use input data, which are believed to be representative at the catchment scale and produce output at a single point, are referred to as lumped models. There are, on the other hand, models that subdivide the catchment into smaller units supposed to be homogeneous in terms of their physical characteristics. Input data are required at this smaller homogeneous scale and the output can also be estimated at different points within the catchment. Such models are referred to as distributed models.

1.2 Challenges of the modelling process

All the rainfall-runoff models that are currently in use are, of course, mere approximations of the catchment processes taking place and none are able to completely describe the actual processes. This is mainly due to the lack of detailed knowledge of the processes involved in the generation of runoff from precipitation. Even those processes, for which sound physical descriptions are available, may not be correctly represented in the models. Many of the physical principles are formulated at point scale and trying to apply them to a catchment scale of practical interest necessitates knowledge of the physical properties of the catchment at all points, which is not practically possible. Even if it were possible, the complexity of the governing mathematical equations in the physical description of the processes wouldn't make it easy getting a closed form of solving them and a numerical approximation is inevitable. Therefore, there is ultimately a need to discretize the catchment into finite areas that are not homogeneous in terms of their physical characteristics. The resulting need to use average physical characteristics over the element is clearly a deviation from the reality.

Both the conceptual idealized models and the complex physically based models in use today are models with a number of parameters that define the characteristics of the catchment, with the number varying from model to model depending on the degree of treatment they give to the different components of the catchment process and the way they idealize them. These parameters need to be established in order to apply the models for the required purposes.

For conceptual models, there is no direct relationship between the parameters and the physical catchment characteristics and, therefore, the parameters are normally established through a

model calibration process by trying to fit the model output with observed data under the assumption that no significant changes in the catchment properties have taken place during the time when observation was made. The same assumption should hold true if the calibrated model is to be used for future use.

Parameters of process oriented physically based models are related to the physical characteristics of the catchment and, therefore, measurement or prior estimation of the parameters should, in theory, be possible. Practically, however, it is not an easy task and even if one were able to do so; they could only be measured at small scales. Upscaling of parameters obtained from small-scale measurements to a catchment scale, which could be orders of magnitudes larger is not a trivial exercise due to the non-homogeneity of the catchment characteristics (Beven, 2000). Therefore, one should go through the same process of model calibration, which is always needed for conceptual models. This has prompted Beven (1989) to an argument that "the current generation of distributed physically based models are lumped conceptual models".

In addition to the problem of correctly representing the real catchment processes in rainfall-runoff models, estimation of their parameters presents a challenge to a handy application of the models to practical problems. Extensive work has been done on the calibration of rainfall-runoff models (Johnston and Pilgrim, 1976; Duan et al., 1992; Yapo et al., 1996; Kuczera, 1997; Gupta and Sorooshian, 1998).

Traditional calibration of a rainfall-runoff model basically involves the following steps for the estimation of its parameters:

- Defining an objective function or a set of objective functions that measure the degree to which one or more model outputs fit with the corresponding observation. Guidelines for selecting an objective function in model calibration were proposed by Diskin and Simon (1977)

- Carrying out repetitive model runs by adjusting the model parameters, either manually or using automatic optimisation algorithms, so that improved values of the objective functions are obtained. One cannot; of course, keep on doing this indefinitely and therefore, a stopping criterion is set beforehand.

In spite of the evolvement of powerful automated techniques of parameter optimisation, one of the major problems of model calibration is that it is very difficult to find a unique set of parameters that leads to acceptable model performance. Since it is the overall interaction of the different parameters that determines the model performance, different combinations of their values may lead to equally acceptable model performances.

1.3 Modelling ungauged catchments and prediction of the effect of changes

The difficulty in estimating model parameters a-priory through measurement and the ultimate necessity of model calibration against observed catchment responses has a serious practical consequence. The non-uniqueness of the model parameters estimated through model calibration makes it difficult to associate any of the parameters with the readily measurable physical catchment characteristics. Therefore, the parameters may partly loose their physical significance; even though they have physical meanings in the model structure they are used in. This, consequently, limits the transferability of the model parameters to other catchments based on physical properties of the catchments. The model should then be calibrated separately for each catchment for which prediction of the catchment response is sought. Since model calibration needs one or more observed response data, application of the model to ungauged catchments will be difficult.

Prediction of the impact of changes in the catchment properties, like land use, on the response of a catchment also requires quantification of the model parameters corresponding to the changed catchment properties. Unless there is a relationship between the model parameters and the catchment properties, such quantification cannot be done in a physically meaningful way, thus limiting the applicability of the model for prediction of the effect of changes.

In order to address the problems mentioned above, several studies have been made during the past years in an attempt to develop schemes of regionalization of model parameters based on readily measurable physiographic, land cover, and climatological attributes of catchments. Many of the works in the earlier days were focused on developing a means of relating event based catchment responses with rainfall and topographic factors using a multiple regression approach (Heerdegen and Reich, 1974; Waylen and Woo, 1984; Nathan and McMahon, 1992).

Recent works, however, have been focusing on development of a regionalization scheme to estimate the parameters of a more general class of continuous water balance models of time scales ranging from monthly to hourly from readily measurable catchment properties. Abdulla and Lettenmaier (1997) applied a method of regionalization of the parameters of the VIC-2L land surface hydrologic model (Liang et al., 1994) for the construction of daily stream flow for catchments in the Arkansas-Red River basin based on distributed land surface characteristics and climatological characteristics derived from station meteorological data. Sefton and Howarth (1998) also employed a similar parameter regionalization scheme for the IHACRES model (Jakeman et al., 1990; Littlewood et al., 1997) to estimate daily flows for catchments in England and Wales using physical catchment descriptors indexing topography, soil type, climate, and land cover. Some more similar works are documented in Xu and Singh (1998) for estimation of monthly flow, Post and Jakeman (1999), and Seibert (1999).

All of the parameter regionalization approaches mentioned in the foregoing paragraph follow a general two-step procedure of parameter regionalization. The first step is to find optimum sets of parameters for a number of gauged catchments by calibrating the model against observed responses for each of the catchments independently. The second step is trying to establish a relationship between the optimum model parameters and the catchment characteristics. In many previous studies, this has taken a linear or non-linear regression form. However, such an approach has met with limited success. As mentioned in the previous section, model calibration results in only one realization among many other possible parameter sets that lead to a similar model performance. The relationships established between such set of model parameters and the catchment characteristics are therefore likely to be weak or “random”.

Fernandez, et al. (2000) implemented a different approach that would take care of the problem cited above. Instead of following the two-step procedure implemented in the previous studies, they treated them concurrently. They calibrated the “abcd” monthly water balance model (Thomas, 1981) for 30 gauged catchments in the South eastern part of the US with the dual objective of reproducing the observed catchment response and, additionally, to obtain good relationships between model parameters and catchment characteristics. Their approach resulted in a nearly perfect regional relationship between model parameters and catchment properties, but didn’t lead to improvement in the ability of the regionalized model to model stream flow at validation catchments located within the same study area. Unfortunately, many

of the catchment descriptors they used for regionalization require analysis of stream flow data and, therefore, its application to ungauged catchments is not possible.

1.4 Objective of the study

The aim of this study was to develop a methodology, which enables regional estimation of parameters of a conceptual continuous water balance model based on catchment characteristics, which include the land cover type, soil type, and topographic attributes of the catchment. It was aimed at improving the weaknesses inherent in the traditional two-step regionalization approach in estimating the relationship between the model parameters and the physical catchment characteristics. The catchment characteristics used for regionalization were all determined from readily measurable physiographic and land cover attributes of the catchments.

The intended use of the methodology is:

- To estimate model parameters to model the rainfall-runoff processes in ungauged catchments. This was verified by validating the regionalized model in gauged catchments within the study region that were not considered in deriving the regional parameters.

- To assess the impact of land use and land cover changes on the runoff generation from a catchment.

2 Study area and data organization

2.1 Description of the study area

The current study was conducted on part of the Rhine basin situated downstream of Maxau (upper Rhine) and upstream of Lobith (Lower Rhine). This part of the Rhine basin has a total drainage area of 109,330km^2 and its major part is located in Germany, with some parts lying in France, Luxemburg and Belgium. The main river stretch is subdivided into three districts: the Upper Rhine, the Middle Rhine, and the Lower Rhine. The upper Rhine begins further upstream of the study area at Basel (Rhine 170km) and stretches down to Bingen (Rhine 530km). Two major tributaries (Neckar and Main) join it in this part of the river stretch. The middle Rhine is that part of the river between Bingen and Bonn. Major tributaries Nahe, Lahn, and Mosel join the river in this part. Further downstream, the lower Rhine receives inflows from other major tributaries Sieg, Erft, Ruhr, and Lippe.

Table 2.1 Summary of the sizes of the major tributaries of the Rhine and their subdivision into sub catchments

River basin	Size (km^2)	Number of subcatchments
Neckar	13953	13
Main	27211	16
Sieg	2861	4
Lippe	4882	3
Lahn	5939	5
Ruhr	4487	4
Mosel and Saar	28152	26
Nahe	4010	3
Erft	1818	3
NUR	6688	7
NMR	5089	10
NLR	4240	7

The whole study area was subdivided into 101 meso-scale subcatchments with sizes ranging between 400 km^2 and 2100 km^2. Part of the Upper Mosel basin lies in France and due to

limitation on the availability of meteorological data from this area, six subcatchments located in France were left out of the study. Therefore, the study was focused on the remaining 95 subcatchments for which meteorological data were available. Table 2.1 shows the sizes and the numbers of subcatchments into which the different parts of the basin were subdivided. These include the major tributaries joining the different stretches of the river as well as parts of the basin in the neighbourhood of these stretches of the river that are not included in the major tributaries, which are designated by NUR, NMR, and NLR respectively for the upper, middle, and lower Rhine stretches. The corresponding schematic representation is shown in figure 2.1.

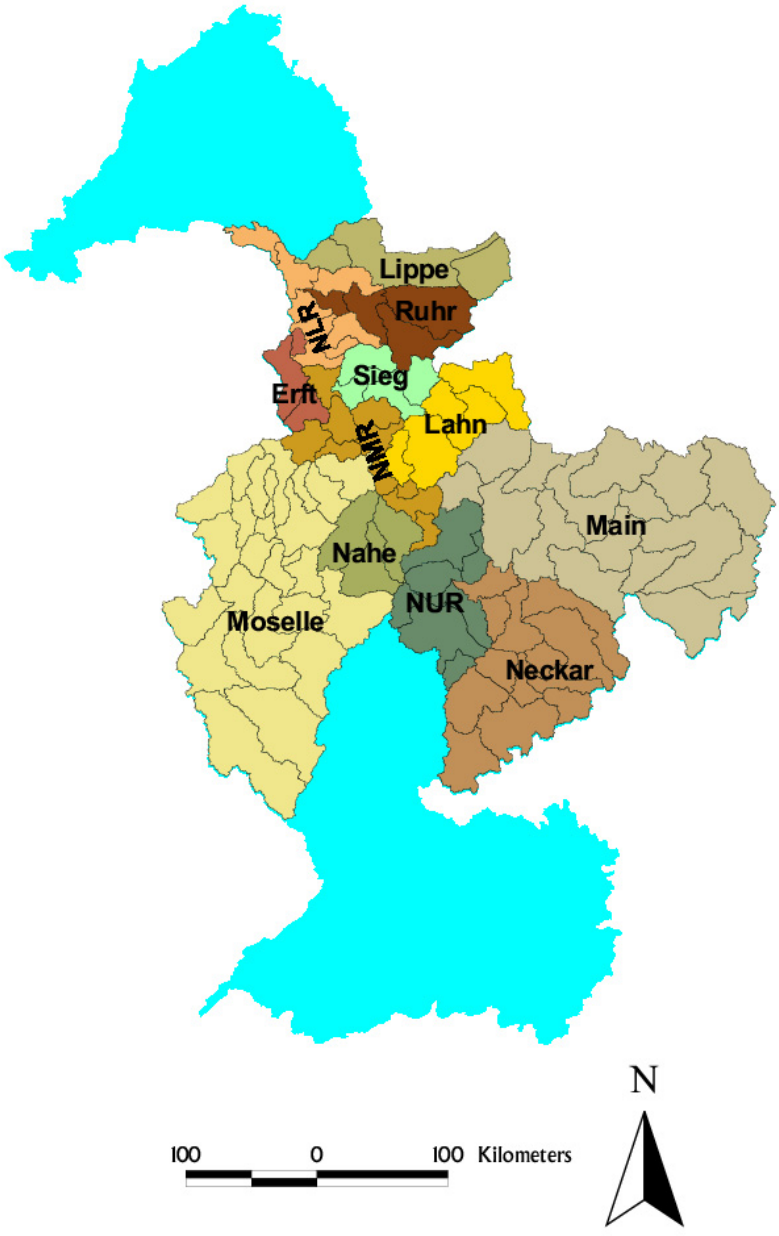

Figure 2.1 The Rhine basin subdivided into higher meso-scale subcatchments

The study area is characterized by different topographic structures and the elevation above sea level ranges from about 1000m in the Fränkische Alb, which forms the south-eastern border of the Main basin, and the black forest area in the south western part of the Neckar basin to as low as 10 m in the lower Rhine district as shown in figure 2.2.

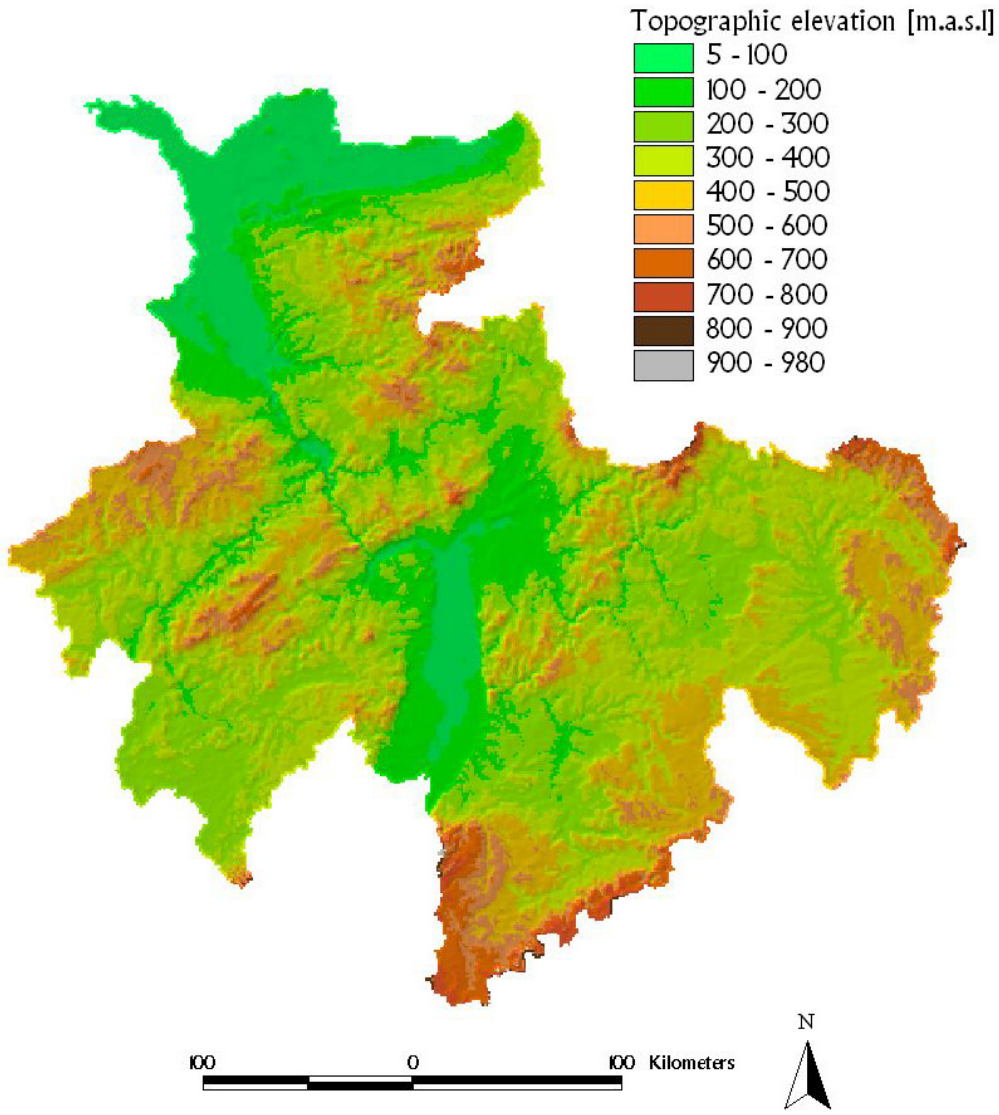

Figure 2.2 Topographic elevation of the study area in meters above sea level (Source: The International Commission for the Hydrology of the Rhine basin, CHR).

Different land cover and land use structures characterize the basin, with different parts of the basin having, on average, their own predominant land use structure prevailing in them. This ranges from a predominantly forest cover structure, for which the Sieg catchment is a typical

example in which the forest cover accounts for 63% of the catchment area, to catchments that are identified by a predominantly urban land use structure, as in the lower Rhine district whose urban area makes up 38% of that part of the basin. Figure 2.3 shows the distribution of different land use classes within the study area.

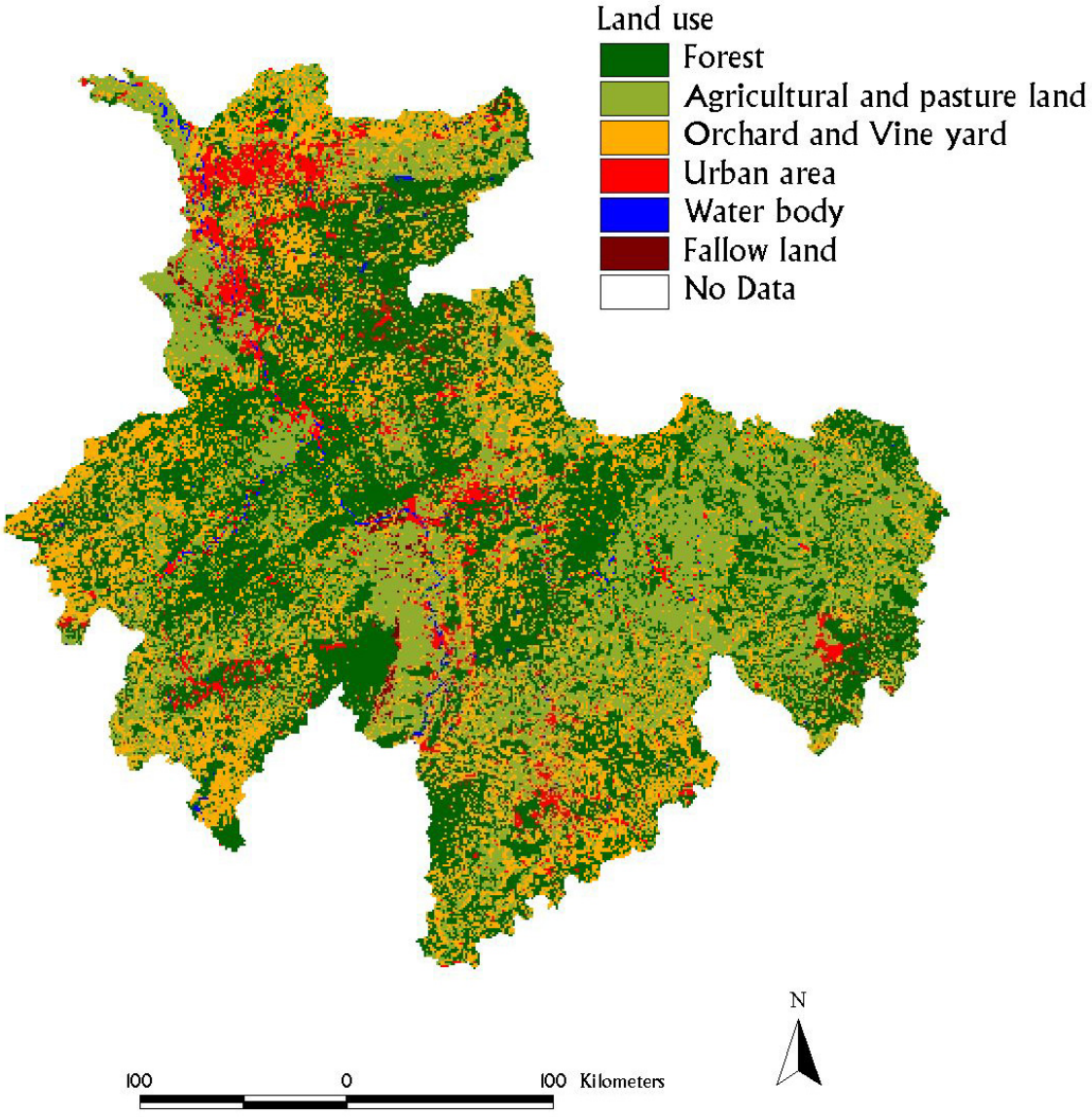

Figure 2.3 Land cover (1993) within the study area (source: The International Commission for the Hydrology of the Rhine basin, CHR).

The geologic formations of the basin are also different for the different tributary catchments. Jurassic and Triassic sediments are the predominant formations in the Neckar catchment. These mainly consist of malm, doggerlime, keuper, shelly limestone and sandstone. Some

parts of this catchment are also known to have karstic rock formation. Jurassic limestone, sandstone, and shelly limestone are the typical formations in the Main catchment, while the Lahn catchment is characterized by Devonian rock and basaltic formations. In the southwestern part of the basin, the Mosel and Saar have mainly Triassic sediment formation, which mainly consists of shelly limestone, sandstone, and keuper, with some parts of the catchment having a Devonian rock formation. Further in the north, the Sieg catchment is formed by mainly Devonian shale and greywacke, while the main formation in the Lippe catchment is Pleistocenic river sediment. Four different zones of geologic formations characterize the Nahe catchment, which is located in the middle Rhine basin district. The northern part is made up of Devonian sediment, which mainly consists of shale and quartzite. The southern part is formed from mainly sandstone and shelly limestone. Near the Nahe-Rhine confluence, marine sand, Tone and Mogel prevail; while in the central part the formation is Taunusquarzitsättel.

2.2 Organization of data

2.2.1 Meteorological data

Precipitation and temperature are by far the most important meteorological variables driving the hydrological processes in a catchment. Precipitation, either in a liquid or snow form is the main input in a rainfall-runoff model. The model tries to simulate its movement within the catchment and its final transformation into runoff. Temperature is another input to a model that influences the amount of evapotranspiration and snowmelt. Proper assessment of their distribution within a catchment under study is, therefore, a crucial step in a rainfall-runoff modelling practice.

Both precipitation and temperature are normally measured at a point scale by conventional measurement gadgets at observation stations. In a rainfall-runoff modelling exercise, however, the amount of precipitation and the magnitude of temperature are required at areal scales, with the areal extent depending on whether a lumped or distributed model is used. For lumped models, average values of precipitation and temperature over the whole catchment area are often sufficient. For grid based distributed models, on the other hand, average values at grids of a few hundred meters to a few kilometres are required. The feasibility of

establishing reasonable estimates of areal averages for small grid sizes depends on the availability of sufficient measurement points around each grid.

Different methods of estimating areal average precipitation are used in practice. These include the simple arithmetic mean, the Thiessen polygon, and the inverse distance method. None of these methods, however, take into consideration the spatial structure of the variation of precipitation. The effect of additional variables that may affect the distribution of precipitation cannot also be integrated in the estimation. Besides, quantification of the uncertainty associated with the estimation is difficult and they do not necessarily lead to an estimate associated with the minimum uncertainty. Geostatistical methods have emerged as alternative approaches to estimate areal average precipitation or temperature from point measurement values. Such approaches incorporate the spatial structure of the variation of precipitation or temperature in estimating the areal average value and lead to a minimum estimation uncertainty. There are also classes of Geostatistical methods that are adopted to include the effect of additional variables that have close relationship with the variable of interest in the estimation process.

The fundamental element in Geostatistical methods is the description of the variability of a regionalized variable by a function known as a variogram. A regionalized variable *Z(u)* is defined as a realization of a set of random variables corresponding to each point *u* within a domain of study. The commonly used hypothesis in Geostatistics is the *intrinsic hypothesis*, which assumes that the expected value of the regionalized variable is constant all over the domain of study and that the variance of the difference in the values of the regionalized variable corresponding to two different locations depends only on the vector separating them, *h*. Based on this hypothesis, the variogram function $\gamma(h)$ is given by:

$$\gamma(h) = \frac{1}{2} E\left[\left(Z(u+h) - Z(u)\right)^2\right] \qquad 2\text{-}1$$

For practical purposes, the variogram function has to be estimated from observed data of the regionalized variable made at different locations within the study domain. The value of the variogram function corresponding to a separation distance, *h*, is calculated as:

$$\hat{\gamma}(h) = \frac{1}{2N_h} \sum_{u_i - u_j = h} \left(Z(u_i) - Z(u_j)\right)^2 \qquad 2\text{-}2$$

where

u_i and u_j are the location vectors of the observation points,

$Z(u_i)$ and $Z(u_j)$ are the observed values at locations u_i and u_j respectively,

N_h is the number of pairs of measurement points separated by a vector h.

The variogram function calculated in this way is known as the *experimental variogram*. The observation points are not usually spaced regularly and, therefore, it may not be easy to get enough points corresponding to a specific separation vector. Therefore, some tolerance is usually applied to the separation vector.

Estimation of the experimental variogram function using equation 2-2 yields values of the variogram at finite number of separation vectors. The function should, however, be continuous and one possibility to make it continuous is to fit linear functions between adjacent calculated points. The fitted linear function, however, may not necessarily meet the criteria a variogram function should fulfil as outlined in Christakos (1984) and Cressie (1993). Therefore, there is a practical need to fit functions that fulfil these criteria to the experimental variogram. Such functions are known as *theoretical variograms*.

There are a number of theoretical variogram models that are used in practice (Kitanidis, 1997). Superposition of two or more of these theoretical variograms will also result in an acceptable variogram model. A combination of two of the common theoretical variogram models is used in this study: the spherical variogram and the pure nugget effect variogram. Isotropy is considered in the variability of both precipitation and temperature and therefore isotropic variogram models are used, i.e., the variogram depends on the scalar separation distance only and not on the direction.

The spherical variogram is a two-parameter function defined as (Kitanidis, 1997):

$$\gamma(h) = \begin{cases} C\left(\frac{3}{2}\frac{h}{a} - \frac{1}{2}\frac{h^3}{a^3}\right), & \text{for } 0 \le h \le a \\ C, & \text{for } h > a \end{cases} \qquad 2\text{-}3$$

where

C is the sill of the variogram, which is the maximum value the variogram attains

a is the range of the variogram, which is the separation distance beyond which there is no correlation between the random variables.

The pure nugget effect variogram is also defined as (Kitanidis, 1997):

$$\gamma(h) = \begin{cases} C_0, & \text{for } h > 0 \\ 0, & \text{for } h = 0 \end{cases} \qquad 2\text{-}4$$

where $C_0 > 0$

The variogram model used in this study, which is a combination of the above two theoretical variograms has, therefore, a form:

$$\gamma(h) = \begin{cases} 0, & \text{for } h = 0 \\ C_0 + C\left(\frac{3}{2}\frac{h}{a} - \frac{1}{2}\frac{h^3}{a^3}\right), & \text{for } 0 < h \le a \\ C_0 + \mathrm{C}, & \text{for } h > a \end{cases} \qquad 2\text{-}5$$

Fitting of the theoretical variogram into the experimental variogram is usually done manually by adjusting the parameters of the theoretical variogram until there is a reasonable match between the two. This procedure can in practice be applied if one has to work only with one or a few realizations of variables. In order to model the spatial variability of precipitation and temperature on the daily basis, one would need to perform this fitting for each day over the study period. The manual fitting procedure is not practical for such a case and a different approach for estimating an approximate variogram function was adopted in this work.

The approach implemented in this work was based on establishing a temporally averaged universal variogram that can be used for all days, which was derived from the spatial cross correlations of the precipitation or the temperature series at the observation points in the study region. It can be shown that the covariance function and the variogram function are related as:

$$\gamma(h) = C(0) - C(h) \qquad 2\text{-}6$$

where,

$C(h)$ is the covariance function

Multiplying the variogram function by any positive constant doesn't lead to a change in the estimated value of the regionalized variable and therefore using the normalized form of the covariance function, which is the correlation function instead of the covariance function can also be used as an approximate simplification to estimate the variogram function. Therefore, a cloud of the points of separation distance versus 1-$r(h)$, where $r(h)$ is the cross correlation of the precipitation or temperature time series between all pairs of observation points is plotted and a theoretical variogram is fitted to the cloud of points. Figure 2.4 shows the h versus 1-$r(h)$ plots and the corresponding fitted theoretical variograms derived from daily time series of precipitation and temperature from stations shown in figure 2.5. Since only the part of the variogram corresponding to smaller separation distances is of importance for interpolation, the theoretical variogram is fitted to the initial part of the h versus 1-$r(h)$ plot.

Since temperature shows less spatial variability, the correlations of the time series between all pairs of stations is high and therefore 1-$r(h)$ tends to be very small. Since multiplying a variogram by a constant number doesn't affect the resulting interpolation result, 1-$r(h)$ was multiplied by 10 so that the parameters of the fitted theoretical variogram can be estimated properly as shown in figure 2.4 b.

The theoretical variograms fitted to the initial parts of the plots shown in figure 2-4 have both the form given in equation 2-5 with h in meters and the following parameters:

$C_0 = 0.055$, $C = 0.40$, $a = 100000m$, for precipitaion interpolation

$C_0 = 0.02$, $C = 0.35$, $a = 300000m$, for temperature interpolation

Daily amount of precipitation and daily mean temperature from 2396 precipitation stations and 509 temperature stations respectively distributed across Germany were acquired from the German Weather Service for the period from 1960 to 1998. Many stations have a lot of missing records and stations with missing data for more than one third of the entire period were discarded and only the remaining stations were considered for further processing. This

brings down the number of precipitation and temperature stations to 1514 and 313 respectively. Missing values in any of these stations were filled in using multiple linear regression from up to 20 nearby stations with no missing record. Based on their proximity to the study area, 949 precipitation and 273 temperature stations were finally used in this study, which are shown in figure 2.5.

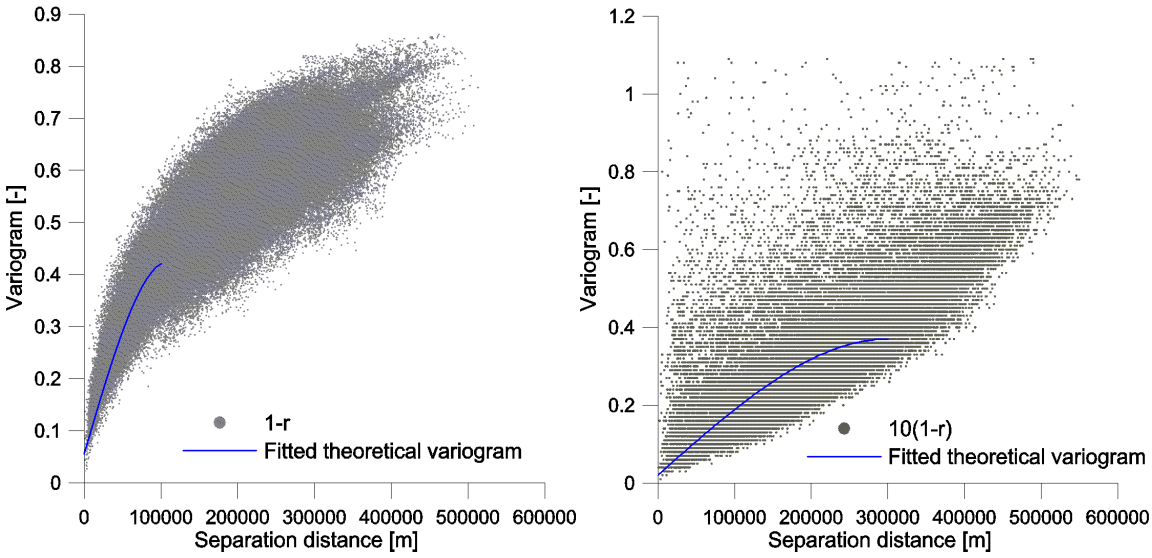

a) Precipitation series

b) Temperature series

Figure 2.4 Plots of the distance between stations versus 1-*r* and the corresponding fitted theoretical variograms for precipitation and temperature interpolation

External Drift Kriging (Ahmed and deMarsily, 1987), which is a geostatistical method of interpolation that takes into account additional variables on which the variable of interest depends, was adapted in this study to estimate precipitation and temperature on a regular grid of 5km × 5km over the whole study area from precipitation and temperature station data distributed within and around the study area. This method was chosen so that the orographic effect on precipitation and the effect of elevation on temperature can be taken account of in estimating them at locations where there are no measurements.

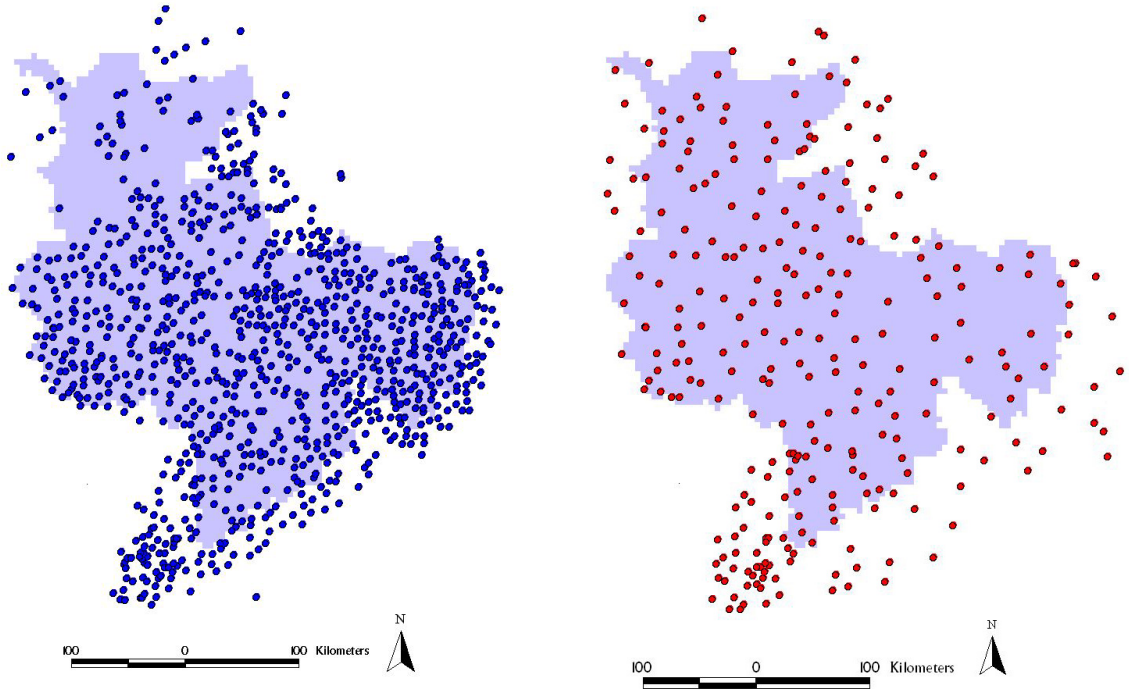

a) Precipitation stations b) Temperature stations

Figure 2.5 Distribution of precipitation and temperature stations used in the study

According to this method, the expected value of the regionalized variable *Z(u)* under consideration (such as precipitation or temperature) at location *u* is assumed to be a linear function of the additional variable *Y(u)* that has an influence on the value of the regionalized variable:

$$E[Z(u) \mid Y(u)] = a + bY(u) \qquad 2\text{-}7$$

where *a* and *b* are unknown constants.

The additional variable has to be numeric, locally linearly dependent, and be available at each point within the domain of the study.

A linear combination of the values of the regionalized variable at locations where the values are known is used to estimate the value at a location where its value is not known:

$$Z^*(u) = \sum_{i=1}^{n} \lambda_i Z(u_i) \qquad 2\text{-}8$$

In order to have an unbiased estimator, equation 2-7 should hold for the estimation:

$$E[Z(u)] = E\left[\sum_{i=1}^{n} \lambda_i Z(u_i)\right] = \sum_{i=1}^{n} \lambda_i E[Z(u_i)] = \sum_{i=1}^{n} \lambda_i [a + bY(u_i)] = a + bY(u) \qquad 2\text{-}9$$

Equation 2-9 leads to a set of two unbiasedness constraints:

$$\sum_{i=1}^{n} \lambda_i = 1 \qquad 2\text{-}10$$

$$\sum_{i=1}^{n} \lambda_i Y(u_i) = Y(u) \qquad 2\text{-}11$$

The above constraints are not enough to get the best estimate of the variable. In addition to the unbaisedness criterion, another criterion to minimize the variance of the estimation is imposed that leads to the *best linear unbiased estimator*:

$$\sigma^2(u) = E\left[\left(Z^*(u) - Z(u)\right)^2\right] \rightarrow \min \qquad 2\text{-}12$$

Equation 2-12 can be rewritten in terms of the variogram function as:

$$\sigma^2(u) = E\left[\left(Z^*(u) - Z(u)\right)^2\right] = -\sum_{i=1}^{n}\sum_{j=1}^{n} \lambda_i \lambda_j \gamma(u_i - u_j) + 2\sum_{i=1}^{n} \lambda_i \gamma(u_i - u) \rightarrow \min \qquad 2\text{-}13$$

Minimizing equation 2-13 subjected to the constraints 2-10 and 2-11 is performed using Lagrange multipliers μ_1 and μ_2, which leads to minimization of the following equation.

$$\sigma^2(u) - 2\mu_1\left(\sum_{i=1}^{n} \lambda_i - 1\right) - 2\mu_2\left(\sum_{i=1}^{n} \lambda_i Y(u_i) - Y(u)\right) \qquad 2\text{-}14$$

This finally leads to the system of external drift equations (Ahmed and de Marsily, 1987):

$$\begin{cases} \sum_{j=1}^{n} \lambda_j \gamma(u_i - u_j) + \mu_1 + \mu_2 Y(u_i) = \gamma(u_i - u), \quad i = 1,...,n \\ \sum_{j=1}^{n} \lambda_j = 1 \\ \sum_{j=1}^{n} \lambda_j Y(u_j) = Y(u) \end{cases} \qquad 2\text{-}15$$

Since temperature shows a fairly uniform lapse rate with elevation, which changes from one day to another mainly due to humidity changes, the additional variable used for interpolating temperature was taken as:

$$Y(u) = z \qquad 2\text{-}16$$

where

z the topographic elevation.

On the other hand, the rate of increase of precipitation decreases with increasing elevation and therefore, in order to take this effect into consideration, the square root of the topographic elevation was used for interpolating precipitation.

$$Y(u) = \sqrt{z} \qquad 2\text{-}17$$

Figure 2.6 shows the interpolated mean annual precipitation and temperature over the study area based on this methodology.

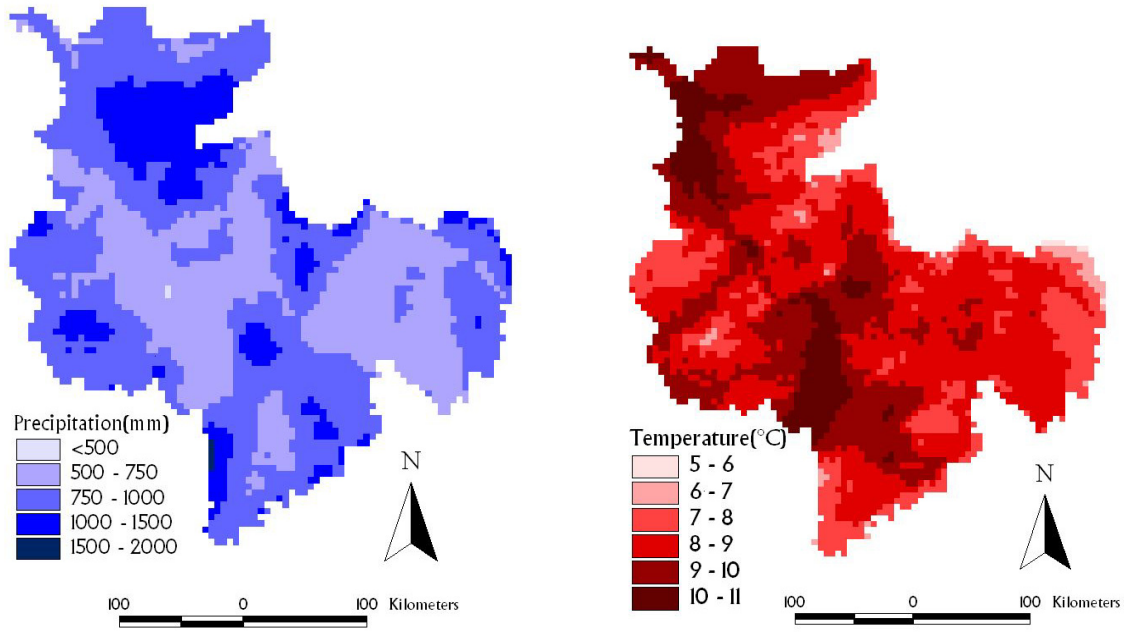

a) Mean annual precipitation b) Mean annual temperature

Figure 2.6 Mean annual precipitation and mean annual temperature in the study area as estimated using the external drift kriging.

Figure 2.7 also shows the distribution of interpolated mean temperature and total precipitation amount within the study area on specific days when extremes were recorded.

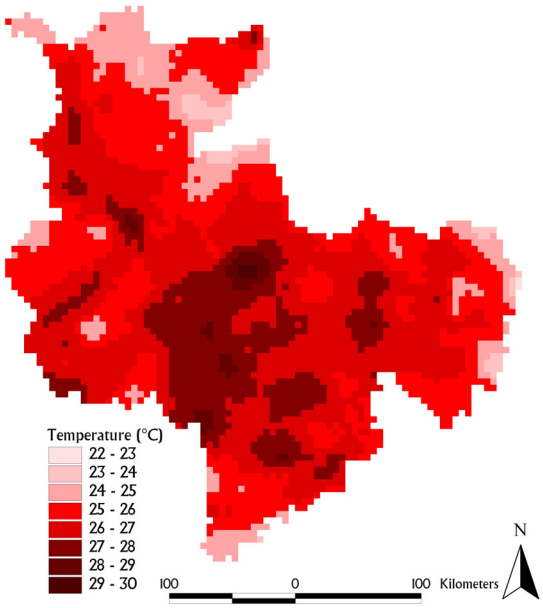

a) Mean temperature on 8.8.92

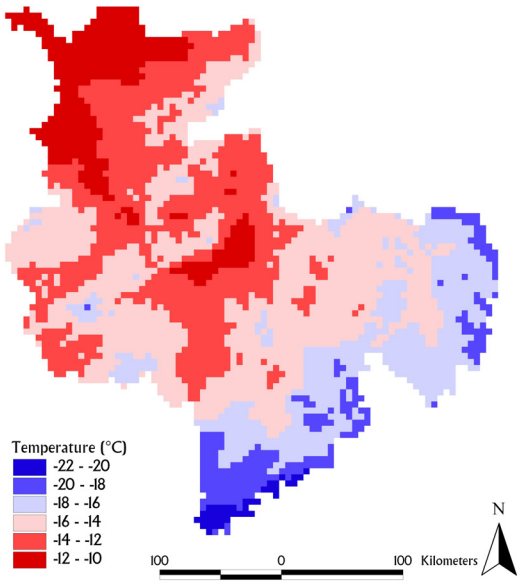

b) Mean temperature on 12.1.87

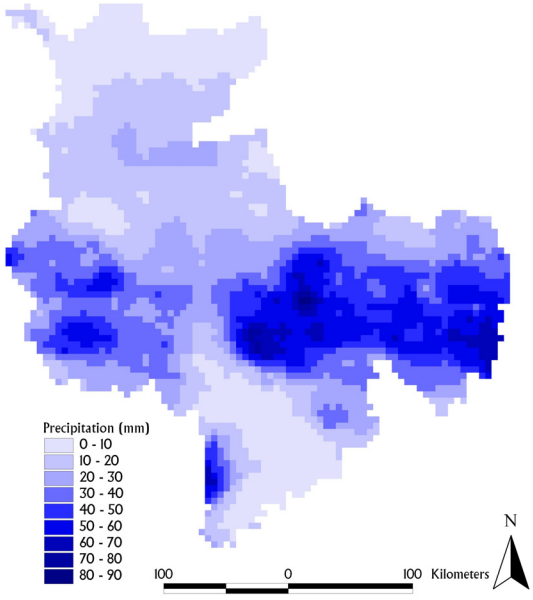

c) Total precipitation amount on 25.1.85

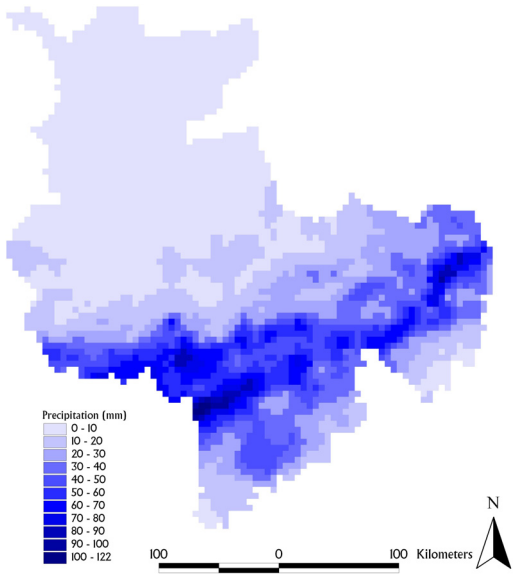

d) Total amount of precipitation on 22.7.95

Figure 2.7 Distribution of mean temperature and amount of precipitation on days of extreme temperature/precipitation.

2.2.2 Evapotranspiration

Evapotranspiration is a process by which water is returned to the atmosphere. It consists of evaporation from open water surface, bare soil surface, and water intercepted by plant surfaces, as well as transpiration by plants from their root zone. It is an important hydrological process that influences the water balance of the catchment. The process of evaporation is influenced by different meteorological variables, the nature of the evaporating surface, and availability of water. The meteorological variables include the energy available from the net radiation and ambient air temperature, which is responsible for converting the liquid water into vapour; the humidity gradient at the evaporating surface, which influences the opportunity of the water vapour on the evaporating surface to move into the atmosphere; and the wind speed, which removes the water vapour from the adjacent air mass and maintains the humidity gradient. Transpiration is a process by which water is taken up by plant roots from the soil and returned to the atmosphere through their leaves as part of their biological activity. The amount and rate of transpiration depends on the type of vegetation cover and their stage of growth, season of the year, time of the day, availability of water in the root zone and the same meteorological factors that affect evaporation. Since it is difficult to quantify evaporation and transpiration separately, they are considered together as evapotranspiration (Jones, 1997).

Evapotranspiration that would take place if there were no limitation on the supply of water is referred to as potential evapotranspiration. Actual evapotranspiration is the amount of water actually removed by the processes of evaporation and transpiration. Depending on the availability of water, it can be equal or lower than the potential evapotranspiration. Although it is the actual evapotranspiration that is used in the water balance computation, an estimate of the potential evapotranspiration for a given catchment condition under the prevailing climatic conditions is an important step in a rainfall-runoff modelling practice. The actual evapotranspiration is then estimated based on the potential value and the availability of moisture supply to meet this demand.

There are different methods available for the estimation of potential evapotranspiration that range from data intensive physical approaches such as the Penman-Monteith equation (Monteith, 1965) to the less demanding empirical approaches such as the Hamon (1961), the Blaney and Criddle (1950), the Turc (1961), and the Haude (1955) methods. Many of the

empirical methods are developed for specific climate regions and shouldn't be used for conditions different from they are developed for.

The Haude approach is a method for estimating long term potential evapotranspiration such as monthly or annual values for the middle European climate. The method has been successfully used by the German Weather Service (Dommermuth and Trampf, 1990). It has been verified to offer realistic results when compared with field measurements of evapotranspiration using Lysimeter for many years. It is based on Dalton's law of evapotranspiration, which considers evapotranspiration as a processes controlled by the vapour pressure difference between the evaporating surface and the atmosphere:

$$ETP = \alpha \cdot (es - ea) = \alpha \cdot es \cdot \left(1 - \frac{f}{100}\right) \qquad 2\text{-}18$$

where:

ETP: potential evapotranspiration (mm/day)
es: saturation vapour pressure of air (hPa)
ea: actual vapour pressure of the air (hPa)
f: relative humidity of the air measured at 2:00 PM
α: monthly crop specific coefficient (mm/hPa)

The saturation vapour pressure is a function of air temperature and is given by the Magnus formula:

$$es = 6.11 \cdot e^{\frac{17.62T}{243.1+T}} \qquad 2\text{-}19$$

where:

T mean air temperature (°C)

The approach needs measurement of only air temperature and relative humidity and knowledge of the type of the vegetation cover. The monthly crop specific coefficients for different common types of plants are shown in table 2.2 (Dommermuth and Trampf, 1990, 1991, 1992).

The Haude factors shown in table 2.2 take the interception loss into consideration. For forest cover, Haude factors were established by Elling, et al.(1990) as shown in table 2.3. However, these coefficients do not take the interception loss into account.

Table 2.2 Monthly crop specific Haude coefficients, α (mm/hPa)

Crop type	Jan.	Feb.	Mar.	Apr.	May	Jun.	Jul.	Aug.	Sep.	Oct.	Nov.	Dec.
Grass	0.20	0.20	0.21	0.29	0.29	0.28	0.26	0.25	0.23	0.22	0.20	0.20
Sugar beets	0.14	0.14	0.14	0.15	0.22	0.30	0.36	0.32	0.26	0.19	0.14	0.14
Maize	0.14	0.14	0.14	0.14	0.18	0.26	0.26	0.26	0.24	0.21	0.14	0.14
Wheat	0.18	0.18	0.19	0.26	0.34	0.38	0.34	0.22	0.21	0.20	0.18	0.18
Summer barley	0.15	0.15	0.18	0.25	0.30	0.36	0.26	0.18	0.18	0.18	0.18	0.18

Table 2.3 Monthly Haude coefficients for forest cover, α(mm/hPa)

Forest type	Jan.	Feb.	Mar.	Apr.	May	Jun.	Jul.	Aug.	Sep.	Oct.	Nov.	Dec.
Deciduous	0.01	0.00	0.04	0.10	0.23	0.28	0.32	0.26	0.17	0.10	0.01	0.00
Coniferous	0.08	0.04	0.14	0.35	0.39	0.34	0.31	0.25	0.20	0.13	0.07	0.05

The long term mean monthly potential evapotranspiration for a reference crop (grass) was estimated using the Haude formula at the climate stations distributed within the study area for the years 1970 to 1998 and interpolated on the same grid used for the interpolation of temperature and precipitation. Depending on the type of vegetation cover, these values were multiplied by the ratio of the Haude factor for the given vegetation type to that of grass to estimate the potential evapotranspiration of other vegetation types. For non-forest areas, this evapotranspiration value accounts for the interception loss and there is no need to further consider interception. In forest areas, since the Haude coefficients do not consider the interception loss, an interception storage, I_{max} was defined. The interception capacity of forest depends on the type and age of the forest cover. This ranges between 3mm and 5mm for coniferous forests and between 2mm and 4mm for deciduous forests (Mitscherlich, 1981; Münch, 1993). While deciduous forests attain their maximum storage in summer due to their leaves, coniferous forests have their maximum storage in winter due to the effect of snow stacking.

3 Modelling of the rainfall-runoff processes

3.1 Introduction

The most rational way of modelling the rainfall-runoff processes would be through the application of the known physical principles to all the processes involved in the generation of runoff from rainfall. However, not all the processes involved are well understood and some approximation that involves aggregation of some of the processes is inevitable. Besides, the physical properties of a catchment and the rainfall may show a high spatial variability within the catchment. This necessitates modelling of the processes using a spatially distributed modelling approach by discretizing the catchment area into finer areas. This requires the availability of the physical parameters and other data needed in the model at all these discrete areas within the catchment. However, measurement of physical parameters is practically done at small scale and upscaling of the small scale measurements to elements treated in the model, which may be orders of magnitudes larger, is a practical necessity. This upscaling doesn't often reproduce the actual variability of the parameters within the area (Binley et al. 1989). Besides, the number of measurements needed may not be practically feasible as the size of the catchment increases. This, therefore, puts a practical limit to its applicability in modelling large-scale catchments.

The difficulty associated with properly estimating the distribution of the model parameters within the catchment a-priory ultimately puts a need to calibrate the model against observed catchment responses. This leads to calibration of an over-parameterised problem and if the model calibration is done against only observed discharge, as is the case in most rainfall-runoff model calibration practices, the parameters may not be well identified. The parameters estimated in this way can only be used to estimate the catchment response the model is calibrated with and if the same set of parameters were to be used for time periods outside the calibration period, the prediction made by the model would be uncertain.

Under conditions where availability of data is limited to enable proper identification of parameters of complex models, implementation of such models is not warranted. Instead, more parsimonious models, which are structured in such a way that their parameters are well posed with respect to the available data would be sufficient. Jakeman and Hornberger (1993) came to a conclusion that if only stream flow data are available to calibrate a model, a model structure based on a quick-flow and a slow-flow component is sufficient to provide an

adequate simulation of the stream flow resulting from rainfall. Moreover, they argued that the addition of more model structure and its associated parameters requiring calibration leads to no significant improvement in model fit yet introduces poorly identified parameters. A study made by Refsgaard and Kundsen (1996) to compare the relative performances of a complex distributed physically based model and a lumped conceptual model when calibrated against observed stream flow also supports this argument.

3.2 Selection of appropriate model for the study

The following criteria had to be considered in choosing the model to be used in this study:

- Since the study is carried out on a large-scale catchment, the model should not be complex and data intensive. Its data requirement should be addressed by the available observations and measurements within the study area.

- The model structure should schematise the most important runoff generating processes in a scientifically reasonable way.

- The model should not have too many parameters.
- The model should be known to be applicable to the study area. This should be evidenced by previous application of the model to parts of the study area.

Based on the above criteria, the HBV model (Bergström, 1995), which is a semi-distributed conceptual model, was chosen. The model was originally developed at the Swedish Meteorological and Hydrological Institute (SMHI) and was first applied in the early 1970s (Bergström and Forsman, 1973). Some modifications were later applied to the structure of the model to improve its potential for making use of spatially distributed data and improve the model performance (Lindström et al., 1997).

The model was implemented in the study of the impact of climate change on a river basin hydrology on the upper Neckar catchment, which is part of the current study area, and was tested to perform very well (CCHYDRO, 1999).

As one of the objectives of the study was to be able to model the impact of land use changes, some more modifications were applied to some of the model components in such a way that

the model can properly represent land use effects. A FORTRAN code for this modified version of the model was written and it is referred to as HBV-IWS[1] model.

3.3 Structure of the HBV-IWS model

The model uses subcatchments as primary hydrological units. Further zoning of the subcatchments into elevation zones and other homogeneous units based on land use, soil type, etc. is also possible. The model consists of three main components:

- snow accumulation and melt routine
- soil moisture accounting routine
- runoff response routine

The model components are classified into two major categories based on the spatial scale on which they work. The first category comprises of components for distributed runoff generation processes at the scale of a homogeneous zone within a subcatchment, while the second one consists of components for a lumped runoff response process at the subcatchment level.

3.3.1 Distributed runoff generation Processes

Snow accumulation and melt

Snow accumulation and melt is modelled by a degree-day method, in which the daily rate of snowmelt in water equivalent is proportional to the increase in daily temperature above a threshold value *TT*:

$$S_{melt} = CC \max(0, T - TT) \qquad 3\text{-}1$$

where

S_{melt} melt rate as water equivalent [mm day^{-1}]
CC degree-day factor [mm °C^{-1} day^{-1}]
T mean daily air temperature [°C]
TT threshold temperature for snow melt initiation [°C]

[1] IWS: *Institut für Wasserbau der Universität Stuttgart*.

If the mean air temperature is less than the threshold temperature, precipitation is assumed to be in snow form. In the original version of the HBV model, the degree-day factor *CC* was set a constant. However, it is known that whenever there is a rainfall, the energy available in the rainwater with positive temperature also forces more snow to melt. In order to include this effect in the rate of snowmelt, the degree-day factor was modified as a linear function of the daily depth of precipitation:

$$CC = \begin{cases} CC_0 + kP & \text{if} \quad \mathrm{P} \le \dfrac{\mathrm{C}_{\max} - CC_0}{k} \\ C_{\max} & \text{else} \end{cases} \qquad 3\text{-}2$$

where

CC_0 degree-day factor when there is no rainfall [mm °C^{-1} day^{-1}]

P daily depth of precipitation [mm]

C_{max} a limiting value to the degree day factor [mm °C^{-1} day^{-1}]

k a positive constant

The limiting value of the degree-day factor C_{max} is introduced in order to avoid unrealistically high snowmelt during very intense rainfall.

Interception

For forest cover, interception storage (I_{max}) was defined. The storage may vary depending on the season. Rainfall is first intercepted until the interception storage is filled. The remaining rainfall reaches the soil surface as through fall and stem flow.

Soil moisture accounting

The soil moisture accounting routine computes the proportion of snowmelt or rainfall that reaches the soil surface, which is ultimately converted to runoff. This proportion is related to the soil moisture deficit and is calculated using the relation:

$$\frac{R}{P} = \left(\frac{SM}{FC} \right)^{\beta} \qquad 3\text{-}3$$

where

R contribution of the zone to runoff [mm]

P rainfall or snowmelt [mm]

SM actual soil moisture [mm]

FC maximum storage capacity of the soil [mm]

β a model parameter

The remaining part of the rainfall or snowmelt is added to the soil moisture until the storage capacity of the soil FC is reached.

Evapotranspiration

The long term mean monthly potential evapotranspiration is used to compute evapotranspiration in each month. Daily values of potential evapotranspiration are adjusted based on the daily mean air temperature according to the relation:

$$PE_A = \left(1 + C_{ET}\left(T - T_M\right)\right)PE_M \qquad 3\text{-}4$$

where

PE_A adjusted potential evapotranspiration [mm/day]

PE_M long term mean evapotranspiration for a given month [mm/day]

T_M long term mean monthly air temperature [°C]

T mean daily air temperature [°C]

C_{ET} model parameter [$°C^{-1}$]

The adjusted daily potential evapotranspiration, PE_A, cannot have a negative value and is not allowed to exceed twice the monthly average.

If separate interception storage is defined and the amount of water in the interception storage is greater than the potential evapotranspiration, the evapotranspiration demand is first met by the water in the interception storage. If it is less than the potential evapotranspiration, all the intercepted water evaporates and the remaining evapotranspiration takes place from the soil moisture. The actual evapotranspiration that takes place from the soil zone depends on the soil moisture. Evapotranspiration equal to the potential value takes place if the soil moisture is greater than a soil parameter LP. If the actual soil moisture is less than this value the actual evapotranspiration is reduced linearly to zero at a completely dry soil.

$$E_{\text{int}} = \min\left(I_{act}, PE_A\right) \qquad 3\text{-}5$$

where

E_{int} evaporation from the interception storage [mm/day]

I_{act} amount of water in the interception storage [mm]

PE_A potential evapotranspiration [mm/day]

The potential value of the evapotranspiration that would take place from the soil zone is then:

$$PE_A^{'} = PE_A - E_{\text{int}} \qquad 3\text{-}6$$

The actual evapotranspiration that takes place from the soil zone is given by:

$$ET = \begin{cases} \min\left(SM, PE_A^{'}\right) & \text{if SM} > LP \\ \min\left(SM, \frac{SM}{LP} PE_A^{'}\right) & \text{else} \end{cases} \qquad 3\text{-}7$$

where

ET actual evapotranspiration from the soil zone [mm]

SM actual soil moisture [mm]

LP limiting soil moisture above which evapotranspiration reaches its potential value [mm]

3.3.2 Lumped runoff response process

The runoff computed in the soil moisture accounting routine is transformed to discharge at the outlet of the subcatchment using the runoff response function. This function controls the time distribution of the generated runoff. The runoff response routine consists of two conceptual reservoirs arranged one over another. The upper reservoir is a non-linear reservoir whose outflow simulates the direct runoff component from the upper soil zone, while the lower one is a linear reservoir whose outflow simulates the base flow component of the runoff.

The upper reservoir is fed by the excess water from the soil moisture accounting routine and its outflow at time step t_i is given by:

$$Q_1(t_i) = k_1 h_1(t_i)^{1+\alpha} \qquad 3\text{-}8$$

where

$Q_1(t_i)$ outflow from the upper reservoir at time step t_i [mm/day]

$h_1(t_i)$ depth of water in the upper reservoir at time step t_i [mm]

k_1 recession coefficient of the upper reservoir [day^{-1}]

α model parameter

The lower reservoir is fed by a percolation rate controlled by a parameter *perc* from the upper reservoir. The outflow at time step t_i is computed as:

$$Q_2(t_i) = k_2 h_2(t_i) \qquad 3\text{-}9$$

where

$Q_2(t_i)$ outflow from the lower reservoir at time step t_i [mm/day]

$h_2(t_i)$ depth of water in the lower reservoir at time step t_i [mm]

k_2 recession coefficient of the lower reservoir [day^{-1}]

The total runoff Q_g is computed as the sum of the outflows from the upper and the lower reservoirs and any other component of the runoff that doesn't enter the reservoirs (see section 3.3.3).

$$Q_g(t_i) = Q_1(t_i) + Q_2(t_i) + q_s(t_i) \qquad 3\text{-}10$$

where

$Q_g(t_i)$ total generated runoff at the outlet of a catchment at time step t_i [mm/day]

$q_s(t_i)$ component of the catchment runoff that doesn't enter the reservoirs generated at time step t_i [mm/day]

The total runoff is then smoothed using a triangular transformation function whose base is defined by a parameter *MAXBAS* [days] as shown in figure 3.1.

$$Q(t_i) = \sum_{j=0}^{T} \tau(j) Q_g(t_{i-j}) \qquad 3\text{-}11$$

where

$Q(t_i)$ final transformed total runoff at the outlet of the catchment at time step t_i [mm/day]

$\tau(j)$ the weighting function at j^{th} time step

T *MAXBAS* expressed as an integer multiple of the time-step used for runoff computation.

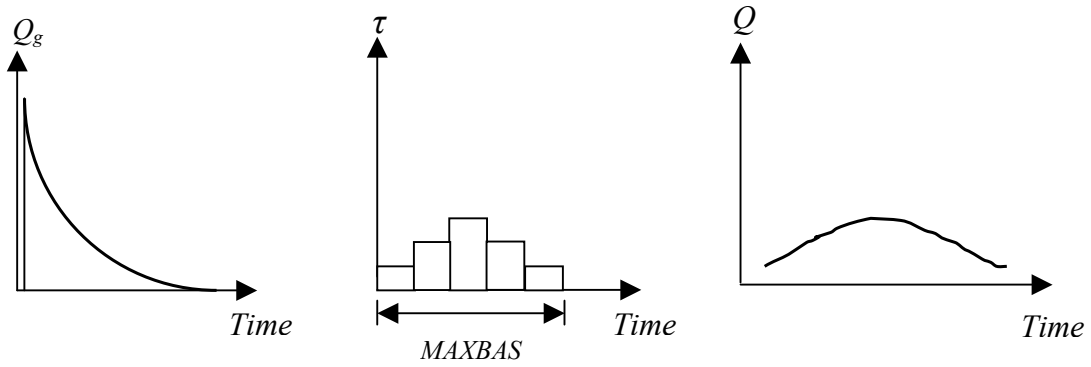

Figure 3.1 Smoothing of the generated runoff Q_g to obtain Q

3.3.3 Additional components

Flows generated from the subcatchments can be routed between subcatchments using the Muskingum hydrological flood routing procedure (Shaw, 1988).

If the model is to be used for prediction of the effect of changes in the land cover characteristics, especially the effect of urbanization, the runoff generated on impervious areas should be handled properly. In the original version of the HBV model this was not accounted for. A component for sealed areas was added in the model structure in this work. The percentage of sealed areas in different zones is given as an input to the model. All the rainfall or snowmelt on sealed areas produces surface runoff and is routed to the outlet of the catchment without entering the reservoirs defined in the runoff response routine.

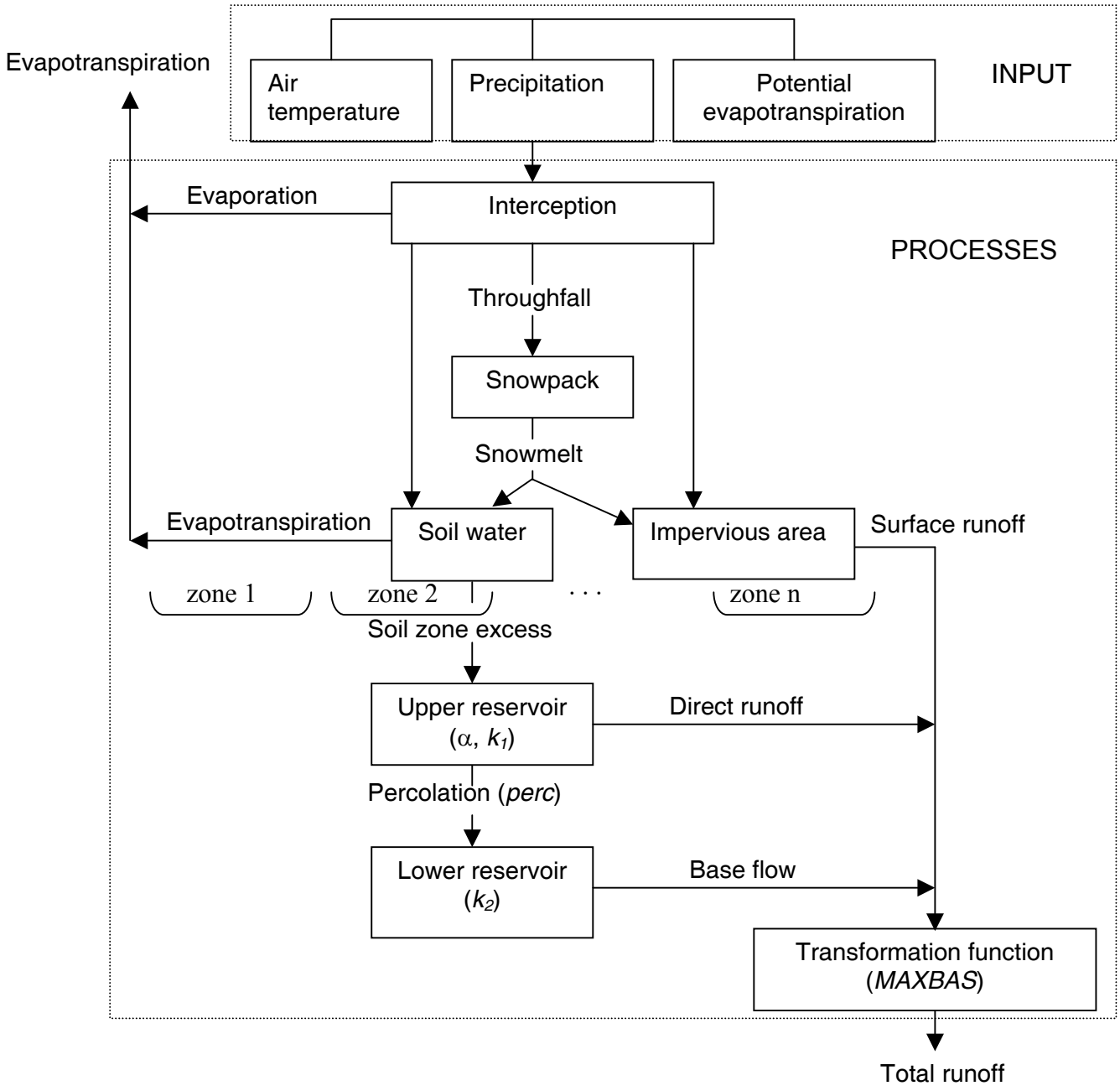

Figure 3.2 Schematic representation of the HBV-IWS model

When the intensity of precipitation is high, infiltration into the soil zone may be limited by the infiltration capacity of the soil and the possible siltation of the soil surface, even if the soil was not saturated. Due to the heterogeneity of the infiltration capacity within a given zone, the entire zone may not produce this infiltration excess overland runoff for a given rainfall intensity. To model this phenomenon, a threshold precipitation intensity (P_{thr}) was defined. When the rainfall intensity exceeds this value, portion of the rainfall in excess of this

threshold value produces direct overland flow that is directly routed to the outlet without entering the reservoirs of the runoff response routine. The ratio between this direct overland flow and the rainfall in excess of P_{thr} is defined as percentage of sealing during heavy rainfall (Ψ_{seal}). Both parameters have to be established through model calibration.

$$q' = \psi_{seal}\left(P - P_{thr}\right) \qquad 3\text{-}12$$

where

q' is the infiltration excess direct overland flow [mm/day]

P is precipitation [mm/day]

Schematic representation of the structure of the HBV-IWS model is shown in Figure 3.2.

3.4 Classification of the subcatchment into homogeneous units for distributed modelling of the runoff generation processes

Since the different runoff generation processes described in the model structure have variable outputs for different catchment characteristics, it is worthwhile to subdivide the subcatchments into different homogenous zones based on the important catchment characteristics that have influence on the runoff generation processes. Topographic elevation, soil type, and land use were used in defining zones in this study. As elevation affects the distribution of the basic meteorological variables such as precipitation and temperature as well as the rate of evapotranspiration, it is an important catchment characteristic that should be considered in defining zones. Elevation zones were defined using a contour interval of 100m. Areas between successive contour intervals were considered homogenous with respect to elevation. The elevation in the study area varies from about 10m to around 1000 and therefore, a maximum of 10 elevation zones were defined in each subcatchment. The water holding capacity of the soil zone, the infiltration capacity and the actual evapotranspiration depend on the soil type and, therefore, soil type should also be used as another basis for zoning the subcatchments. Based on the soil map of the study area, 13 different soil types were identified. Among them, only six types make up the major portion of the study area. Each of the remaining types accounts for less than 1% of the area and were included in the neighbouring dominant soil type. Another catchment characteristic that has an important influence on many of the catchment processes is the land use class. The rate of

evapotranspiration, the infiltration rate, and the rate of snowmelt all depend on the land use type. Four land use classes were defined: urban, agricultural, forest, and water body.

For each subcatchment, homogenous zones were formed by intersecting the elevation classes and the soil types. A maximum of 60 homogenous zones were formed in each subcatchment depending on the range of the elevation and the number of soil types in the subcatchment. In each of the zones formed in this way, the percentage of each of the four land use classes was calculated from the intersection of the three maps.

For the modelling of the processes in each zone, the daily precipitation amount and mean temperature were interpolated on a regular grid of 5km × 5km and the values in each zone were estimated as the mean of the values on the grids located within a given zone. The runoff was computed for each land use class within the zone defined by the intersection of the elevation and soil class using the routines discussed in section 3.3.1. The runoff from the zone was then calculated as the weighted mean runoff from each land use class, the weights being the proportions of the different land use classes. Finally, the subcatchment runoff was computed as the sum of the runoff from each zone weighted by the relative area of each zone before being routed by the reservoirs of the runoff response module to the outlet of the subcatchment.

4 Regionalization of model parameters

4.1 Introduction

In spite of their attractiveness due to their few number of parameters compared to distributed physically based models, the major shortcoming of the parsimonious conceptual models is that their parameters are not physically measurable. Therefore, there is a need to establish the parameters through model calibration against observed catchment responses. Traditional model calibration approaches try to establish a set of model parameters that lead to maximum matching between the model output and the observed response without any reference to the physical catchment descriptors. A model calibrated in this way can only be used to simulate the runoff in the catchment it is calibrated for and its application to other catchments is not possible, as the parameters are not related to catchment properties. Application of such a modelling approach is therefore limited to catchments for which there are observed responses that are needed for model calibration.

In practice, however, there is a need to model runoff in catchments that are not gauged as well. Application of a physically based model may seem to be the best choice in such a case. Although the parameters of a physically based model have physical meanings and can be related to the physical catchment properties, their measurement is usually limited to small scales and estimation of their values at a scale relevant to the model used to predict the catchment response is not practically feasible. Therefore, calibration of the model against observed catchment response is necessary to estimate at least some of the parameters of a physically based model too. Due to the reason discussed in chapter 3, however, there is no gain in implementing the data intensive physically based models to estimate the catchment response in ungauged catchments of larger size in which availability of data is a limiting factor for the proper identification of the model parameters.

Estimating the impact of changes within a catchment, such as changes in land use or land cover are also important considerations that need to be addressed by an operational model. Unless the parameters of the model are related to the catchment attributes that are prone to change, prediction of the effect of these changes is not possible. Relating parameters of a conceptual rainfall-runoff model with the relevant catchment attributes is not, however, a trivial task.

The classical approach to relate the parameters of a conceptual rainfall-runoff model with the physical catchment descriptors follows a two-step procedure. The model is calibrated for a number of subcatchments within the area of interest independently and a set of optimum parameters is estimated for each subcatchment. The relationship between each of the model parameters and the physical catchment attributes is then estimated using a regression approach. This approach has been implemented for different conceptual rainfall-runoff models (Waylen and Woo, 1984; Weeks and Ashkanasy, 1985; Abdulla and Lettenmaier, 1997; Sefton and Howarth,1998; Post and Jakeman, 1999).

4.2 A transfer function approach for parameter regionalization

The classical approach of regionalization of the parameters of a rainfall-runoff model doesn't generally lead to a strong relationship between the model parameters and the catchment descriptors. Calibration of the model against observed discharge doesn't lead to a unique set of parameters. There could be a high degree of parameter interaction and as a consequence, many different sets of parameters may lead to similar model performance. The parameter set obtained through calibration is therefore a single realization among a large number of equally competing parameter sets in terms of their performance. The parameters estimated in this way may not properly reflect the dependency they have with the catchment descriptors. Therefore, the relationship established is likely to be weak. In addition, catchment descriptors that may not have any influence on a given parameter may be included in deriving the regional relationships, as there is no indication from the 'optimum' parameter which descriptors are important in describing it.

Recently, a modelling paradigm that rejects the idea of an 'optimum' parameter set has been in use. Instead of trying to get a single set of parameters through model calibration, many sets of parameters that lead to acceptable model performance are used with their corresponding likelihood weights determined based on pre-specified likelihood functions to make prediction by the model. Such a methodology, referred to as a Generalized Likelihood Uncertainty Estimation (GLUE), is outlined by Beven and Binley (1992) and takes implicitly into account all the uncertainties resulting from the model structure and the data used for model calibration and enables quantification of the total uncertainty in the model prediction. It is based on randomly sampling a parameter set from the feasible parameter space and making a model run using the parameter set thus sampled. Whether to accept or reject the parameter set is decided

based on a pre-defined threshold value of a model performance measure and if it is accepted a likelihood weight is assigned to it based on the defined likelihood function. The procedure is repeated many times so that the entire parameter space is well sampled. The required number of samples increases with the number of model parameters and the associated requirement of computing resources usually limits the applicability of the methodology for models with many parameters.

The intention in this work is to solve the problem of identifying a unique optimum set of parameters and fitting the relationship between the parameters and the catchment descriptors that is inherent in the classical method of parameter regionalization by implementing a different approach. Instead of calibrating the model for the individual subcatchments separately and then trying to fit a relationship between the parameters and the catchment descriptors, the calibration process is begun by first expressing the model parameters as functions of the catchment descriptors using functions whose form is assumed a priori. The model is then calibrated for many subcatchments simultaneously. The model calibration is performed without making any direct reference to the model parameters. Instead, the calibration yields other set of parameters that are used to relate the model parameters with the catchment descriptors in the initially assumed function.

4.2.1 Defining the transfer function

The model parameters are categorized in to two groups. The first group of parameters are related to the runoff generation processes in different zones within the subcatchments. These parameters are estimated based on the soil type or the land use class of the zones or both, depending on which of these catchment attributes influence the parameter values. For the runoff generation processes, the attributes that have a major influence are usually known from physically based models developed to model different components of a catchment process separately. Table 4.1 shows the most important catchment attributes that influence the parameters of the runoff generation processes of the HBV-IWS model. These attributes are used as the bases of regionalization of the parameters.

Table 4.1 Basis of regionalization of parameters of the runoff generation processes

Parameter	basis of regionalization
Snowmelt:	
CC	land use
TT	land use
Soil water and evapotranspiration	
FC	soil type, landuse
LP	soil type
β	soil type,landuse

The second group of parameters are related to the runoff response process at the subcatchment level. Since the runoff response module consists of a series of fictitious reservoirs, its parameters are not physically measurable. Therefore, it is hardly possible to tell which catchment descriptors have an influence on the parameters. Each of the model parameters of this module, p_k, are initially associated with all the catchment descriptors using a transfer function *G* as:

$$p_k = G_{pk}(l_i, s_j, A, \hat{S}, SF; i = 1,..., I, j = 1,...J) \qquad 4\text{-}1$$

where

l and *s* relative areas corresponding to different land use and soil type classes respectively.

I and *J* the number of land use classes and sol types respectively

k an index for the parameter (k = 1,…,N, where N is the number of parameters)

A area of the subcatchment

$\hat{S}$ average slope of the subcatchment

SF an index defined as the ratio between area of the catchment and the square of the distance from the outlet of the catchment to the farthest point in the catchment.

The transfer function G may take different forms. The most common form of the transfer function used for regional parameter estimation in hydrological applications is a multivariate linear function, which was used in this work. Accordingly, the transfer function has the form:

$$G_{pk}\left(l_i, s_j, A, \hat{S}, SF, i = 1,...,I, j = 1,...,J\right) = \sum_{i=1}^{I} \lambda_{ki} l_i + \sum_{j=1}^{J} \gamma_{kj} s_j + \psi_k A + \xi_k \hat{S} + \mu_k SF \qquad 4\text{-}2$$

where

λ_{ki} parameter of the transfer function relating land use class i with the k^{th} model parameter

γ_{kj} parameter of the transfer function relating soil class j with the k^{th} model parameter

ψ_k parameter of the transfer function relating the size of the subcatchment with the k^{th} model parameter.

ξ_k parameter of the transfer function relating the average slope of the subcatchment with the k^{th} model parameter.

μ_k parameter of the transfer function relating the shape of the subcatchment with the k^{th} model parameter.

4.2.2 Estimation of the parameters of the transfer function

The parameters of the transfer function in equation 4-2 are the characteristic values that relate the different catchment attributes with the model parameters and each of them has a constant value throughout the study area. The actual value of each of the model parameters corresponding to a given subcatchment depends solely on the catchment attributes, which are usually available in digital form. The objective of model calibration is therefore to estimate

the parameters of the transfer function that lead to optimum performance of the model in all subcatchments within the study area.

Table 4.2 Ranges of catchment attributes used for parameter regionalization in the calibration and validation set of subcatchments

Catchment attribute	Calibration set		Validation set	
	Max.(%)	Min. (%)	Max. (%)	Min. (%)
Land use class (%)				
Forest	69.2	14.6	76.6	10.1
Urban	34.0	8.0	49.5	8.3
Agricultural	69.7	14.3	73.2	5.6
Water bodies	1.1	0.0	1.2	0.0
Soil type (%)				
Lithosol	18.7	0.0	16.3	0.0
Ranker	18.0	0.0	13.1	0.0
Gleysol + Rendzina	50.3	0.0	22.7	0.0
Cambisol	87.9	8.6	100.0	0.0
Luvisol	67.4	1.8	87.8	0.0
Podzol	31.7	0.0	15.0	0.0
Mean slope (%)	3.75	0.6	3.51	0.44
Shape factor (-)	1.35	0.13	1.33	0.18
Area (km^2)	2879.0	507.0	2009.0	107.0

In order to estimate the parameters of the transfer function that can be applied to the entire study area, the model should be calibrated simultaneously for many subcatchments within the study area with contrasting catchment attributes so that all possible ranges of the different catchment attributes are considered. Thirty subcatchments from different parts of the study area were selected in this study as a set of calibration subcatchments to estimate the parameters. The parameters estimated by calibrating the model for this set of subcatchments

were subsequently validated by applying them in the remaining subcatchments, which constitute a validation set of subcatchments. Table 4.2 shows the ranges of the different catchment attributes that are used for regionalization of the model parameters in the calibration and validation sets of subcatchments.

As calibration of rainfall-runoff models is a process to seek a set of model parameters that leads to the best matching between the model simulated and the observed catchment responses, the objective of the model calibration was to minimise the sum of the square of the differences between the model simulated and the observed discharges from each of the subcatchments that constitute the calibration set. Therefore, an objective function O_m was defined, which needs to be minimised:

$$O_m = \frac{1}{N}\sum_{i=1}^{N} w(t_i)\left(Q_c(t_i) - Q_0(t_i)\right)^2 \qquad 4\text{-}3$$

where

O_m objective function for subcatchment m

$Q_c(t_i)$ model simulated discharge at time step i

$Q_o(t_i)$ observed discharge at time step i

$w(t_i)$ a weight that gives emphasis to certain attributes of the discharge hydrograph at time step i

N number of time steps in the calibration period

The weight $w(t_i)$ used in this work is the observed discharge at time step t_i to give more weight to estimation of the higher flows, as it is more important to capture them.

The model is calibrated for all subcatchments in the calibration set simultaneously and therefore, there are as many objective functions as the number of subcatchments. These objective functions need to be aggregated into a single objective function to simplify handling of the optimisation problem.

The subcatchments that constitute the calibration set may have different sizes or the effective rainfall that produces runoff within different subcatchments may be different due to the spatial non-uniformity of rainfall and therefore the scale of the discharges coming from them may be different. Therefore it would be difficult to use the objective function given in

equation 4-3 to inter-compare the model performances in different subcatchments. In order to avoid this scale inconsistency, equation 4-3 was normalized by the weighted variance of the observed discharge from each subcatchment and a weighted form of the commonly used model efficiency measure, the Nash-Sutcliffe coefficient (Nash and Sutcliffe, 1970), was introduced:

$$R_m^2 = 1 - \frac{\sum_{i=1}^{N} w(t_i)(Q_c(t_i) - Q_o(t_i))^2}{\sum_{i=1}^{N} w(t_i)(Q_o(t_i) - \overline{Q_o})^2} \qquad 4\text{-}4$$

where

R_m^2 the weighted Nash-Sutcliffe coefficient for subcatchment *m*

$\overline{Q_o}$ the mean observed discharge over t_i, $i=1,\ldots,N$

R_m^2 can have a maximum value of 1.0 for a perfect match between the model simulated and the observed discharge hydrographs and it can have a negative value for poorly simulated discharge. The model calibration should therefore be performed to maximise R_m^2.

There are as many objective functions as the number of subcatchments to be calibrated simultaneously and there is a need to aggregate them into one objective function to simplify the optimisation process. A possible aggregation technique is to sum up the Nash-Sutcliffe coefficients in the subcatchments making up the calibration set and maximise the resulting sum:

$$O = \sum_{m=1}^{M} R_m^2 \rightarrow \max \qquad 4\text{-}5$$

However, this aggregated objective function only measures the average performance of the model over all the subcatchments. A poor performance of the model in some subcatchments might be offset by a good performance in other subcatchments. Therefore, the aggregated objective function was modified in such a way that much emphasis is given to the R_m^2 value of the subcatchment in which the model performance is the worst:

$$O = \sum_{m=1}^{M} R_m^2 + M \min R_m^2 \rightarrow \max \qquad 4\text{-}6$$

where M is the number of subcatchments used for simultaneous calibration.

The model calibration procedure adapted in this work followed the automatic parameter estimation technique. Numerical optimization was implemented to estimate optimum values of the parameters of the transfer function by maximizing the objective function given in equation 4-6. Due to its robustness and reliability in handling difficult non-linear optimization problems, the Generalized Reduced Gradient algorithm (Lasdon, et.al., 1978; Lasdon and Waren, 1979) was used. Like any other non-linear optimisation algorithm, however, this method doesn't guarantee finding a global optimum solution in case where there are distinct local optima, which is the case in rainfall-runoff models attributed to their highly non-linear behaviour. One way to check if the global optimum has been achieved is to vary some of the parameters at the estimated optimum set and see if a new optimum set would be obtained by further continuing the optimisation process.

Table 4.3 Constraints imposed on the parameters of the runoff generation routines

Model parameter	Range	Other constraints
Snow accumulation and melt:		
CC_0 (mm/°C/day)	0.5 – 5	$CC_0(forest) \le CC_0(agricultural) \le CC_0(urban)$
C_{max} (mm/°C/day)	10	
k (-)	0 – 0.5	
TT (°C)	-2 – 1	
Evapotranspiration:		
$C_{ET}(°C^{-1})$	0 – 0.5	
Soil parameters:		
β (-)	1.0 – 5.0	
P_{thr}(mm/day)	10.0 – 50.0	
Ψ_{seal}(-)	0.0 – 1.0	
Landuse multiplier for β	0.5 – 1.5	$\beta(urban) \le \beta(agricultural) \le \beta(forest)$

Appropriate constraints were put on the ranges of the parameters of the transfer function based on previous modeling experience on the ranges of the actual model parameters. Besides, other physically meaningful constraints were put on some of the parameters. For example, the degree-day factor in forest should be less than in urban areas and the soil parameter β, which controls the runoff coefficient, should be larger in forest areas than agricultural areas. Table 4.3 shows the constraints imposed on the parameters of the runoff generation routines and table 4.4 shows the constraints applied to the parameters of the transfer functions corresponding to the runoff response routines.

Table 4.4 Constraints applied to the parameters of the transfer function corresponding to the runoff response routine

Model parameter	Range of parameters of the transfer function
α [-]	0.0 – 1.0
k_1 [1/day]	0.01 – 0.1
k_2 [1/day]	5×10^{-5} – 0.1
perc [1/day]	10^{-6} – 10^{-3}
MAXBAS [hours]	2 – 48

4.2.3 Application of the calibration procedure

The standard split sampling model calibration procedure was followed and the model calibration period runs from 1980 to 1988. The subsequent period until 1995 was used to validate the calibrated model. In order to minimize the effect of the initial states of the subcatchments on the model performance, the first six months were used as a warm up period and the model simulation results during this period were not used to judge the model performance.

The meteorological conditions in different parts of the study area for the calibration and validation periods are summarized in table 4.5. As can be seen in the table, the mean daily temperature in the validation period is slightly higher than that of the calibration period in all parts of the study area. The difference in the mean daily temperature between the validation

and calibration periods ranges between 0.83 °C in the Neckar basin and 1°C in the Nahe catchment. The stronger increase is on the minimum mean daily temperature than the maximum mean daily temperature. On the other hand, the mean daily precipitation over the validation period in different parts of the study area is between 3.5% and 10% less than the corresponding value in the calibration period. The highest difference is in the Neckar catchment while the lowest is in the Lippe catchment. Similarly, the mean annual number of dry days (here defined as days with precipitation less than 1.0 mm) is larger in the validation period than in the calibration period. The variability of both the daily mean temperature and the daily amount of precipitation are more or less similar in the calibration and validation periods, with both variables showing only slightly more variability in the calibration period. In general, the validation period is a bit warmer and drier than the calibration period.

In order to properly model the magnitude and the time distribution of flood flows from a catchment, rainfall series of higher time resolution is required, since high rainfall intensities over shorter periods have a significant effect on the peak of a flood. However, only daily records of meteorological data are available from observation stations for this study. Different methods of disaggregating the daily amount of rainfall into finer time resolution, such as hourly series, are widely used. The simplest method, which doesn't require any additional information, is to evenly distribute the daily amount throughout the day. However, storm events that cause flood may have only a limited duration within the day with higher intensity, which has a very important implication on the magnitude of the peak of the flood. Other methods that take into account the variability of precipitation at finer time scales are also available. Most of these methods are stochastic in their nature. They include methods that are based on fitting theoretical probability distribution functions to attributes of the precipitation such as the number of events per day, starting time of an event within a day, event duration and event volume (Econopouly, et al., 1990; Connolly et al., 1998). But these approaches need additional information from observations made at the required time resolution at one or more observation stations. Since this information was not available for this study, the first approach, i.e., disaggregation of the daily amount by uniformly distributing it throughout the day, was implemented and the model was run at a time step of 1 hour.

Table 4.5 Summary of the meteorological variables in the calibration and validation periods in the study area

River basin	Calibration period								Validation period							
	Mean daily temperature				Daily amount of precipitation			Mean ann.no. of dry days	Mean daily temperature				Daily amount of precipitation			Mean ann.no. of dry days
	min.	mean	max.	St. Dev.	mean	max.	St. Dev.		min.	mean	max.	St. Dev.	mean	max	St. Dev.	
Neckar	-18.46	8.50	27.09	7.59	2.67	46.84	4.50	204	-11.20	9.33	26.36	7.06	2.39	45.63	4.24	213
Main	-16.07	8.28	26.76	7.74	2.29	31.14	3.80	206	-11.66	9.23	26.77	7.29	2.10	49.59	3.74	219
Ruhr	-15.07	8.17	24.62	7.03	3.25	51.33	5.26	189	-10.62	9.08	26.73	6.65	3.03	46.66	5.25	204
Lahn	-14.36	8.23	24.58	7.36	2.47	50.12	4.30	205	-10.32	9.16	27.03	7.03	2.24	36.39	4.13	225
Mosel	-14.46	8.67	25.46	7.15	2.67	33.62	4.35	199	-11.12	9.62	26.48	6.87	2.41	43.46	4.23	215
Lippe	-15.07	9.21	25.67	7.01	2.33	59.35	4.00	205	-9.36	10.06	27.63	6.57	2.25	30.44	3.96	218
nahe	-14.93	8.51	25.24	7.32	2.26	32.51	4.00	217	-11.17	9.51	26.52	7.02	2.05	41.80	3.80	227
Sieg	-14.24	8.47	24.67	7.11	3.35	62.04	5.55	192	-10.45	9.41	26.80	6.81	3.03	56.81	5.50	210
Erft	-12.41	9.61	25.49	6.94	2.24	36.98	3.72	202	-10.29	10.56	27.26	6.59	2.02	33.60	3.58	222

The model was calibrated with the dual objective of simulating the observed daily discharge and preserving the mean runoff over longer periods. This was achieved by a simultaneous calibration of the model for the daily, 2 days total, 4 days total, 7 days total, and 15 days total discharges. This means, multiple objectives were considered to calibrate the model. For each subcatchment, the objective function to be optimized is then the arithmetic sum of the Nash-Sutcliffe coefficients corresponding to the discharges at the different time scales. The aggregated objective function used to calibrate the entire calibration set of subcatchments is related to the objective function of each of the subcatchments using equation 4-6.

For time scales greater than 1 day, the comparison of the observed and the model simulated discharges was done on the basis of a moving time window. That is, for a given time scale, the total discharges for consecutive time steps are calculated over the same number of days but each of them shifted by only one day. This can be mathematically expressed as:

$$QT_N(t_i) = \sum_{j=1}^{N} Q(t_{i-j+1}) \quad \text{for } i \geq N \qquad 4\text{-}7$$

where

$QT_N(t_i)$ the N day total discharge at time step t_i

$Q(t_i)$ the daily discharge at time step t_i

Tables 4.6 - 4.8 show the optimum model parameters for the distributed runoff generation processes corresponding to the catchment descriptors they are regionalized on. The parameters shown in table 4.6 are for those runoff generation processes related to land use.

As the rate of snowmelt tends to be faster in urban areas and slower in forests, the parameters of the snow accumulation and melt process were regionalized based on land use. However, regionalizing all the parameters of the routine to the different land use classes would lead to over parameterisation of the model and therefore the limiting value of the degree-day factor (C_{max}), the rate of increase of the degree-day factor with precipitation amount (k), and the threshold temperature (TT) were left to be constant for all land use classes. Similarly, the adjustment parameter of the evapotranspiration for temperature anomalies (C_{ET}) was also set a constant for all land use classes.

Table 4.6 Calibrated regional values of the parameters of the runoff generation processes that are mainly related to land use.

Model parameter	Land use		
	Forest	Urban	Agricultural
Snow accumulation and melt:			
CC_0 (mm/°C/day)	2.2	2.95	2.2
C_{max} (mm/°C/day)	7.5	7.5	7.5
k (-)	0.15	0.15	0.15
TT (°C)	0	0	0
Evapotranspiration:			
$C_{ET}(°C^{-1})$	0.15	0.15	0.15

The parameters shown in table 4.7 pertain to the runoff generation processes that are mainly dependent on the soil type. As land use, in addition to the soil type, influences the runoff coefficient, the soil parameter β, which relates the amount of precipitation or snowmelt with the portion that is converted to runoff was regionalized based on both soil type and land use. In order to reduce the number of parameters, a multiplier of the values of the parameter corresponding to the different soil types (table 4.7), was introduced whose value is dependent on the land use class. Infiltration tends to be higher in forest-covered soil due to the development of root channels within the soil and earthworm activities. On the other hand, due to the presence of sealed areas, infiltration in urban areas is lower. Therefore the multiplier is constrained in such a way that this effect is taken account of. From equation 3-3 it can be seen that a higher value of β is associated with higher infiltration and therefore the land use multiplier for this parameter should be higher for forest and lower for urban areas. Table 4.8 shows the calibrated values of the multiplier for the different land use classes under this constraint. The parameters introduced in the modification of the infiltration process for higher precipitation intensity, P_{thr} and Ψ_{seal} were left to have the same value each for all soil types in order to avoid over parameterisation of the model.

The parameters discussed so far are related to the distributed runoff generation processes, which were obtained after a simultaneous calibration of the model for the calibration set of subcatchments. The remaining model parameters pertain to the lumped runoff response

process and they are related to the different catchment descriptors through the parameters of the transfer function using equation 4-2.

Table 4.7 Calibrated regional values of the parameters of the runoff generation processes that are mainly related to soil type.

Model parameter	Soil type					
	Lithosol	Ranker	Gleysol	Cambisol	Luvisol	Podzol
β (-)	1.45	2	2.06	1.7	1.85	2
P_{thr}(mm/day)	40	40	40	40	40	40
Ψ_{seal}(-)	0.3	0.3	0.3	0.3	0.3	0.3

Table 4.8 Calibrated land use adjustment factors for soil parameter β

Parameter	Land use		
	Forest	Urban	Agricultural
Land use multiplier for β	1.17	0.825	1

The three parameters of the runoff concentration process pertaining to outflows from the upper and lower reservoirs; α, k_1, and k_2 were all initially regionalized based on all the catchment descriptors. A sensitivity study of the parameters with respect to the different catchment descriptors, however, showed that the parameter α is less sensitive to the size, slope, and shape factor of the subcatchments than the land use and soil types. Therefore, in order to reduce the number of parameters, this parameter was regionalized based only on soil type and land use. The percolation parameter, *perc*, was regionalized based on soil type, as the process takes place in the lower soil zone and is more dependent on the soil type or the geology, even though the model considers this differently. The smoothing function of the generated runoff, *MAXBAS*, was set as a function of the size, shape, and mean slope of the catchment to keep the number of parameters a minimum. The optimum values of the parameters of the transfer functions for all the parameters of the runoff response process corresponding to the different catchment descriptors are shown in table 4.9.

Summary of the performance of the regionalized model in the calibration set of subcatchments during the calibration period (1980 – 1988) after the model was calibrated simultaneously for them is shown in table 4.10. The table shows the discharge weighted Nash-Sutcliffe coefficient, which is used as the objective function to calibrate the model; the relative accumulated difference between the model simulated and the observed discharges; and the peak error, which is an index used to judge whether the high flows are estimated well or not.

The relative accumulated difference is defined as:

$$rel-accdif = \frac{\sum_{i=1}^{N}(Q_c(t_i) - Q_o(t_i))}{\sum_{i=1}^{N} Q_o(t_i)} \qquad 4\text{-}8$$

where:

$Q_c(t_i)$	model simulated discharge at time step *i*
$Q_o(t_i)$	observed discharge at time step *i*
N	the number of time steps

Similarly, the peak error is defined based on the relative difference of the mean annual simulated and observed peak discharges:

$$peak-error = \frac{\overline{Q}_{c(\max)} - \overline{Q}_{o(\max)}}{\overline{Q}_{o(\max)}} \qquad 4\text{-}9$$

where:

$\overline{Q}_{c(\max)}$	mean annual simulated peak discharge
$\overline{Q}_{o(\max)}$	mean annual observed peak discharge

Table 4.9 Calibrated parameters of the transfer function relating the parameters of the lumped runoff response process with catchment descriptors

Model parameter	Catchment descriptor											
	Soil type [%]						Land use [%]			Area[$km^2 \times 10^3$]	Slope [%]	Shape [-]
	Lithosol	Ranker	Gleysol	Cambisol	Luvisol	Podzol	Forest	Urban	Agricultural			
α [-]	0.0415	0.047	0	0.214	0	0.023	0.027	0.107	0.062	-	-	-
k_1 [1/day]	0.013	0.033	0.017	0.094	0.013	0.093	0.0186	0.0282	0.027	0.0064*	0.0171	0.0142
k_2 [1/day]	4.4×10^{-4}	2×10^{-3}	10^{-3}	2×10^{-3}	2.7×10^{-3}	1.3×10^{-3}	1.3×10^{-3}	3×10^{-3}	2×10^{-3}	6.6×10^{-4}	2.7×10^{-3}	2×10^{-3}
perc [1/day]	2×10^{-5}	2.81×10^{-4}	1.67×10^{-4}	2.81×10^{-4}	2.08×10^{-4}	2.08×10^{-5}	-	-	-	-	-	-
MAXBAS [hours]	-	-	-	-	-	-	-	-	-	10	6.42	13.5

* The transfer function value is related to the inverse of the area

As can be seen in table 4.10, the weighted Nash-Sutcliffe coefficient for the simulation of the daily discharge in the calibration set of subcatchments during the calibration period has values ranging between 0.802 and 0.942, with a mean value of 0.874. This indicates a reasonably good performance of the model in all the calibration subcatchments. The highest value was obtained in the lower part of the Lippe catchment, while the lowest was in the Sauer subcatchment, which is a tributary of the Mosel. Figure 4.1 shows the scatter plot of the model simulated and the observed daily discharges in these subcatchments over the calibration period and figure 4.2 shows the simulated and observed daily discharge hydrographs for the same subcatchments for the year 1988, when one of the extreme floods in the Rhine was recorded.

There is no clear pattern on the underestimation or overestimation of the mean daily discharge over the calibration period. In some subcatchments, the mean daily discharge is underestimated by as much as 22%, while at the same time overestimation by up to a similar magnitude is noticed in some others.

Based on daily simulation, the mean annual peak discharge is, however, generally underestimated in most subcatchments. The maximum underestimation of the peak by about 30% is noticed in parts of the Mosel (see table 4.10). The model shows an overestimation of the peak discharge in some subcatchments in the lower region of the Main basin and the upper region of the Lippe.

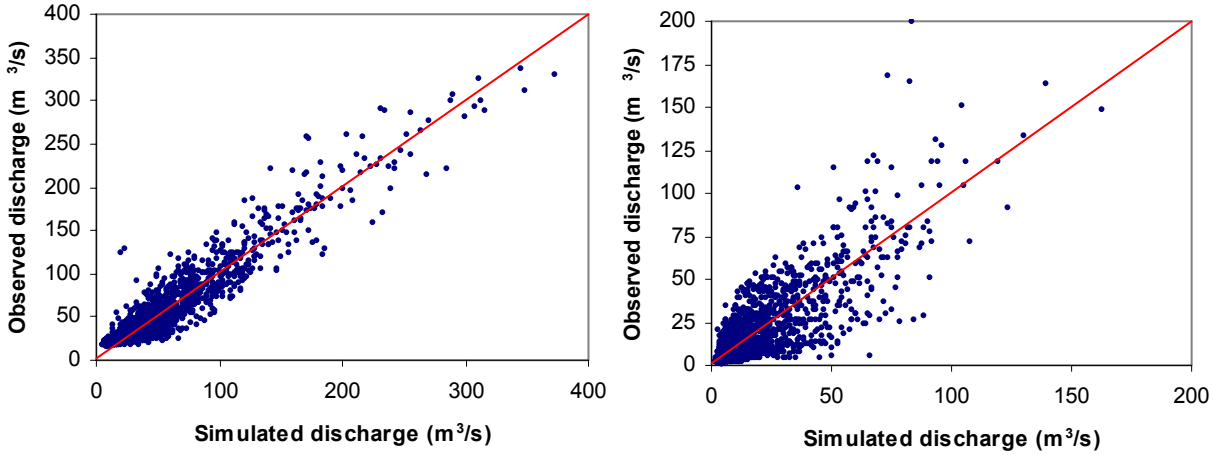

a) Schermbeck (Lippe), $R_m^2 = 0.942$ b) Michelau (Sauer), $R_m^2 = 0.802$

Figure 4.1 Scatter plots of the model simulated and the observed daily discharges over the model calibration period at gauges where the model performances are the best and the worst respectively.

Table 4.10 Performance measures of the regionalized model in the calibration set of subcatchments during the calibration period (1980-1988).

Gauge	River Basin	Drainage area [km^2]	Daily			4 days total over moving window		7 days total over moving window		15 days total over moving window	
			R_m^2	rel-accdif	Peak-error	R_m^2	Peak-error	R_m^2	Peak-error	R_m^2	Peak-error
Plochingen (Fils)	Neckar	706	0.901	-0.016	-0.209	0.927	-0.180	0.935	-0.175	0.940	-0.166
Neustadt (Rems)	Neckar	581	0.856	0.099	0.011	0.895	0.174	0.917	0.123	0.933	0.147
Stein (Kocher)	Neckar	1957	0.913	0.014	-0.099	0.945	-0.052	0.955	-0.092	0.963	-0.068
Untergriesheim (Jagst)	Neckar	1836	0.889	0.095	-0.203	0.924	-0.162	0.935	-0.163	0.944	-0.103
Pforzheim (Enz)	Neckar	1477	0.828	0.188	0.047	0.851	0.149	0.873	0.141	0.894	0.115
Schwuerbitz	Main	2426	0.843	-0.185	-0.235	0.854	-0.123	0.862	-0.131	0.865	-0.136
Kemmern	Main	4253	0.874	-0.155	-0.150	0.883	-0.090	0.889	-0.090	0.891	-0.090
Wolfsmuenster (Fraenkische saale)	Main	2131	0.921	-0.131	-0.071	0.931	-0.012	0.938	-0.025	0.942	-0.007
Waldenhausen (Tauber)	Main	1810	0.887	0.038	-0.282	0.930	-0.150	0.941	-0.080	0.949	0.015
Hanau (Kinzig)	Main	921	0.830	0.068	0.387	0.902	0.140	0.924	0.079	0.941	0.033
Bad Viebel (Nidda)	Main	1619	0.885	0.105	0.426	0.919	0.063	0.927	-0.026	0.932	-0.048
Marburg	Lahn	1666	0.877	-0.005	-0.009	0.929	0.084	0.946	0.048	0.955	-0.002
Asslar (Dill)	Lahn	717	0.849	-0.012	-0.079	0.914	0.066	0.935	0.072	0.953	0.028
Kalkofen	Lahn	5304	0.918	0.077	0.080	0.933	0.103	0.942	0.113	0.950	0.099
Nalbach (Prims)	Mosel	734	0.891	-0.124	0.011	0.905	0.121	0.915	0.056	0.924	-0.009
Michelau (Sauer)	Mosel	933	0.802	-0.061	-0.101	0.842	-0.134	0.866	-0.124	0.899	-0.177
Gemuend (Our)	Mosel	613	0.851	-0.040	-0.303	0.872	-0.222	0.886	-0.228	0.908	-0.207
Bollendorf (Sauer)	Mosel	3222	0.894	0.158	-0.091	0.908	-0.003	0.919	0.056	0.934	0.011
Pruemzurlay (Pruem)	Mosel	574	0.890	0.089	-0.201	0.910	-0.076	0.925	-0.036	0.942	0.009
Alsdorf-Oberecken (Nims)	Mosel	264	0.858	0.058	-0.117	0.894	0.062	0.915	0.132	0.936	0.120
Kordel (Kyll)	Mosel	817	0.897	0.089	-0.077	0.918	-0.002	0.926	0.057	0.935	0.079
Platten (Lieser)	Mosel	377	0.867	0.157	0.000	0.890	0.113	0.902	0.129	0.916	0.144
Lippstadt	Lippe	1394	0.805	-0.221	0.185	0.816	0.060	0.827	0.038	0.836	-0.047
Haltern	Lippe	4273	0.938	0.062	-0.174	0.950	-0.096	0.954	-0.085	0.956	-0.104
Schermbeck	Lippe	4783	0.942	0.062	-0.087	0.951	-0.004	0.956	0.005	0.960	-0.028
Martinstein	Nahe	1435	0.861	0.047	-0.167	0.902	-0.017	0.913	-0.005	0.922	0.010
Boos	Nahe	2832	0.831	0.226	0.031	0.860	0.125	0.872	0.123	0.883	0.129
Grolsheim	Nahe	4013	0.871	0.168	-0.150	0.900	-0.084	0.906	-0.084	0.910	-0.058

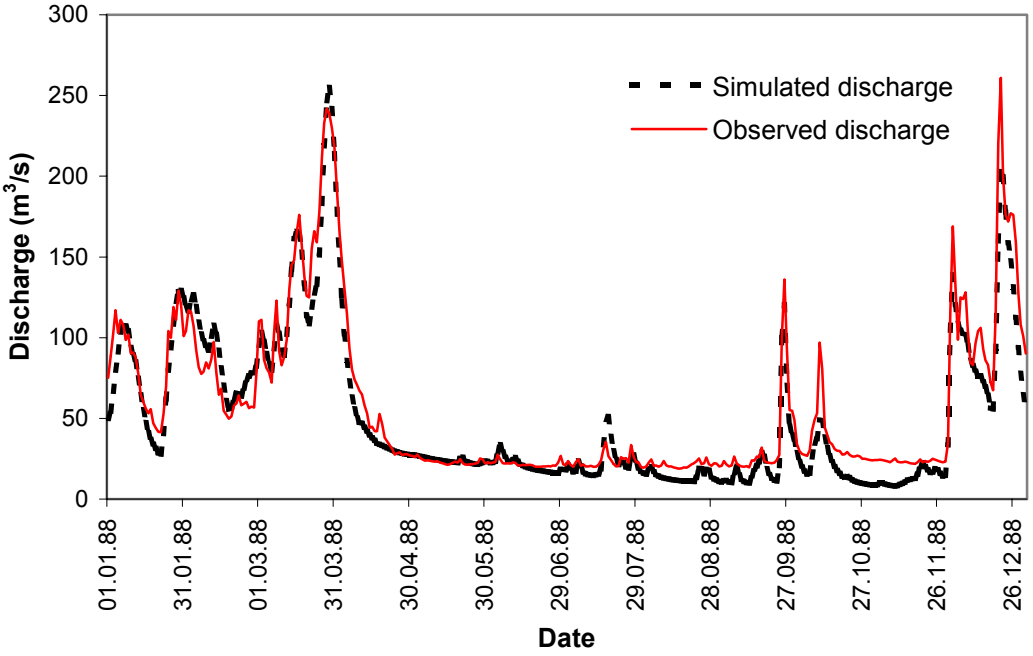

a) Schermbeck (Lippe)

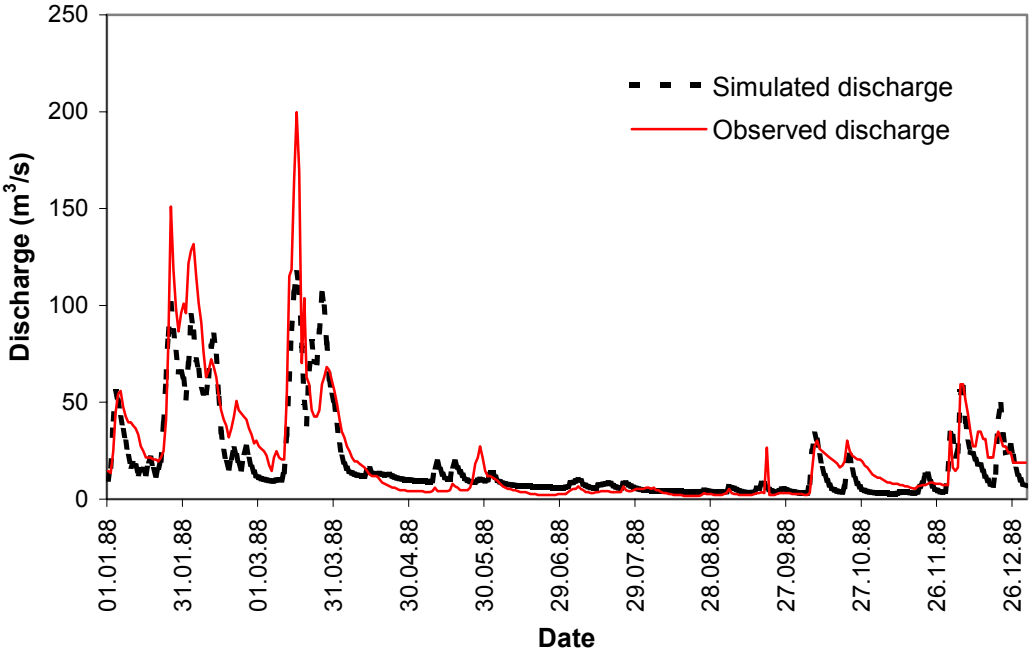

b) Michelau (Sauer)

Figure 4.2 Simulated and observed daily discharge hydrographs at two of the gauges located in the calibration set of subcatchments over the year in which there was an extreme flood event.

Simulation of the aggregated discharge for larger time scales clearly shows an improvement in the model performance measures, as can be seen in table 4.10, which also shows summary of the model performance in simulating the 4 days, 7 days and 15 days total discharges over moving windows. The Nash-Sutcliffe coefficient is seen to progressively increase with the time scale. Generally, estimation of the peak of the aggregated mean discharge is also noticed to improve for higher time scales, although there are still some outliers from this general trend. Since the relative bias is scale invariant, it doesn't show any change.

4.2.4 Validation of the regionalized model

Validation of the regionalized model was performed in two ways. The first approach follows the standard split sampling method, in which the available discharge observation is split in to two series and model calibration is performed on one of the series while the other series is latter used to validate the calibrated model. This approach was used to validate the model in the calibration set of subcatchments for which there is enough observed discharge data beyond the calibration period. Summary of the performance of the regionalized model in this set of subcatchments during the validation period is shown in table 4.11, which shows performance of the model at different time scales at gauging stations for which at least a four years data is available beyond the calibration period.

The validation result shows that the performance of the regionalized model in terms of the weighted Nash-Sutcliffe efficiency measure is more or less similar to that of the calibration period. However, the mean daily discharge appears to be a bit overestimated in most of the subcatchments, while the mean annual peak discharge is more underestimated in the validation period. Exceptions are those subcatchments with in the Main basin, in which there is some improvement in all performance measures; and the Lahn basin, in which there is some improvement in the estimation of the mean annual peak discharge. Scatter plots of the observed and the model simulated daily discharges for subcatchments in which the model performances in terms of the Nash-Sutcliffe coefficient are the highest and the lowest during the validation period are shown in figure 4.3. Comparison of the simulated and observed daily discharge hydrographs in the same subcatchments for the year 1995 is shown in figure 4.4.

A similar observation in the performance of the model at higher time scales as in the case of the calibration period is notice, as one can see in table 4.11.

Table 4.11 Performance of the regionalized model in the calibration set of subcatchments during the validation period.

Gauge	River Basin	Drainage area [km^2]	Daily			4 days total over moving window		7 days total over moving window		15 days total over moving window		Validation period
			R_m^2	rel-accdif	Peak-error	R_m^2	Peak-error	R_m^2	Peak-error	R_m^2	Peak-error	
Plochingen (Fils)	Neckar	706	0.895	0.012	-0.330	0.936	-0.125	0.941	-0.097	0.944	-0.090	1989 - 1995
Neustadt (Rems)	Neckar	581	0.863	0.150	-0.223	0.894	0.096	0.897	0.162	0.897	0.162	1989 - 1995
Stein (Kocher)	Neckar	1957	0.877	0.109	-0.221	0.912	-0.010	0.919	0.026	0.926	0.014	1989 - 1995
Untergriesheim (Jagst)	Neckar	1836	0.870	0.184	-0.319	0.922	-0.114	0.932	-0.021	0.935	0.008	1989 - 1995
Pforzheim (Enz)	Neckar	1477	0.859	0.153	-0.014	0.872	0.172	0.886	0.162	0.903	0.126	1989 - 1995
Schwuerbitz	Main	2426	0.915	-0.141	-0.162	0.927	-0.034	0.937	-0.113	0.942	-0.133	1989 - 1995
Kemmern	Main	4253	0.923	-0.108	-0.002	0.937	0.032	0.947	-0.065	0.953	-0.081	1989 - 1995
Wolfsmuenster (Fraenkische saale)	Main	2131	0.943	-0.060	0.061	0.956	0.114	0.967	0.042	0.976	0.038	1989 - 1995
Asslar (Dill)	Lahn	717	0.808	0.108	0.087	0.887	0.238	0.927	0.129	0.958	0.056	1989 - 1995
Kalkofen	Lahn	5304	0.900	0.175	0.069	0.921	0.176	0.938	0.087	0.953	0.076	1989 - 1995
Pruemzurlay (Pruem)	Mosel	574	0.909	0.123	-0.330	0.940	-0.160	0.951	-0.136	0.959	-0.121	1989 - 1995
Grolsheim	Nahe	4013	0.863	0.359	-0.201	0.894	-0.141	0.910	-0.103	0.931	-0.082	1989 - 1992

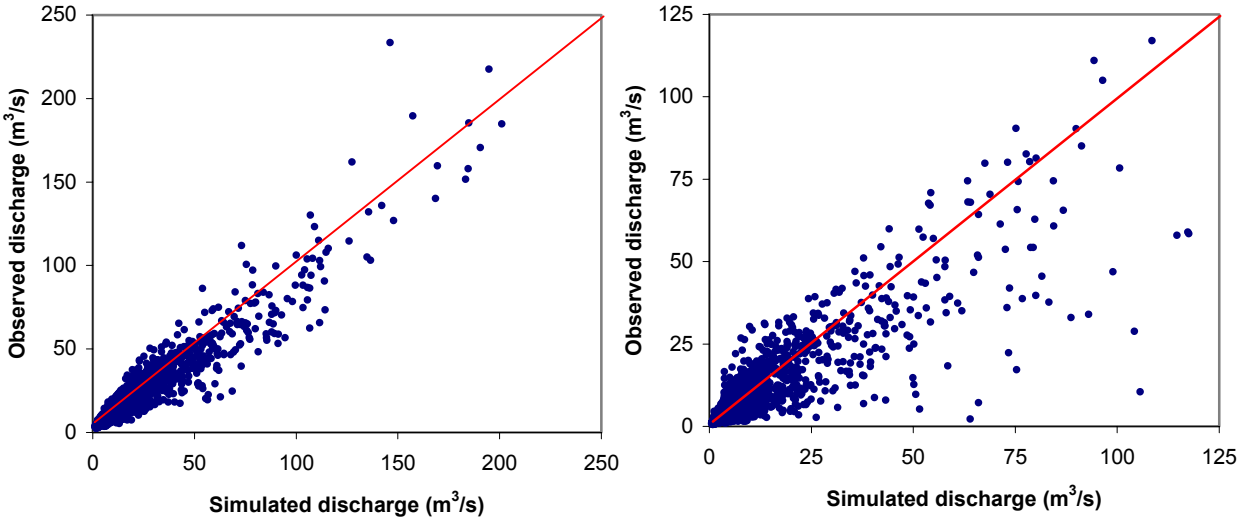

a) Wolfsmuenster (Main), $R_m^2 = 0.943$ b) Asslar (Lahn), $R_m^2 = 0.808$

Figure 4.3 Scatter plots of the model simulated and the observed daily discharges over the model validation period at gauges where the model performances are the best and the worst respectively.

The second approach of validating the regionalized model consists of applying the regional relationship between the model parameters and the catchment descriptors derived in the calibration set of subcatchments to the other subcatchments within the study area that were not used to derive the regional relationship. These subcatchments constitute a validation set of subcatchments. This approach is the most important part of the model validation exercise in this particular work. As the core objective of the methodology implemented here is to derive a regional relationship between the model parameters and the catchment descriptors, which can later be used to predict the runoff from ungauged catchments, one should test whether the relationships established are valid by testing their applicability to subcatchments that were not used in deriving the relationship between the model parameters and the catchment descriptors. This approach, therefore, is a crucial step in validating the methodology as a whole.

Performance of the regionalized model in the validation set of subcatchments was evaluated separately for the calibration and validation periods used in the calibration set of subcatchments so that comparison of the performance of the model in the calibration set and

the validation set of subcatchments can be compared over similar periods of model simulation.

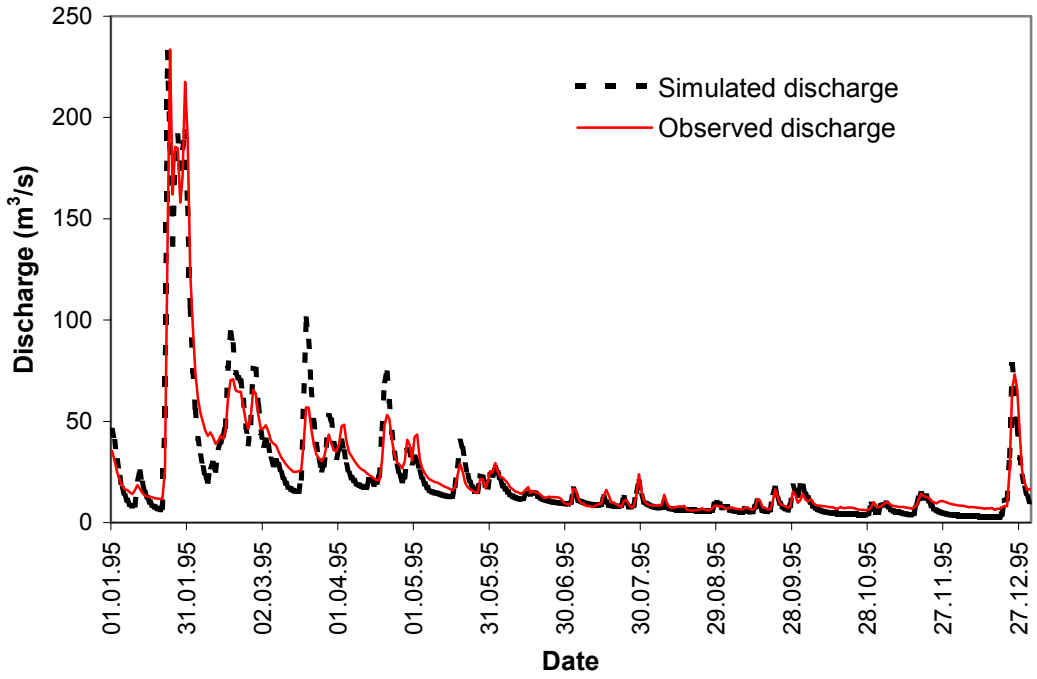

a) Wolfsmuenster (Main)

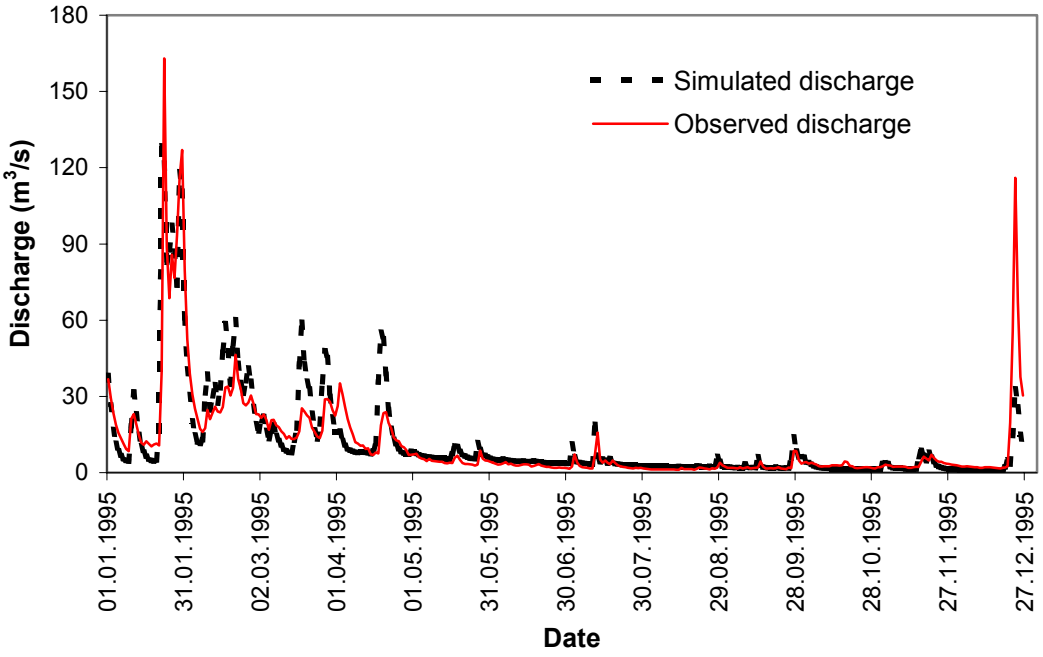

b) Asslar (Lahn)

Figure 4.4 Simulated and observed hydrographs at selected gauges in the calibration set of subcatchments in the validation period.

Table 4.12 shows a summary of the performance of the regionalized model when applied to the validation set of subcatchments during the calibration period. The weighted Nash-Sutcliffe coefficient for the daily simulation at all the gauging stations within the validation set during the calibration period shows values above 0.83, with an average value of 0.88. This is without considering subcatchments within the Erft catchment, in which the regionalized model performance is generally very poor with even a negative value of the Nash-Sutcliffe coefficient. This ill-performance of the regionalized model in this part of the study area is attributed to the extensive coal mining practice within the basin, which has an important implication on the runoff generation dynamics. The parameter estimation approach implemented in this work doesn't consider land use classes other than forest, urban, and agricultural. A mining activity leads to introduction of a different runoff generation dynamics within the catchment, which is not considered in the land use classes used to regionalize the model parameters. Therefore, the model is not suitable for modelling the runoff from catchments where activities that lead to a different runoff generation dynamics are taking place.

The mean daily discharge is estimated reasonably well in all the validation subcatchments during the calibration period except in those within the Main basin, where it is generally underestimated. The mean annual peak discharge is also estimated better in the validation set of subcatchments than in the calibration set, although the general trend is still underestimation of the peak. The scatter plots of the simulated and the observed daily discharges in the upper part of the Ruhr basin and the lower part of the Neckar basin over the calibration period are shown in figure 4.5. Also figure 4.6 shows the corresponding simulated and the observed daily discharge hydrographs using meteorological data of the year 1988. From the scatter plots and figure 4.6, it can be seen that the lower peak discharges are generally overestimated by the regionalized model, while the extremely high peak flood flows are underestimated. This observation is not limited to the specific gauges for which comparisons are shown in the figures, but also applies to all gauges shown in table 4.12.

The performance of the regionalized model in the validation subcatchments during the validation period in terms of the Nash-Sutcliffe coefficient shows only a slight difference from its performance during the calibration period. It shows a slight improvement in subcatchments in the Ruhr and Main catchments while it shows slightly less value at Gauge Rockenau in the Neckar catchment. The relative bias between the simulated and the observed

daily discharges remains more or less the same in the two periods except at gauges in the lower part of the Main basin, at which a slight improvement in the bias is observed in the validation period. Similarly, a slight over estimation of the mean annual peak discharge is observed in subcatchments in the Main basin during the validation period. These are summarized in table 4.13. Figure 4.7 shows scatter plots of the simulated and the observed daily discharges over the validation period at Gauge Steinbach in the Main catchment and Gauge Villigst in the Rhur catchment. Figure 4.8 also shows the simulated and the observed daily discharge hydrographs at the same gauges for the year 1995.

Regarding modelling of runoff at higher time scales, the performance of the model in terms of the Nash-Sutcliffe coefficient shows a similar trend as in the calibration set of subcatchments. The performance shows improvement with increasing time scale. The performance in terms of estimating the peak of the aggregated mean runoff, however, doesn't show any clear trend of improvement with increasing time scale as was observed in the calibration set. One can notice in tables 4.12 and 4.13 that it is even more underestimated at higher time scales in some cases.

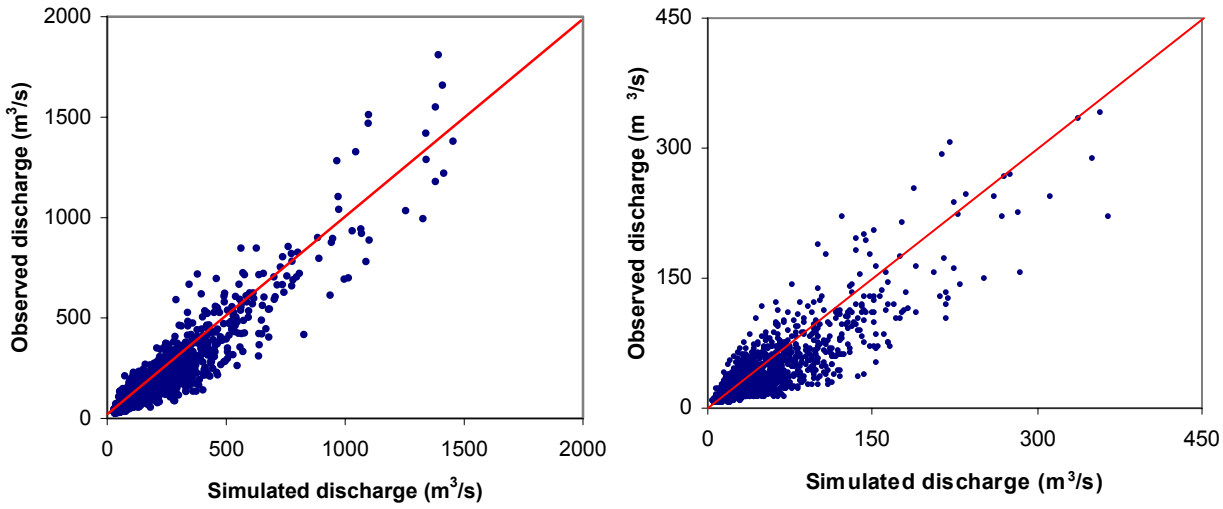

a) Rockenau (Neckar), $R_m^2 = 0.926$ b) Villigst (Ruhr), $R_m^2 = 0.835$

Figure 4.5 Scatter plots of the model simulated and the observed daily discharges at selected gauges in the validation set of subcatchments over the calibration period.

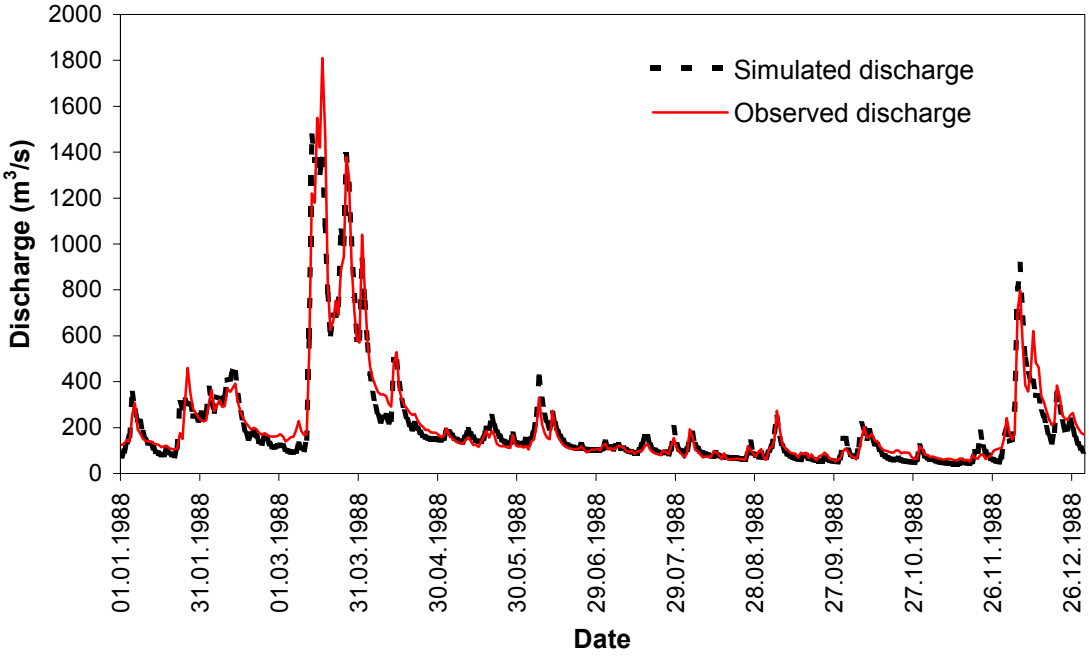

a) Rockenau (Neckar)

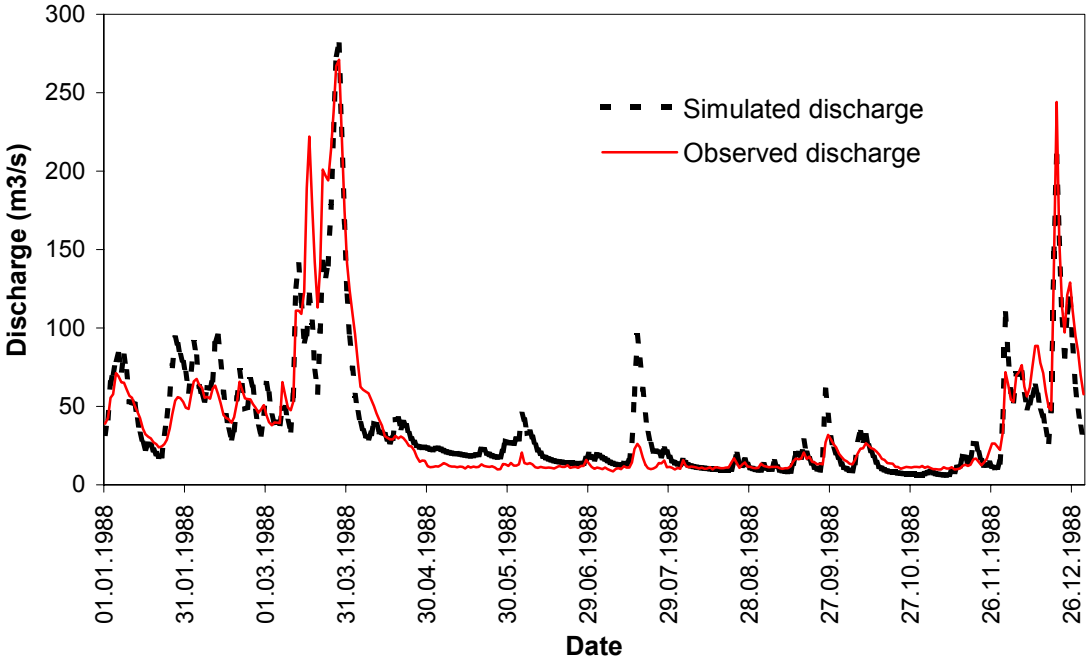

b) Villigst (Ruhr)

Figure 4.6 Model simulated and observed daily discharges at two gauges from the validation set of subcatchments in the calibration period.

Table 4.12 Performance of the regionalized model in the validation set of subcatchments during the calibration period.

Gauge	River Basin	Drainage area [km^2]	Daily			4 days moving average		7 days moving average		15 days moving average		Simulation period
			R_m^2	rel-accdif	Peak-error	R_m^2	Peak-error	R_m^2	Peak-error	R_m^2	Peak-error	
Villigst	Ruhr	2009	0.835	0.064	-0.053	0.851	-0.044	0.872	-0.084	0.894	-0.116	1980 - 1988
Hagen-Hohenlimburg (Lenne)	Ruhr	1322	0.844	-0.053	0.034	0.865	0.060	0.891	0.020	0.914	-0.064	1980 - 1988
Hattingen	Ruhr	4118	0.862	-0.005	-0.042	0.883	0.036	0.902	0.000	0.921	-0.057	1980 - 1988
Betzdorf	Sieg	755	0.873	0.014	-0.033	0.884	0.022	0.900	0.010	0.910	-0.068	1980 - 1988
Eitorf	Sieg	1468	0.897	-0.001	-0.026	0.907	-0.007	0.918	-0.011	0.925	-0.083	1980 - 1988
Lohmar	Sieg	820	0.884	0.019	-0.070	0.886	0.047	0.899	0.089	0.909	0.048	1980 - 1988
Menden	Sieg	2825	0.920	0.040	-0.051	0.922	-0.017	0.931	-0.005	0.938	-0.047	1980 - 1988
Rockenau	Neckar	12655	0.926	0.076	-0.064	0.941	-0.031	0.949	-0.034	0.955	-0.012	1980 - 1988
Trunstadt	Main	12010	0.875	-0.228	-0.076	0.883	-0.064	0.888	-0.074	0.890	-0.063	1980 - 1988
Schweinfurt	Main	12715	0.878	-0.225	-0.072	0.886	-0.071	0.893	-0.082	0.895	-0.063	1980 - 1988
Wuerzburg	Main	13979	0.879	-0.232	-0.061	0.887	-0.079	0.893	-0.077	0.894	-0.072	1980 - 1988
Steinbach	Main	17914	0.896	-0.166	-0.064	0.907	-0.079	0.918	-0.038	0.924	-0.036	1980 - 1988
Kleinheubach	Main	21505	0.907	-0.112	-0.044	0.920	-0.063	0.933	0.002	0.942	-0.005	1980 - 1988
Bliesheim	Erft	604	0.811	0.167	-0.221	0.835	-0.179	0.846	-0.146	0.863	-0.025	1980 - 1988
Neubrueck	Erft	1596	-5.306	-0.336	1.132	-5.292	0.925	-5.084	0.733	-4.707	0.469	1980 - 1988

Table 4.13 Performance of the regionalized model in the validation set of subcatchments during the validation period.

Gauge	River Basin	Drainage area [km^2]	Daily			4 days moving average		7 days moving average		15 days moving average		Simulation period
			R_m^2	rel-accdif	Peak-error	R_m^2	Peak-error	R_m^2	Peak-error	R_m^2	Peak-error	
Villigst	Ruhr	2009	0.867	0.072	-0.035	0.882	0.007	0.899	-0.095	0.914	-0.140	1989 - 1995
Hagen-Hohenlimburg (Lenne)	Ruhr	1322	0.884	0.028	0.153	0.904	0.180	0.929	0.019	0.952	-0.039	1989 - 1995
Hattingen	Ruhr	4118	0.914	0.038	0.041	0.930	0.089	0.945	-0.032	0.959	-0.084	1989 - 1995
Rockenau	Neckar	12655	0.894	0.061	-0.090	0.932	0.037	0.940	0.073	0.949	0.076	1989 - 1995
Trunstadt	Main	12010	0.885	-0.250	0.057	0.893	0.100	0.896	0.040	0.892	-0.009	1989 - 1995
Schweinfurt	Main	12715	0.895	-0.224	0.064	0.907	0.105	0.913	0.051	0.914	-0.007	1989 - 1995
Wuerzburg	Main	13979	0.881	-0.228	0.061	0.896	0.111	0.903	0.057	0.904	0.005	1989 - 1995
Steinbach	Main	17914	0.921	-0.098	0.135	0.933	0.131	0.944	0.103	0.953	0.065	1989 - 1995
Kleinheubach	Main	21505	0.923	-0.092	0.102	0.935	0.108	0.967	0.110	0.974	0.094	1989 - 1995
Bliesheim	Erft	604	0.718	0.191	-0.010	0.729	0.075	0.730	0.115	0.733	0.172	1989 - 1995
Neubrueck	Erft	1596	-1.329	-0.058	1.069	-1.170	1.063	-0.979	0.941	-0.729	0.765	1989 - 1993

One logical consideration in choosing catchments that are to be used to validate the regional relationship between the model parameters and the catchment descriptors is that the ranges of the catchment descriptors used to regionalize the model parameters within them should be within the corresponding ranges of the descriptors in the calibration set of subcatchments. As one can see in table 4.2, however, there are subcatchments in the validation set in which some of the descriptors are a bit outside their range in the calibration set. The performance of the regionalized model in such subcatchments was found to be promising, suggesting the possibility of applying the regional relationship for a slight extrapolation of the catchment descriptors outside the range within which they were derived. This can be seen in the subcatchments of the Ruhr catchment, in which the urban area proportion exceeds the maximum proportion of urban area in the calibration set of subcatchments. Similarly, the proportion of forest areas in some of the subcatchments of the Sieg catchment exceeds the corresponding proportion in the calibration set.

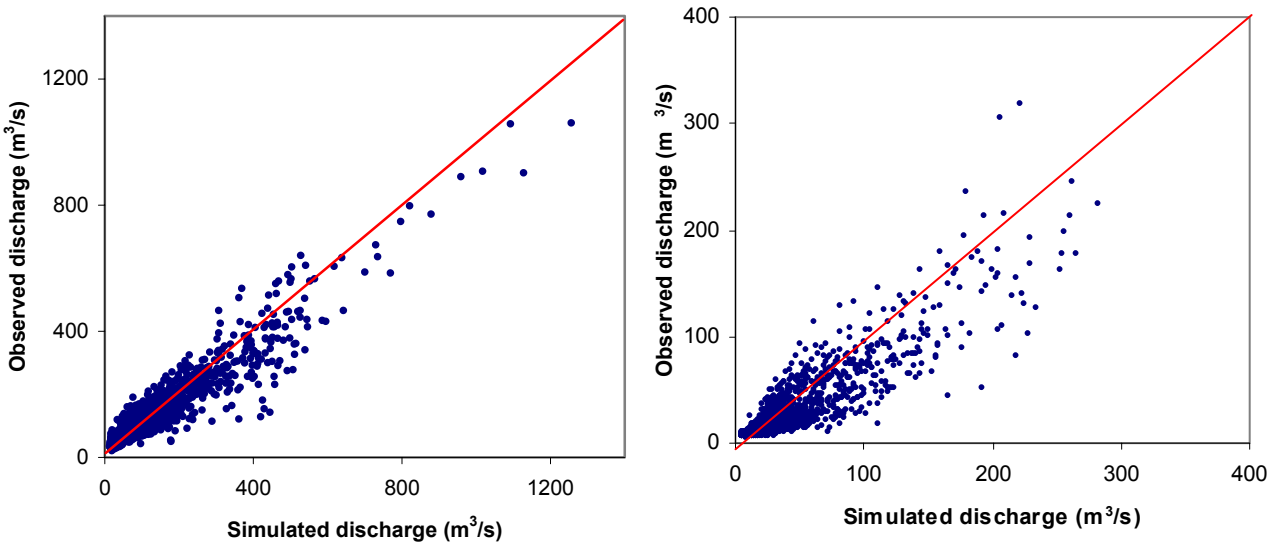

a) Steinbach (Main), $R_m^2 = 0.921$ b) Villigst (Ruhr), $R_m^2 = 0.867$

Figure 4.7 Scatter plots of the model simulated and observed daily discharges at selected gauges in the validation set of subcatchments over the validation period.

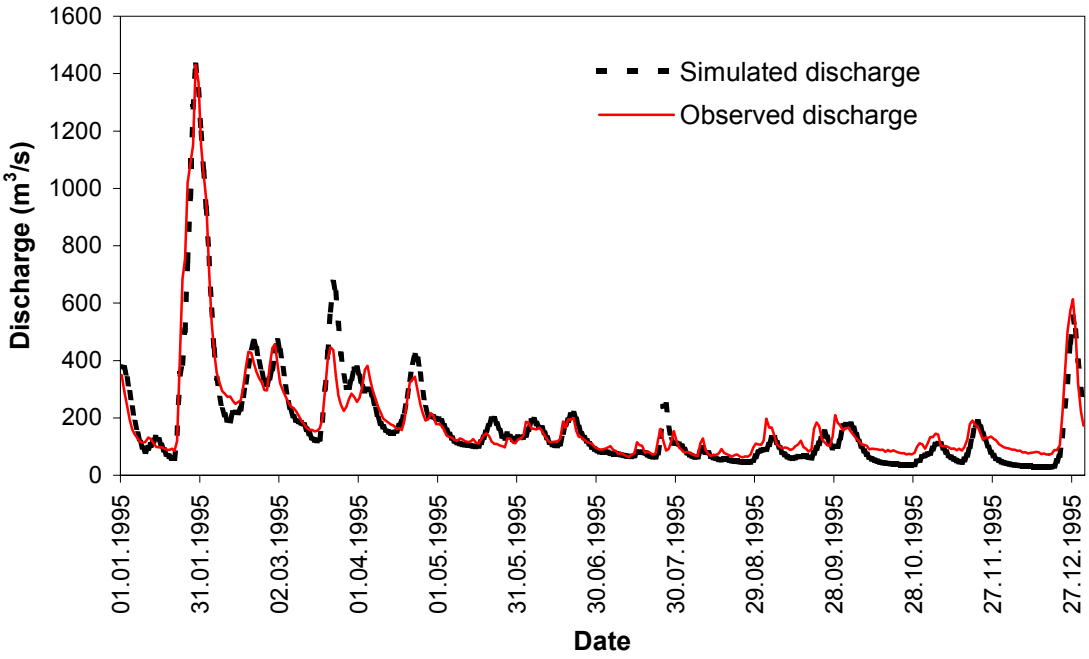

a) Steinbach (Main)

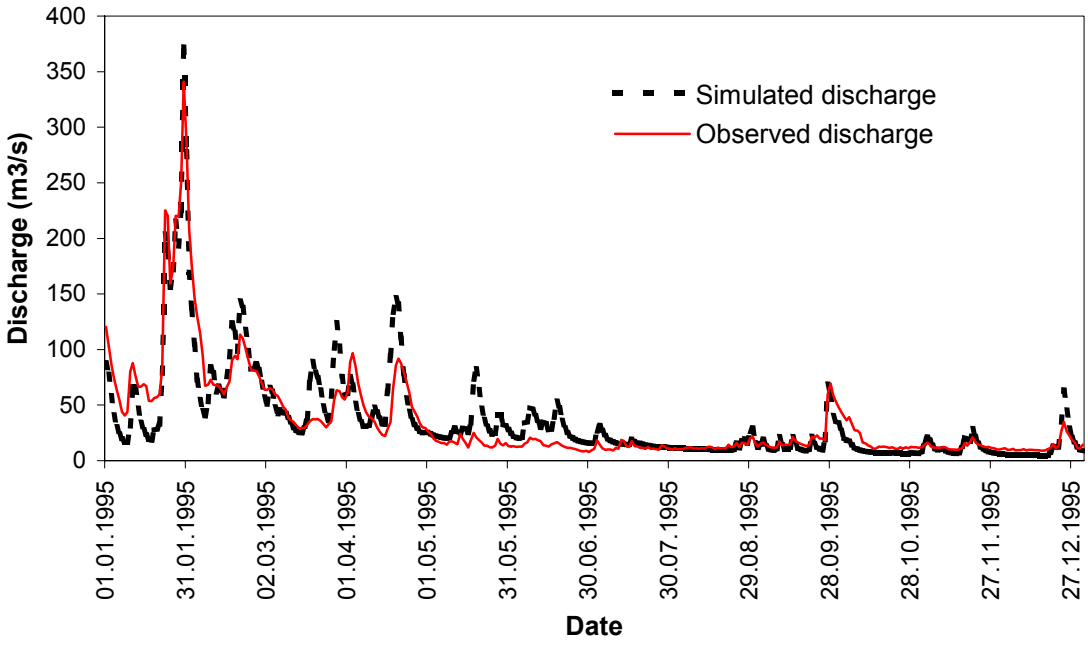

b) Villigst (Ruhr)

Figure 4.8 Model simulated and observed daily discharges at two gauges from the validation set of subcatchments in the validation period.

4.2.5 Sensitivity Analysis

The study of the impact of changes in the model parameters and other variables used in a model on the model output is an important phase of a modeling practice. All parameters and variables used in a rainfall-runoff model do not have a similar level of effect on the sensitivity of the model simulation. A slight change in some parameters or variables may lead to a significant change in the model simulation result. The model is said to be sensitive to such parameters or variables. On the other hand, no noticeable change is felt due to a change in others and they constitute a group of parameters or variables to which the model is insensitive. Study of the sensitivity of the model simulation results to changes in the model parameters or other input variables gives an insight to the model user into which parameters or variables contribute most to the variability of the simulation result and which are insignificant in terms of their influence on the uncertainty associated with the model prediction.

4.2.5.1 Sensitivity to model parameters

The classical method of analyzing the sensitivity of a model simulation for a given parameter is through the evaluation of the local gradient of the model simulation result or the model performance measure with respect to the parameter at a given set of model parameters (McCuen, 1973). The gradient of the model performance measure, i.e., the objective function defined in section 4.2.2 was used in this study.

$$S_j = \frac{\partial O}{\partial p_j} \qquad 4\text{-}11$$

where

S_j sensitivity index with respect to parameter j at a given set of model parameters

O model performance measure

p_j value of parameter j for which sensitivity is evaluated

The sensitivity index defined in equation 4-11 gives the absolute sensitivity of the model to the change in parameter p_j. Such an index is not an appropriate measure to compare the model sensitivity to different parameters, since S_j is not invariant to either the model performance measure or the parameter value. Dividing the numerator of equation 4-11 by the performance

measure and the denominator by the parameter value gives the relative sensitivity, which can be used as an index to compare sensitivity of the model to different parameters.

$$R_j = \frac{\partial O / O}{\partial p_i / p_i} \qquad 4\text{-}12$$

Equation 4-12 only gives the local sensitivity of the model to parameter p_i at a specific point in the parameter space of all the model parameters. R_j therefore depends on the point in the parameter space at which it is evaluated. As knowledge of the sensitivity of the model parameters is more important near the set of model parameters values at which the model is used for simulation, sensitivity analysis of a model with respect to parameters is normally done near the optimum set after model calibration.

One way of presenting the sensitivity of a model simulation result to a change in a given parameter is by plotting the percentage changes in the model output or the objective function corresponding to different percentage changes in the parameter value. Such a plot is referred to as a sensitivity plot (Dawdy, 1969) and it can be used to examine the stability of a given parameter in the optimum set of parameters. Figures 4.9 and 4.10 show the sensitivity plots for the parameters of the lumped runoff response routine and the distributed runoff generation routines respectively. To derive the sensitivity plot, the model was run for all subcatchments in the calibration set by uniformly varying the given parameter by the same percentage in all subcatchments and the corresponding objective function from each subcatchment was calculated. The plot shows the percentage change in the average objective function from all the subcatchments against the percentage change in the parameter value.

It can be seen in figure 4.9 that the parameters of the runoff response routine show higher sensitivity except parameter *MAXBAS,* which shows only a slight sensitivity around the optimum. Especially parameters α and k_1, which control the outflow from the upper reservoir, are highly sensitive. This is, of course, what is expected since these parameters are related to the relatively fast response of the catchment and control the peak runoff, which highly affects the objective function since the error term in the objective function is weighted by the runoff. One can also notice from the sensitivity plots of these two parameters that the model simulation result is more sensitive to an increase in the values of these parameters than a decrease in their values. An opposite behavior is noticed in the sensitivity of the parameter

perc, which again controls the rate at which water is transferred from the upper to the lower reservoir. The model reacts more to a decrease in the value of *perc* than an increase in its value.

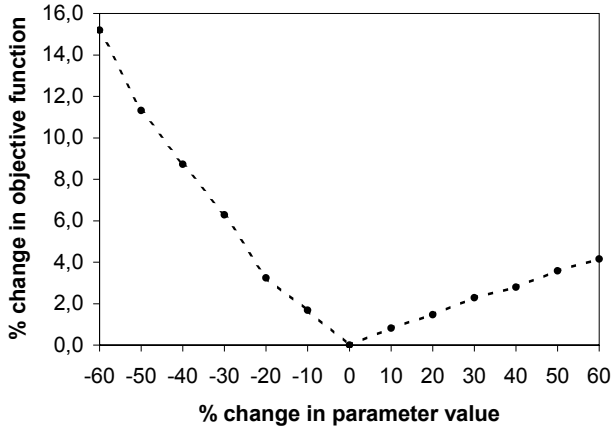

a) parameter α

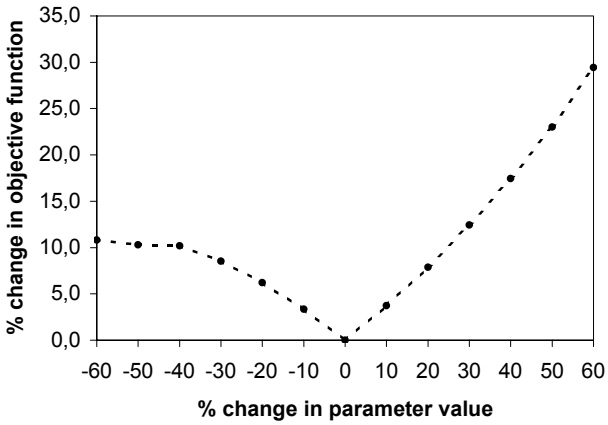

b) parameter k_1

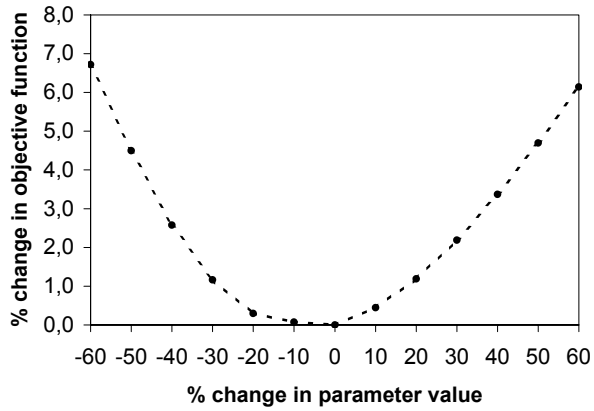

c) parameter k_2

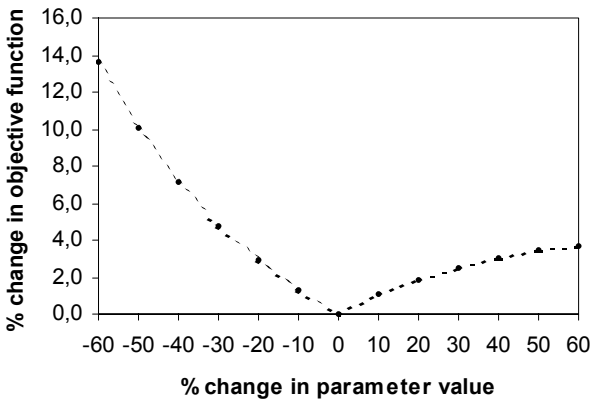

d) parameter *perc*

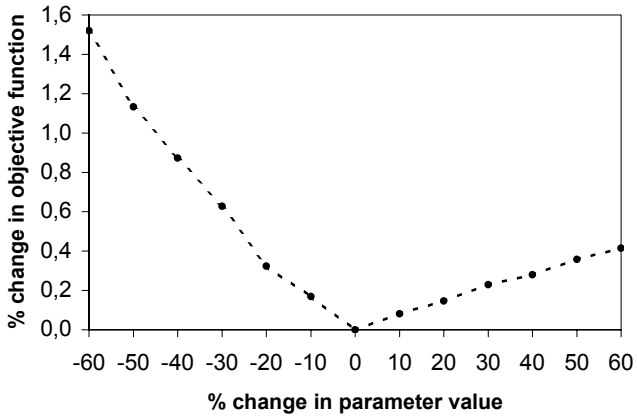

e) parameter *MAXBAS*

Figure 4.9 Sensitivity plots of the parameters of the lumped runoff response module around the optimum set of model parameters.

Parameter k_2, which controls the slower outflow from the lower reservoir, on the other hand shows a somewhat lower sensitivity than the parameters that control emptying of the upper reservoir. This parameter controls the low flow part of the modeled hydrograph and the effect of this part of the hydrograph on the objective function is less compared to part of the hydrograph around the peak flow and this explains the lower sensitivity of this parameter compared to the parameters of the upper reservoir. The sensitivity of the model simulation result also shows similar behavior both for a decrease and an increase of the parameter value.

The parameters of the runoff generation routines pertaining to different processes show different sensitivities. The degree-day factor, for example shows a high sensitivity when the sensitivity analysis is performed for periods when there is snowmelt. The threshold temperature, on the other hand, shows no significant sensitivity around the optimum solution, indicating that it is more important to focus on the degree-day factor in estimating the parameters of the snow accumulation and melt routine.

The parameters of the soil moisture accounting routine show moderate to high sensitivity. The field capacity of the soil shows high sensitivity. As the storage capacity of the soil controls the amount of rain or snowmelt that would be trapped in the catchment, this parameter has an important influence on the generated runoff at lower precipitation magnitudes and during the early phase of a long lasting precipitation. The same is with parameter β, which controls the proportion of rainfall or snowmelt that turns into runoff depending on the soil water deficit in the catchment. The effect of both parameters is significant only if the soil is not saturated and they have no influence once the soil is saturated.

The parameters of the evapotranspiration routine, C_{ET} and LP, on the other hand show very low sensitivity. Especially, the parameter C_{ET}, which is a parameter used to adjust the daily potential evapotranspiration for temperature anomalies, shows an asymptotic behavior for larger increases in its value. This is due to the fact that the maximum adjusted daily potential evapotranspiration is limited to twice the mean daily value estimated based on the monthly average and a further increase in the parameter value doesn't lead to an increase in the evapotranspiration and thus the model output.

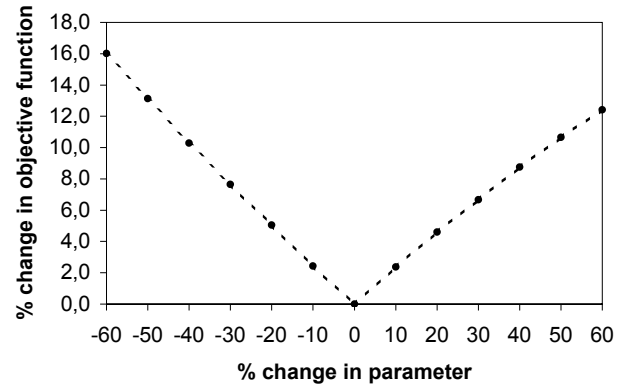

a) Parameter *CC*

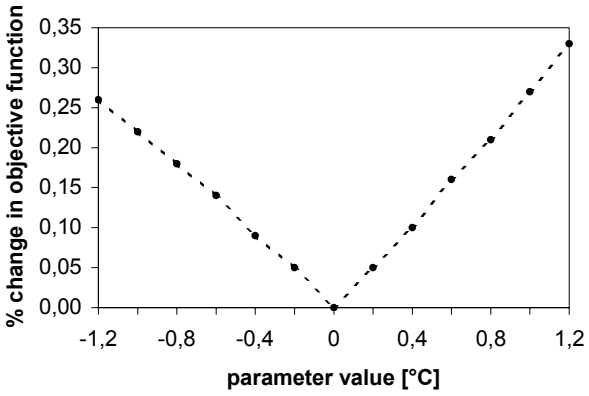

b) Parameter *TT*

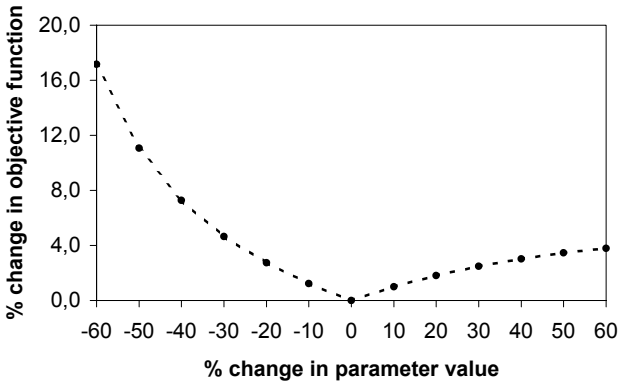

c) Parameter *FC*

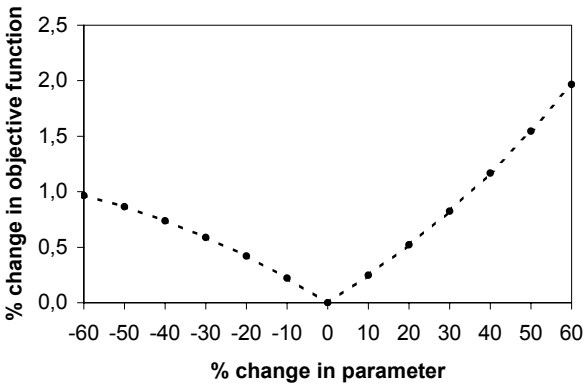

d) Parameter *LP*

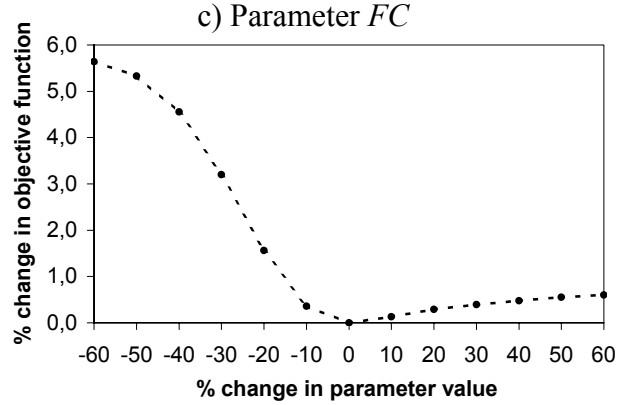

e) Parameter β

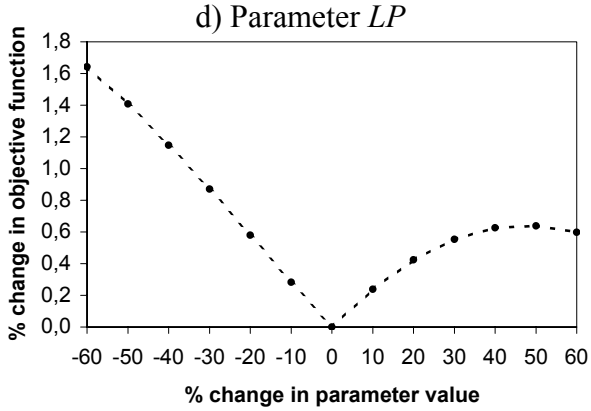

f) Parameter C_{ET}

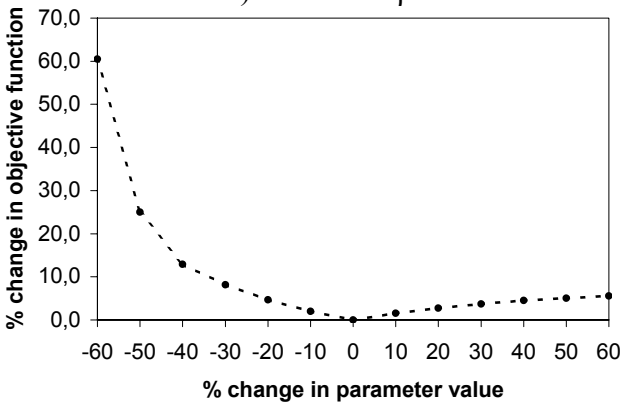

g) Parameter P_{thr}

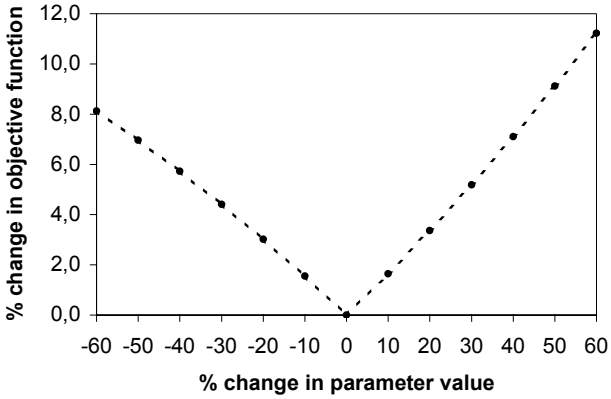

h) Parameter Ψ_{seal}

Figure 4.10 Sensitivity plots of the parameters of the distributed runoff generation routines around the optimum parameter set.

The parameters of the routine that are added to adjust the infiltration process for higher intensity of precipitation show higher sensitivity. These parameters obviously should show such a behavior in terms of their sensitivity. The threshold precipitation magnitude, P_{thr}, determines the daily precipitation amount above which part of it produces fast direct runoff. As is shown in the sensitivity plot, a decrease in its value leads to a very fast change in the model performance. This is because decreasing its value causes a large proportion of the rainfall to produce fast direct runoff and this affects not only the magnitude of the runoff but also the timing of the runoff at the outlet of the catchments since this component of the runoff is not routed in the reservoirs of the runoff response routine, which leads to a tremendous increases in the error term in the objective function. An increase in its value, on the other hand, leads to a relatively smaller change in the model performance. This is due to the fact that increasing further the value of this parameter affects only the runoff produced from very large rainfall events, which are not that frequent and their effect on the model performance over longer period is minimal. Its effect would be more significant if the model performance were evaluated based on event-based simulation. The parameter Ψ_{seal} also determines the proportion of the rainfall in excess of P_{thr} that produces fast direct runoff and a change in its value significantly affects the peak runoff, which is manifested in the model performance.

Summary of the degree of sensitivity of the model performance to the different model parameters around the optimum set of parameters estimated through calibration of the model is shown in table 4.14. The sensitivity of the model is categorized in to three different levels. Those parameters to which the model performance shows higher sensitivity are indicated by three plus signs and parameters whose change affects the model performance moderately are indicated by a single plus sign. Parameters to which no significant sensitivity of the model performance is noticed are indicated by a minus sign.

It should be noted that the foregoing sensitivity study evaluates the sensitivity of the model performance due to a change in a given parameter only around the optimum set of parameters. In addition, the sensitivity was investigated by changing only one parameter at a time and the effect of the possible interaction between the different parameters on the sensitivity of the model performance is not taken into consideration. Although this approach gives an insight into the parameters that contribute more to the variability of the model prediction locally near the optimum set, it tells little about the overall importance of the parameter within the model,

since it is not able to determine the variation of the model result at other points in the feasible parameter space due to a change in a given parameter value.

Table 4.14 Sensitivities of the HBV-IWS model to the different model parameters.

Parameter	Model sensitivity
Snow accumulation and melt:	
CC	+++
TT	-
Soil water and evapotranspiration:	
FC	+++
LP	-
β	+
C_{ET}	-
Runoff concentration:	
α	+++
k_1	+++
k_2	+
perc	+++
MAXBAS	-
Others:	
P_{thr}, Ψ_{seal}	+++

\+ model is moderately sensitive
+++ model is highly sensitive
\- model is not sensitive

In order to investigate the importance of a given parameter within the model structure, one would need to carry out a sensitivity study of all the model parameters over the entire feasible parameter space. This needs implementation of a global sensitivity analysis technique that also takes into account the possible interaction between parameters. In addition to evaluating the sensitivity of the parameter at all points within the feasible parameter range, such an approach enables one to estimate the uncertainty in the prediction of the model due to uncertainty in estimating the model parameter over the entire feasible range of the parameter. This needs making appropriate assumption about the probability distribution of the

parameters and running the model for many parameter sets sampled from this distribution and evaluating the model result. A Monte Carlo type sampling would give the best result. However, the need to make a large number of samples doesn't make the approach attractive due to the associated huge computer time. This is not included in this work.

4.2.5.2 Sensitivity to input variables

In addition to the sensitivity of the model to its parameters, it is worthwhile to investigate the model sensitivity to the catchment descriptors on which the model parameters are regionalized. This study enables one to understand how changes within the catchment due to human interaction, such as alteration of the prevailing land use property affect the response of the catchment. A similar procedure like in the previous sub-section was followed to investigate the sensitivity of the model to the catchment descriptors.

The investigation was focused on those descriptors that are likely to change. The sensitivity of the model to changes in the proportions of the different land use classes and the size of the catchment were investigated. Investigation of the sensitivity to catchment size was performed in order to assess how important the areal scale of a catchment is in the regionalized model. The sensitivity of the individual model parameters to the size of the catchment can be directly estimated from the partial derivatives of the parameters with respect to the size of the catchment from the transfer function of section 4.2.1. However, since more than one model parameters are functions of the catchment size, it is difficult to assess the sensitivity of the model to catchment size from this information and therefore the model sensitivity should be assessed by directly varying the catchment size and investigating the change in the model performance.

Figure 4.11 shows the sensitivity plots of the different classes of land use and the catchment size. One can see in the figure that generally, the model sensitivity to the different classes of land use, when evaluated based on the Nash-Sutcliffe model performance measure, is low. The sensitivity to the proportion of urban area is a bit higher than to the other classes of land use. Quantitative impacts of the changes in the proportions of the different land use classes on the model output are discussed to more detail in chapter 5. The model also shows a moderate sensitivity to catchment size.

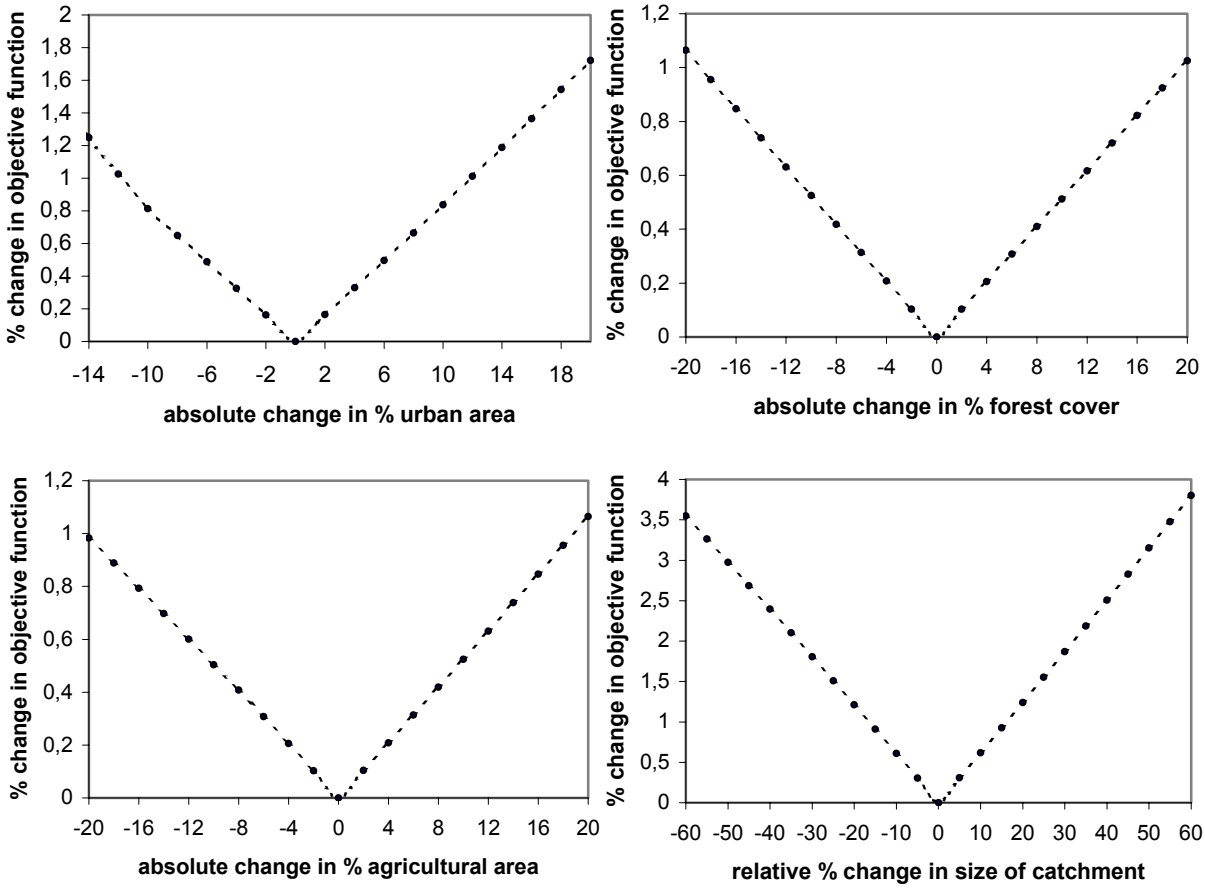

Figure 4.11 Sensitivity plots of the catchment descriptors that are likely to change.

Finally, the sensitivity of the model to the most important meteorological input variable (precipitation) was investigated in order to get an insight into how uncertainty in estimating the variable is reflected in the model performance. Figure 4.12 shows the sensitivity plot of precipitation using the optimum set of model parameters. It can be seen that the model is highly sensitive to a change in the amount of precipitation. This is, of course, what one would expect as the model is driven by precipitation. One can also see from the sensitivity plot that the change in the model performance increases indefinitely with an increase in the amount of precipitation while it becomes stable for larger decrease in the amount of precipitation. This is due to the fact that while an increase in the amount of precipitation adds more to the resulting runoff, a decrease in its amount finally leads to a situation in which more portion of the precipitation is abstracted within the catchment due to interception and infiltration. A further reduction in the precipitation amount doesn't therefore result in any noticeable difference in the generated runoff.

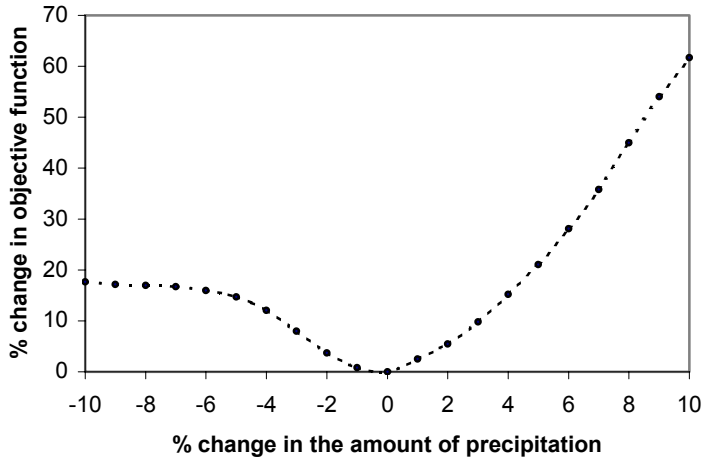

Figure 4.12 Sensitivity plot of precipitation amount.

5 Application in quantifying the hydrologic effect of land use changes

5.1 Introduction

Quantifying the hydrological impact of land use and land cover changes has always been a challenging task to hydrologists. Little is known if there is a well-defined relationship between land use or land cover and the runoff generation mechanism within a catchment. Different methodologies have been implemented to quantify the effect of changes in land use and land cover on the runoff generation, but none of them have been adopted as a general and standard approach of handling the problem. These approaches range from assessment of changes through catchment experiments, which were mainly applied in the earlier times, to the application of a mathematical modelling approach.

The lack of any general approach to assess the hydrological impact of changes in land use or land cover has also been manifested by the different, even sometimes contradictory, results reported by different researchers. Langford (1976), for example, found out that there is no significant increase in water yield as a result of burning down of a stand of Eucalyptus in Australia. In contrast, after reviewing results from a number of catchment experiments, Hibbert (1967) concluded that there is clearly an increase in water yield due to reduction of forest cover, while he underlined on the unpredictability of the response. On the other hand, Bosch and Hewlett (1982) argued on Hibbert's later conclusion, giving specific figures on the changes of water yield due to changes in the amount of cover of different types of vegetations. Most studies done on the effect of urbanization, however, seem to have come up with similar results with regard to the direction of the change in the response of a catchment. After synthesizing the results from a number of previous studies, Hollis (1975) came to a summary that whilst small frequent floods are increased many times by urbanization, large rare floods are not significantly affected.

5.2 Mathematical modelling of the effect of changes in land use

A mathematical modelling approach has been implemented extensively in the past years to assess the hydrological impact of changes in land use and land cover within a catchment. Different methodologies have been implemented, although all of them used rainfall-runoff modelling for the catchments. Lørup, et al. (1998) and Schreider, et al. (2002), for example,

calibrated lumped models for a reference period when there was little change in land use and later applied the calibrated model to a subsequent period in which changes in land use had taken place. They implemented trend analysis to the bias between the modeled and the observed runoff over the later period to investigate changes in the catchment runoff that were believed to have been caused by land use changes. In another approach, Wooldridge, et al. (2001) attempted to regionalize the parameters of a simple semi-distributed conceptual model for forest and non-forest land use classification and different climate regions with the aim of predicting the influence of land use change on the hydrologic response of a catchment. Samaniego (2003) implemented empirical models to relate a set of runoff characteristics of a meso-scale catchment with a set of predictor variables, which constitute morphologic, climatologic, and land cover properties of a catchment. These models were integrated with a simple spatially distributed stochastic land cover change model to quantify the hydrologic impacts of different land cover and climate change scenarios.

A modeling approach that seems to have a sound scientific ground to quantify the effect of land use changes is implementation of a spatially distributed physically based hydrological model, in which the land surface characteristics of the catchment are represented and all the processes influenced by them are modeled using parameters that can physically be estimated a-priori. However, prior estimation of model parameters is not an easy task due to inconsistency of the scale at which measurements are made and the scale at which they are represented in the model. Attempts to simulate a catchment response using such a modeling approach with prior estimation of model parameters did not give promising results (Parkin et al, 1996).

Attempts have, however, been made to still use a physically based distributed model to model the impact of land use changes by setting some of the model parameters a-priori using information from previous modeling experience or field measurements and estimating the others through model calibration against observed catchment responses. However, model calibration leads to a non-unique set of parameters (Beven, 2000) and this makes it difficult to associate the parameters estimated through calibration with the land surface characteristics of the catchment. Therefore, the faith one can put on such models in predicting the effect of changes in land use depends on the uncertainty associated with estimating the model parameters. Application of such an approach to assess the impact of land use changes in

meso-scale catchments has been reported in Bronstert, et al.(2002); Ranzi, et al.(2002); and Brath, et al.(2003).

Application of the modeling approach just mentioned to large-scale or higher meso-scale catchments is not practical, as upscaling of parameters obtained at small scales to the spatial units considered in modeling such sizes of catchments doesn't lead to a reasonable representation of the parameters. If smaller spatial units were used, the associated number of model parameters and the computational resources requirement would be extremely high. Since the modeling approach implemented in this study to model the rainfall-runoff relationship in higher meso-scale catchments makes use of functions that associate the model parameters with the physical catchment properties including land use, it can be used as a tool to estimate the effect of land use changes in the runoff of higher meso-scale catchments. Therefore, one important application of the methodology presented in the foregoing chapters is the quantification of the hydrological impact of changes in land use. Application of the regionalized model in quantifying the effect of land use changes to different land use scenarios will be presented in the following sections.

5.3 Land use scenarios

Before pursuing to quantifying the hydrologic impact of possible future land use scenarios, the sensitivity of the response of the catchment to changes in land use needs to be investigated. Changes in the catchment response corresponding to different scenarios depicting extreme changes in land use were investigated. Two different hypothetical land use scenarios were generated and their associated impacts were assessed by running the regionalized model with parameters corresponding to the changed situations using the same meteorological inputs used to calibrate and validate the model.

5.3.1 Intensive urbanization

The impact of strong urbanization on the runoff generation of a catchment was investigated by uniformly doubling the proportion of urban area in the current land use state. The proportion of forest land use was maintained as it was and the increase in the urban area was made at the expense of agricultural land use. The proportions of the different land use

categories in the current state of land use in the different parts of the study area are shown in table 5.1.

Table 5.1 Percentages of the different landuse classes in the major tributary catchments of the Rhine (Source: Landuse map of the Rhine from CHR).

River basin	Percentage of landuse categories			
	Urban	Agricultural	Forest	Water body
Neckar	14.9	46.6	38.4	0.1
Main	11.7	48.9	39.1	0.3
Sieg	18.4	18.8	62.5	0.3
Lippe	18.1	60.0	21.5	0.4
Lahn	14.0	34.3	51.6	0.1
Ruhr	19.0	20.5	59.4	1.1
Mosel	12.0	43.6	43.9	0.5
Nahe	11.6	40.7	47.6	0.1
Erft	17.8	65.1	17.0	0.1

The simulation result for this scenario shows an increase in the peak runoff resulting from all rainfall events. However, the degree of increase varies from event to event. The increase in the runoff resulting from summer storm events was found to be higher than the increase in the higher runoff resulting from winter precipitation events. This is mainly due to the fact that storm events in summer are generally preceded by a dry soil condition with higher potential for infiltration than in winter. Therefore, the increase in urban area at the expense of agricultural land use would lead to less possibility for infiltration due to surface sealing and consequently, the runoff would be higher as the precipitation that otherwise would infiltrate also contributes to the runoff. This is especially the case during events of smaller magnitude that may not be enough to saturate the soil. A similar result was reported by Niehoff, et al. (2002) for a meso-scale catchment within the Rhine basin through the application of a spatially distributed process based model together with a spatially distributed land-use scenario generation approach. Figure 5.1 shows the rise in the peak runoff for selected events in summer and winter in catchments where the urban area proportion is the maximum and the

minimum. In the upper panel of the figure, one can notice the difference in the degree of increase in the peak runoff of similar magnitude in the Ruhr catchment (a return period of approximately 1.5 years) in summer and winter. The lower panel shows the effect on summer and winter flood events of return periods approximately 1 and 6 years respectively in the Nahe catchment.

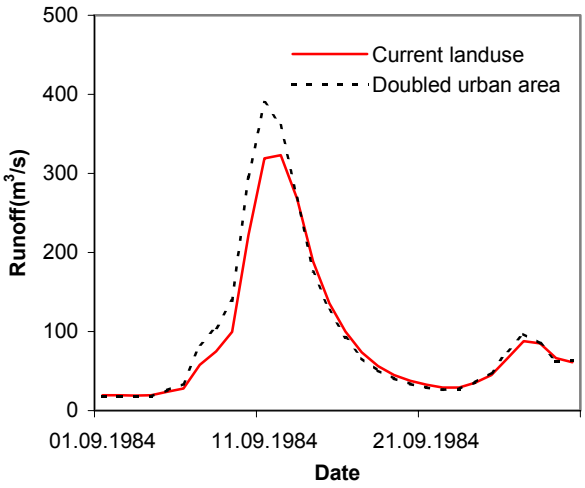

a) Hattingen (Ruhr) - Summer

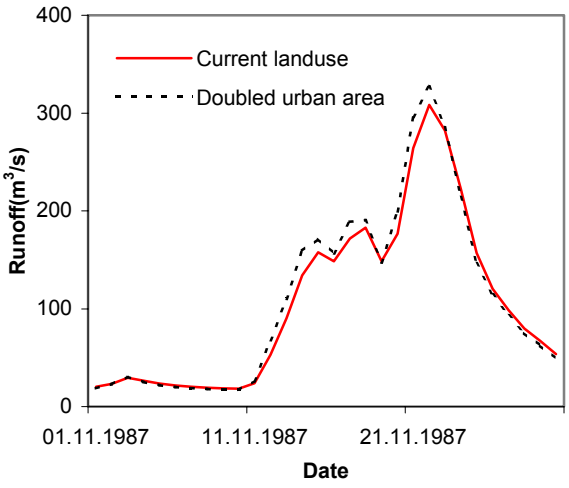

b) Hattingen (Ruhr) -Winter

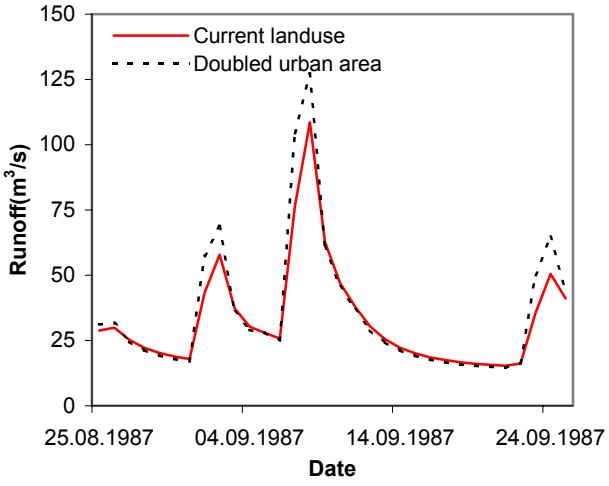

a) Grolsheim (Nahe)- Summer

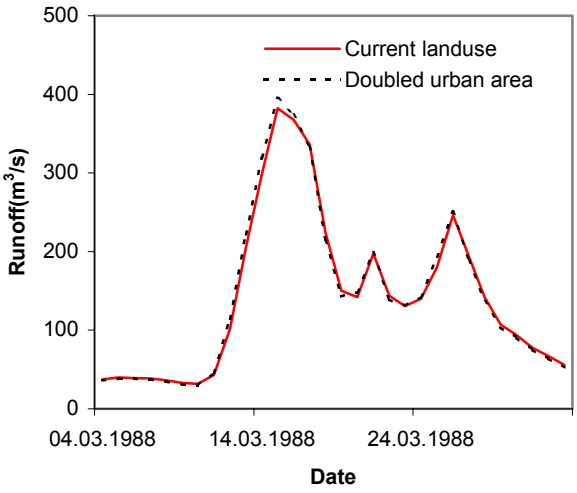

b) Grolsheim (Nahe) - Winter

Figure 5.1 Effect of intensive urbanization on the peak discharges resulting from summer and winter events.

In addition, it could also be reasoned out that the evapotranspiration in agricultural areas is generally higher than in urban areas and the resulting reduction in evapotranspiration loss due

to urbanization also contributes to the increase in the runoff. Some increase in the mean runoff ranging between 0.58% and 4.5% was obtained from the different major tributaries over the period 1980 to 1995.

The increase in the peak runoff due to urbanization is accompanied by a reduction in the arrival time of the peak at the outlet of the catchment. This reduction actually depends on the size of the catchment, in addition to the degree of increase of the urban area. It should also be noted that computation of the runoff at finer time scale with precipitation data at the corresponding time scale is needed to investigate the effect of urbanization on the runoff. As mentioned in section 4.2.3, the daily precipitation was uniformly disaggregated in to hourly values and the model run was made for a time step of 1 hour. Table 5.3 shows the increase in the peak runoff and the corresponding reduction in the arrival time in different parts of the study area for selected flood events.

5.3.2 Afforestation

Another land use scenario used to assess the impact of extreme change in land use was an extensive afforestation scenario. This scenario represents a hypothetical situation where the entire catchment area is covered by forest.

A considerable reduction in the peak runoff in all seasons was observed for a completely forest covered land use scenario. This is mainly due to the absence of sealed area, from which fast direct runoff is generated, leading to the reduction in the peak runoff. In addition, the higher evapotranspiration rate in forests, which becomes even more significant in summer accounts for the reduction of the peak flow to some extent. The removal of soil water through the evapotranspiration process leads to an increase in the infiltration rate, which consequently leads to a reduction in the portion of the rainfall that produces runoff. The higher interception capacity of forests also leads to a reduction of the net precipitation reaching the soil surface and hence a reduction in the resulting runoff. This, however, has a significant effect only on small storm events and the effect is minimal on large storm and flood events (Calder, 1992).

Figure 5.2 shows the relative impact on the peak runoff of removing the urban area from the current land use (replacing it by forest) and covering the entire catchment by forest. It can be

seen that a larger proportion of the reduction in the peak runoff is caused by the removal of urban area.

In addition to its effect on smaller storms, interception loss in forests is found to account for a substantial amount of loss in the total rainfall over longer period (Rutter, 1963; Stewart, 1977). This coupled with the higher transpiration in forests attributed to their larger rooting depth and their access to more soil moisture from deeper zones leads to a reduction in seasonal and long-term mean runoff. The mean runoff in the different major tributary catchments of the study area between 1980 and 1995 for a completely forest cover scenario was found to be 6 to 14% lower than in the current land use scenario.

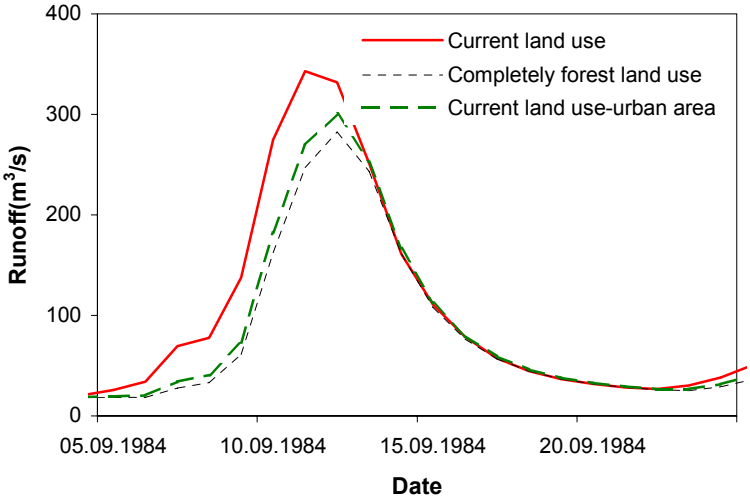

Figure 5.2 Reduction of the peak runoff due to replacement of the urban area by forest and covering the entire catchment by forest respectively in the Ruhr catchment (Gauge Hattingen).

Figure 5.3 shows the reductions in the peak runoff pertaining to flood events of different magnitudes in two different catchments in which the increases in forest cover due to the completely forest cover scenario are the highest and the lowest respectively. The upper panel shows the impact on summer and winter flood events of approximate return periods 1 and 2 years respectively in the Sieg catchment, while the lower panel shows the impact on flood events of approximate return periods 1.5 and 12 years respectively in the Lippe catchment.

It should also be noted that the proportion of forest cover in this scenario is very much away from the range of the proportions used in deriving the regional relationships between the

model parameters and the land use attributes of the catchment. Since the performance of the regional relationships was not validated for catchment attributes showing large deviation from their respective ranges within which the regional relationships were derived, the results obtained for this change scenario may be uncertain. However, they may give an insight into the direction of the change in the catchment response.

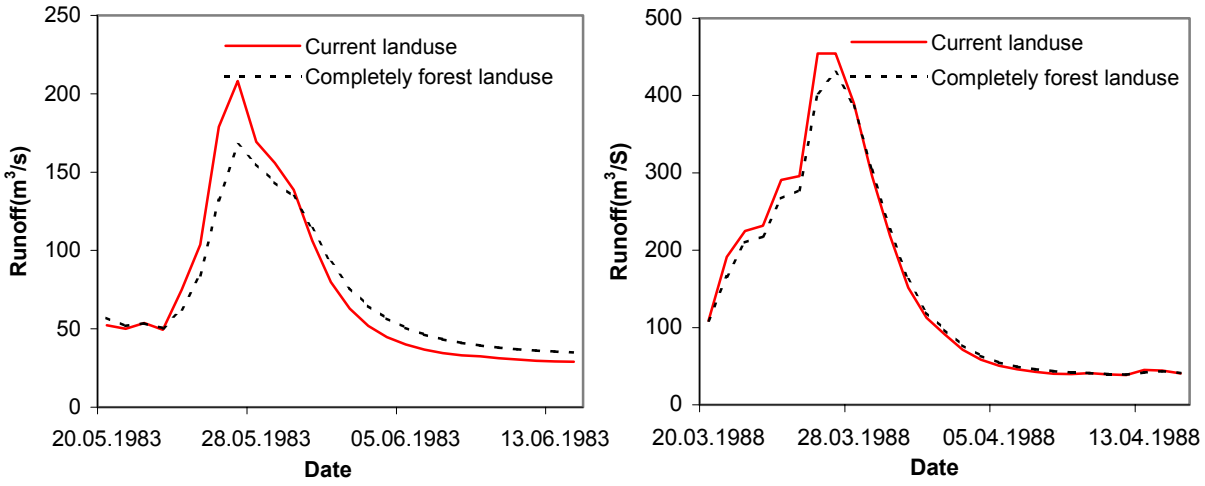

a) Menden (Sieg) – Summer

b) Menden (Sieg) - Winter

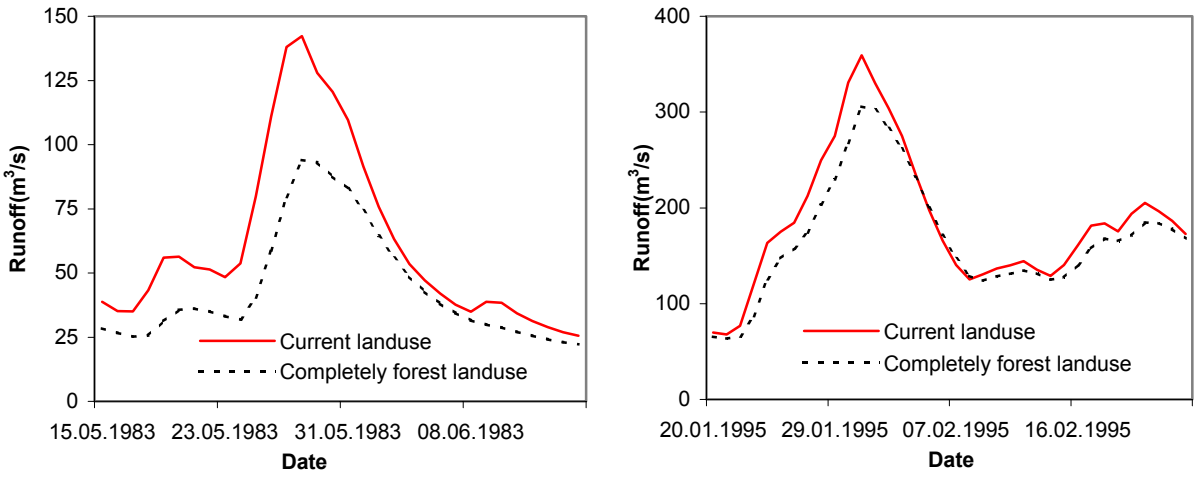

a) Schermbeck (Lippe) – Summer

b) Schermbeck (Lippe) - Winter

Figure 5.3 Effect of extensive afforestation on the peak discharge resulting from summer and winter precipitation events.

5.3.3 Future land use scenario

In addition to the hypothetical land use change scenarios that were used to test the sensitivity of the regionalized model to changes in land use, a more realistic land use change scenario for the year 2010 was also considered to quantify a possible future change in the hydrologic regime of the study area. The generation of the change scenario was based on the work by Dosch and Beckmann (1999). The approach makes use of statistical extrapolation of the prevailing usage of area in different districts within the study area and a modulation by the population prognosis for the year 2015. Administrative districts within the area were classified in to nine different types of settlements and their percentage changes were projected based on the trend of their expansion. Figure 5.4 shows the percentage increase of settlement and traffic areas between 1996 and 2010 and the proportion of settlement and traffic areas in the different districts within the study area in the year 2010 as projected by this approach.

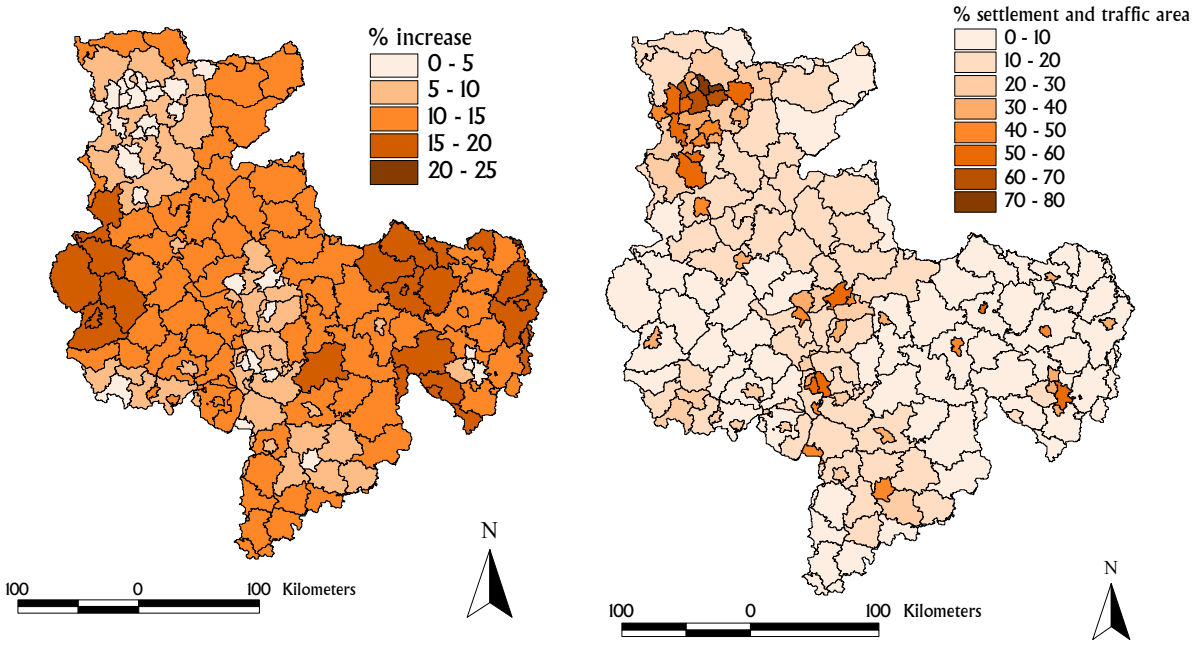

Figure 5.4 Projected increase in settlement and traffic areas between 1996 and 2010 and the corresponding proportion of settlement and traffic areas in 2010 (Based on Dosch and Beckmann,1999).

Table 5.2 summarizes the percentages of urban area in 2010 for the scenario in the major tributary catchments of the German side of the Rhine basin. The increase in the urban area proportion from the current state to the year 2010 was made at the expense of agricultural land use and the proportion of forest areas remains the same as its current state. The average increase in urban land use over the whole study area for this scenario accounts for 12.8% of the proportion of urban area in the current state of land use, which is considerably less than the intensive urbanization scenario discussed in section 5.3.1.

Table 5.2 Relative increase of urban area in different parts of the study area for scenario 2010 (Based on Dosch and Beckmann, 1999).

River basin	% urban area current	% urban area 2010	relative increase (%)
Neckar	14.9	16.8	12.9
Main	11.7	13.8	17.2
Sieg	18.4	20.7	12.2
Lippe	18.1	20.5	13.2
Lahn	14.0	16.1	15
Ruhr	19.0	21	10.3
Mosel	12.0	13.3	11.3
Nahe	11.6	13.5	16
Erft	17.8	20.1	12.9

The direction of the change in the hydrological response of the catchments to this change scenario is similar to that of the intensified urbanization scenario. However, the extent of the change is much less, since the relative increase in the urban area is less compared to the double urban area scenario. Especially, flows resulting from winter events were little affected. A maximum increase of 0.7 % in the mean runoff between 1980 and 1995 was found, indicating almost no effect on the long-term water balance. Figure 5.5 shows the changes in the peak runoff for summer and winter events from two different catchments, in which the relative increases in urban areas are the highest and the lowest respectively. One can see from the figure that the hydrographs are almost indistinguishable in the Ruhr catchment, in which a 10% increase in the urban area is considered.

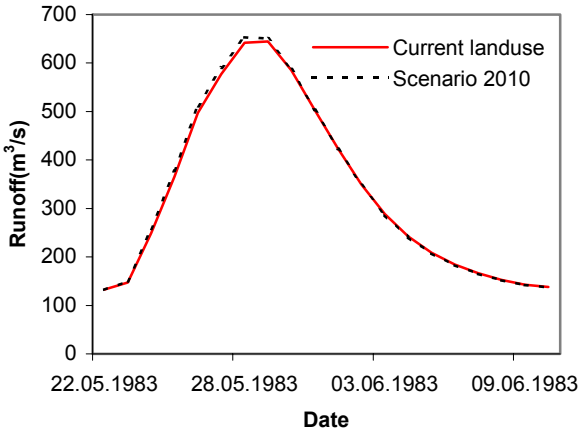

a) Kleinheubach (Main) – Summer

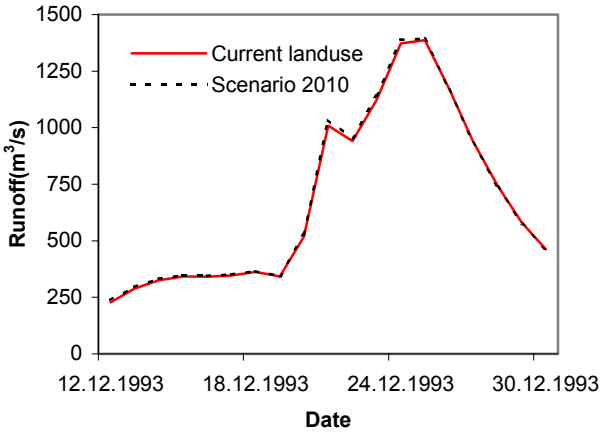

b) Kleinheubach (Main) - Winter

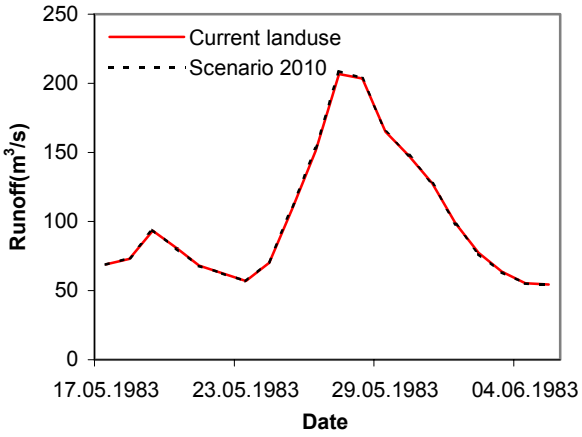

a) Hattingen (Ruhr) – Summer

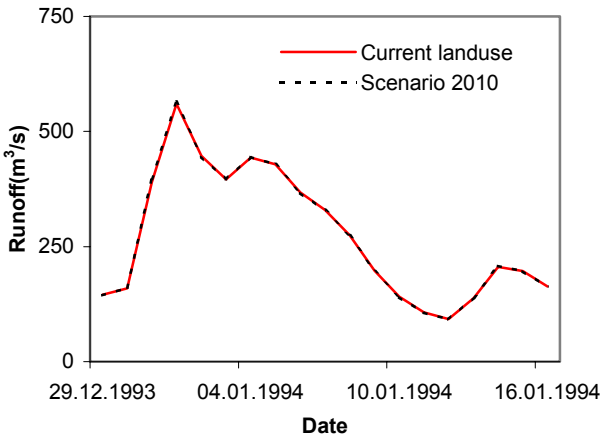

b) Hattingen (Ruhr) – Winter

Figure 5.5 Effect of urban area increases for scenario 2010 on the runoff from events in summer and winter in the Main and Ruhr catchments.

Table 5.3 shows summary of the peak runoff resulting from selected rainfall events for the different land use scenarios presented in the foregoing sections. The table shows specific discharges from catchments producing the maximum and the minimum specific discharges for each event together with their corresponding approximate return periods, as well as the area weighted average specific discharge from all the major catchments within the study area. The catchments corresponding to the maximum and the minimum specific discharges are different for the different events, although in many of the events shown in the table the Sieg and the Lippe catchments produce the maximum and the minimum specific discharges respectively. The percentage changes of these specific discharges resulting from different land

use scenarios are also presented. In addition, the effect of the land use changes on the arrival time of the peak, which is estimated by disaggregating the daily precipitation into hourly values using a uniform distribution, is shown. It can be seen from the table that it is difficult to derive a definite relationship between the return period of a flood event and the impact of a land use change on the flood. The reason for this is that the impact of land use changes on the runoff depends mainly on the antecedent moisture condition within the catchment as discussed in the previous sections.

Table 5.3 Summary of changes in peak runoff and their arrival time for selected events due to different land use scenarios.

Event date	Present landuse			Landuse scenario 2010				Doubled urban area				Entire basin forested			
	q(liter/s/km^2) with app. return period			% increase in discharge			avg. Peak arrival time diff.[h]	% increase in discharge			avg. Peak arrival time diff.[h]	% increase in discharge			avg. Peak arrival time diff.[h]
	Max	min	avg	Max*	Min*	avg		Max*	Min*	avg		Max*	Min*	avg	
27.05.1983	131.56 (Mosel) 20 Yrs.	28.43 (Lippe) 1.5 yrs.	75.14	0.94	2.00	1.14	-1	8.24	15.09	8.49	-3	-14.18	-32.99	-14.36	7
04.06.1984	112.49 (Sieg) 1.5 yrs.	38.01(Mosel) 1 yr.	69.20	0.99	1.52	1.58	-1	8.48	7.77	11.66	-2	-9.75	-20.95	-18.92	7
04.03.1987	173.7 (Sieg) 2.5 yrs.	53.4 (Lippe) 3 yrs.	98.58	0.89	1.31	0.74	-1	7.48	9.74	5.52	-3	-9.27	-17.12	-9.46	5
28.03.1988	154.11 (Sieg) 2 yrs	45.94 (Lippe) 2 yrs.	100.74	0.95	0.63	0.76	-1	7.99	4.27	6.03	-3	-7.69	-17.02	-9.48	7
23.04.1989	75.63 (Sieg) 1yr.	17.5 (Lippe) 1 yr.	43.87	1.31	3.03	1.06	0	10.95	22.80	8.34	-3	-12.02	-37.60	-14.66	5
15.02.1990	163.11 (Sieg) 2 yrs.	29.31 (Lippe) 1.5 yrs.	91.14	0.85	0.38	1.04	-1	7.17	2.08	7.75	-3	-8.41	-9.66	-10.71	6
21.11.1990	88.1 (Sieg) 1 yr.	19.6 (Lippe) 1 yr.	43.63	1.88	3.06	1.77	-1	15.89	23.16	12.48	-3	-18.80	-40.82	-17.55	8
22.12.1991	183.6 (Sieg) 3 yrs.	38.94 (Lippe) 1.5 yrs.	78.03	1.13	1.54	1.01	-1	8.75	11.63	6.97	-3	-10.47	-24.07	-11.15	8
21.12.1993	214 (Nahe) 50 yrs.	51.91 (Lippe) 3 yrs.	129.12	1.68	0.44	1.17	0	10.56	2.56	8.08	-2	-16.74	-13.35	-13.47	4
23.01.1995	203 (Nahe) 50 yrs.	77.03 (Lippe) 12 yrs.	154.65	1.61	1.08	1.64	0	9.98	7.46	10.24	-2	-14.80	-15.19	-15.56	5

* percentage increases in the maximum or minimum specific discharges.

6 Conclusions and outlook

A regional estimation scheme of parameters of a rainfall-runoff model as functions of physical catchment descriptors has been developed and applied giving good results in terms of the ability of the model to predict a continuous runoff hydrograph from catchments based on daily input meteorological variables. The scheme, which is based on estimating the model parameters that lead to acceptable model performance in terms of some predefined objective function for a number of gauged subcatchments, imposes a constraint on the model parameters by associating them with the catchment descriptors before the calibration process. This, although doesn't entirely avoid the problem of having a number of equally competing model parameters, leads to a considerable reduction of the feasible parameter space over which calibration is made, while at the same time maximising the regional relationship between the model parameters and the catchment descriptors. This renders the approach more attractive than the traditional two-step regionalization scheme in that it avoids calibrating subcatchments individually over wider feasible parameter space and reduces considerably the difficulty associated with fitting the regional relationship between the parameters thus obtained and the catchment descriptors.

Since the model parameters are estimated based on readily measurable catchment descriptors, the scheme makes it possible to estimate model parameters corresponding to ungauged catchments, rendering it potentially suitable for modelling the runoff from such catchments. This was validated by implementing the parameter estimation scheme in gauged subcatchments that were not used in deriving the regional relationship between the model parameters and the catchment descriptors. The result obtained suggests that the model performances in terms of different evaluation criteria in the subcatchments used to validate the scheme and the catchments used to derive the regional relationship are comparable.

The catchment descriptors used in deriving the regional relationship include the land use properties of the catchment in addition to other physiographic attributes of the catchment. Therefore a change in the land use attribute of the catchment is manifested in the parameter values and hence in the response of the catchment. This potentially makes the approach useful in predicting the hydrological consequences of changes in land use within a catchment, as was demonstrated through sensitivity study of the regionalized model to different scenarios of changes in land use.

The direction of the catchment reaction predicted by the regionalized model to land use changes is consistent with the physical explanations that can be given to the effect of the different change scenarios tested in the study and is supportive to findings of many of the previous works conducted on assessment of the impact of land use changes. The results indicate that there is an increase both in the long-term water yield and event based runoff from catchments due to urbanization, while they indicate a reduction in both attributes of the catchment response due to afforestation.

One should, however, be cautious in interpreting the modelled responses of the catchment due to land use changes when one or more of the land use classes in the changed scenario have a proportion outside the range of their proportion in the subcatchments used to derive the regional relationship between the model parameters and the catchment descriptors. As can be seen in table 4.2, the proportions of some classes of land use in the validation set of subcatchments fall slightly outside their corresponding ranges in the calibration set of subcatchments that were used for the derivation of the regional relationship between the model parameters and the catchment descriptors. Since the performance of the regionalized model in the validation subcatchments was found to be within a reasonable degree of acceptance, this suggests that the regionalization approach implemented works well for slight extrapolation of the proportion of land use classes beyond the range considered in deriving the regional relationships. However, for larger extrapolation, the model was not validated and the prediction of the model for such a situation could be more uncertain.

The above remark applies to the other catchment attributes that are used to regionalize the model parameters as well. This implies that the spatial scale of the subcatchment is an important factor that needs to be taken into consideration in using the regional parameter equations in modelling the rainfall-runoff relationship for the subcatchment, since size of the subcatchment is also used as a catchment attribute to regionalize some of the model parameters. The subcatchments used in deriving the regional equations range from the lower to the upper meso-scale subcatchments and applicability of the equations to small and large-scale catchments could also be more uncertain. For large scale catchments, the problem can, however, be handled by subdividing them into meso-scale subcatchments and integrating a flood routing model from the subcatchments down to the outlet of the whole catchment.

The regional parameter estimation methodology implemented in this work considers land use classes that are mainly related to the type of land cover. Other land use classes are not explicitly considered in deriving the regional parameter estimation equations. Therefore, if a land use type other than those considered in deriving the regional equations is introduced in a catchment, the rainfall-runoff relationship for the catchment may not be modelled by the regionalized model used in this study. The introduced land use type may alter the runoff generation mechanism that may necessitate even a change in the structure of the model. This problem was noticed in modelling the rainfall-runoff relationship in the Erft catchment, where an extensive coal mining activity takes place. The regionalized model was not able to capture any part of the runoff hydrograph generated from the catchment.

It needs to be pointed out that the regional equations developed in this work are applicable only within the study area they are established for and within the particular model implemented in the study. The general methodology, however, can be extended to other models and other regions as well.

Based on the observations made during the modelling procedure and the scope of the work presented here, it is also worthwhile to put the following outlooks on the direction of future work that can be done:

- Estimation of the model parameters and their corresponding regional relationships with the catchment attributes was done by calibrating the model based only on simulating the runoff observed at the outlet points of the subcatchments. Simulating the runoff at the outlet needs consideration of all the catchment processes simultaneously and this leads to an interaction of the model parameters pertaining to the different hydrological processes. This obviously increases the freedom of the individual model parameters and parameter values spanning over a wide range can lead to similar model performance. This consequently reduces identifiability of the model parameters. Although the regionalization approach implemented in this work imposes constraints on the parameters, further improvement of estimation of the parameters may be achieved by incorporating other catchment responses or state variables corresponding to different phases of the runoff generation process, if it is feasible to obtain such data. This may suggest a direction for future parameter regionalization works.

- It might also be worthwhile to extend the model structure so that the effect of soil management on the runoff generation, i.e., the effect of macropore flow and the effect of surface siltation due to high intensity of precipitation are considered explicitly for arable land. These processes mainly depend on the intensity of precipitation, soil moisture at the beginning of the event, and the land tillage practice. It might be possible to account for these effects by modelling the infiltration parameters as functions of soil moisture, intensity of precipitation and the land management by making use of information on the dynamics of the land management practice at different times of the year.

- The transfer function relating the model parameters with the catchment attributes was set to have a linear form in this work. It would be worthwhile to try and test other non-linear forms of transfer functions.

- Although the methodology reported in this work reduces the feasible parameter space over which model calibration is done due to a constraint imposed by the functional relationship between the model parameters and the catchment descriptors established a priori, it doesn't lead to estimation of a unique set of model parameters. This implies that there are uncertainties associated with the prediction made by the regionalized model. This suggests a need to carry out a comprehensive uncertainty analysis coupled with the regional parameter estimation in order to assess the reliability of the regionalized model. Future regionalization works should also focus on this issue as well.

References

Abbott, M.B., Bathurst, J.C., Cung, J.A., O'Connell, P.E., and Rasmussen, J., 1986a. An introduction to the European Hydrologic System-Systeme Hydrologique Europeen, SHE, 1: History and philosophy of a physically-based, distributed modeling system. *Journal of Hydrology*, 87: 45-59.

Abbott, M.B., Bathurst, J.C., Cung, J.A., O'Connell, P.E., and Rasmussen, J., 1986b. An introduction to the European Hydrologic System-Systeme Hydrologique Europeen, SHE, 2: Structure of a physically-based, distributed modelling system. *Journal of Hydrology*, 87: 61-77.

Abdulla, F.A., and Lettenmaier, D.P., 1997. Development of regional parameter estimation equations for a macroscale hydrologic model. *Journal of Hydrology*, 197: 230-257.

Ahmed, S., and deMarsily, G., 1987. Comparison of geostatistical methods for estimating transmissivity using data on transmissivity and specific capacity. *Water Resources Research*, 23(9): 1717-1737.

Bárdossy, A., 1996. The use of fuzzy rules for the description of elements of the hydrological cycle. *Ecological Modelling*, 85: 59-65.

Bergström, S., 1995. The HBV model. In: Computer Models of Watershed Hydrology. V.P. Singh(Editor). Water Resources Publications, Littleton, Colorado, USA, 443-476.

Bergström, S., and Forsman, A., 1973. Development of a conceptual deterministic rainfall-runoff model. *Nordic Hydrology,* 4: 147-170.

Beven, K.J., 1989. Changing ideas in hydrology-the case of physically based models. *Journal of hydrology,* 105:157-172.

Beven, K.J., 2000. Rainfall-Runoff Modelling: The Primer. Wiley, 360pp.

Beven, K. and Binley, A., 1992. The future of distributed models: model calibration and uncertainty prediction. *Hydrological Processes*, 6: 279-298.

Beven, K.J., Calver, A. and Morris, E.M., 1987. The Institute of Hydrology Distributed Model. Institute of Hydrology, *Report* No.98, Wallingford (UK), 33 p.

Binley, A.M., Beven, K.J., and Elgy, J., 1989. A physically-based model of heterogeneous hillslopes. II. Effective hydraulic conductivities. *Water Resources Research*, 25(6): 1227-1233.

Blaney, H.F., Criddle, W.D., 1950. Determining Water Requirements in Irrigated Areas from Climatological and Irrigation Data. -US Dep. Agr., Soil Sci. Techn. Paper No. 96.

Bosch, J.M. and Hewlett, J.D., 1982. A review of catchment experiments to determine the effect of vegetation changes on water yield and evapotranspiration. *Journal of Hydrology*, 55: 3-23.

Brath, A., Montanari, A. and Moretti, G., 2003. Assessing the effects on flood risk of the land-use changes in the last five decades: an Italian case study. *IAHS Publs*. 278: 435-441.

Bronstert, A., Niehoff, D. and Bürger, G., 2002. Effects of climate and land-use change on storm runoff generation: present knowledge and modelling capabilities. *Hydrological processes*, 16(2): 509-529.

Calder, I. R., 1992. Hydrologic effects of land-use change. D.R. Maidment (Editor). *Handbook of Hydrology*: 13.1–13.50.

CCHYDRO, 1999. Impact of Climate Change on River Basin hydrology Under Different Climatic Conditions, Final Report. ENV4-CT195-0133, IWHW-BOKU, Muthg. 18, A-1190 Vienna, Austria.

Christakos, G., 1984. On the problem of permissible covariance and variogram models. *Water Resources Research*, 20(2): 251-265.

Clark, C.O., 1945. Storage and unit hydrograph. *Transactions of the American Society of Civil Engineers,* 110: 1416-1446.

Connolly, R.D., Schirmer, J., and Dunn, P.K., 1998: A daily rainfall disaggregation model. *Agricultural and Fores Meteorology*, 92: 105-117.

Crawford, N. H., and Linsley, R.K., 1966. Digital Simulation in hydrology: Stanford Watershed Model IV. Tech. Rep. N. 39, Stanford Univ., Palo Alto, California, USA.

Cressie, N.A.C., 1993. Statistics for spatial data. Wiley, New York, 900pp.

Dawdy, D.R., and O'Donnell, T., 1965. Mathematical models of catchmant behaviour. *Journal of the Hydraulics Division*, ASCE, 91 (HY4): 123-137.

Diskin, M.H., and Simon, E., 1979. The relationship between the time bases of simulation models and their structure. *Water Resources Bulletin*, 15(6): 1716-1732.

Dommermuth, H. and Trampf, W., 1990. Die Verdunstung in der Bundesrepublik Deutschland, Zeitraum 1951-1980, Teil I , Selbstverlag des Deutschen Wetterdienstes, Offenbach am Main.

Dommermuth, H. and Trampf, W., 1991. Die Verdunstung in der Bundesrepublik Deutschland, Zeitraum 1951-1980, Teil II , Selbstverlag des Deutschen Wetterdienstes, Offenbach am Main.

Dommermuth, H. and Trampf, W., 1992. Die Verdunstung in der Bundesrepublik Deutschland, Zeitraum 1951-1980, Teil III , Selbstverlag des Deutschen Wetterdienstes, Offenbach am Main.

Dosch, F. and Beckman, G., 1999. Trends und Szenarien der Siedlungsflächenentwicklung bis 2010. In: Bundesamt für Bauwesen und Raumordnung (Ed.): Perspektiven der zukünftigen Raum- und Stadtentwicklung, Berlin,11, 827-842.

Duan, Q., Gupta, V.K., and Sorooshian, S., 1992. Effective and efficient global optimisation for conceptual rainfall-runoff models. *Water Resources Research*, 28: 1015-1031.

Econopouly, T.W., Davis, D.R., and Woolhiser, D.A., 1990. Parameter transferability for a daily rainfall disaggregation model. *Journal of Hydrology,* 118: 209-228.

Elling, W., Häckel, H., and Ohmayer, G., 1990. Schätzung der aktuellen nutzbaren Wasser-speicherung(ANWS) des Wurzelraumes von Waldbeständen mit Hilfe eines Simulations-modells. - Forstwirtschaftliche Bl.; 109: 210-219.; Hamburg und Berlin.

Fernandez, W., Vogel, R.M., and Sankarasubramanian, A., 2000. Regional calibration of a watershed model. *Hydrological Sciences Journal*, 45(5): 689-707.

Freeze, R.A. and Harlan, R.L., 1969. Blueprint for a physically-based digitally simulated hydrologic response model. *Journal of Hydrology,* 9: 237-258.

Gupta, H.V., and Sorooshian, S., 1998. Toward improved calibration of hydrologic models: Multiple and noncommensurable measures of information. *Water Resources Research,* 34(4):751-763.

Haberlandt, U., Krysanova, V., and Bárdossy, A., 2001. Assessment of nitrogen leaching from arable land in large river basins, Part II: Regionalisation using fuzzy rule based modelling. *Ecological Modelling*, 150 (3): 255-276

Hamon, W.R., 1961. Estimating potential evapo-transpiration. *Journal of the Hydraulics Division, ASCE,* 87: 107-120.

Haude, W., 1955. Zur Bestimmung der Verdunstung auf möglichst einfache Weise. Mitt. Deutscher Wetterdienst, 11.

Heerdegen, R.G., Reich, B.M., 1974. Unit Hydrographs for catchments of different sizes and dissimilar regions. *Journal of Hydrology* 22: 143-153.

Hibbert, A.R., 1967. Forest treatment effects on water yield. In: W.E. Sopper and H.W. Lull (Editors), Int. Symp. For. Hydrol., Pergmon, Oxford, 813 pp.

Hirsch, R. M., 1982. A comparison of four streamflow record extension techniques. *Water Resources Research*, 18(4): 1081-1088.

Hollis, G.E. 1975. The effect of urbanization on flood of different recurrence interval. *Water Resources Research*, 11(3): 431-435.

Hromadka, T.V. II and Whitley, R.J., 1994. The rational method for peak flow rate estimation. *Water Resources Bulletin* 30: 1001.

Hundecha, Y., Bardossy, A. and Theisen, H.W., 2001. Development of a fuzzy logic-based rainfall-runoff model. *Hydrological Sciences Journal,* 46(3): 363-376.

Jakeman, A., and Hornberger, G., 1993. How much complexity is warranted in a rainfall-runoff model? *Water Resources Research*, 29(8): 2637-2649.

Jakeman, A.J., Littlewood, I.G., and Whitehead, P.G., 1990. Computation of the instantaneous unit hydrograph and identifiable component flows with application to two small upland catchments. *Journal of Hydrology*, 117: 275-300.

Johnston, P.R., and Pilgrim, D.H., 1976. Parameter optimisation for watershed models. *Water Resources Research*, 12: 477-486.

Jones, J. A. A., 1997: Global hydrology. Processes, resources and environmental management. Longman, Harlow, 399pp.

Kitanidis, P.K., 1997. Introduction to geostatistics: applications in hydrogeology. Cambridge university press, 249pp.

Kletti, L.L., and Stefan, H. G., 1997. Correlations of climate and streamflow in three minesota streams. *Climate Change*, 37: 575-600.

Kuczera, G., 1997. Efficient subspace probabilistic parameter optimisation for catchment models. *Water Resources Research*, 33: 177-185.

Langford, K.J., 1976. Change in yield of water following a bush fire in a forest of *Eucalyptus regnans*. *Journal of Hydrology*, 29: 87-114.

Lasdon, L.S. and Waren, A.D., 1979. Generalized Reduced Gradient Software for Linearly and Nonlinearly Constrained Problems. H. Greenberg (Editor), Sijithoff and Noordhoff (Pubs.)

Lasdon, L.S., Warren, A.D., Jain, A., and Ratner, M., 1978. Design and testing of a generalized reduced gradient code for nonlinear programming, *ACM Trans. Math. Software*, 4: 34-50.

Liang, X., Lettenmaier, D.P., Wood, E.F., and Burges, S.J., 1994. A simple hydrologically based model of land surface water and energy fluxes for GCMs. *Journal of Geophysical Research*, 99(D7): 14,415-14,428.

Lindström, G. et al.,1997. Development and test of the distributed HBV-96 hydrological model. *Journal of Hydrology*, 201: 272-288.

Littlewood, I.G., Down, K., Parker, J.R., and Post, D.A., 1997. The PC version of IHACRES for catchment-scale rainfall-streamflow modelling. Version 1.0. User Guide. Institute of Hydrology, 89 p.

Lørup, J.K., Refsgaard, J.C. and Mazvimavi, D., 1998. Assessing the effect of land use change on catchment runoff by combined use of statistical tests and hydrological modeling: Case studies from Zimbabwe. *Journal of Hydrology*, 205: 147-163.

McCuen, R.H., 1973. The role of sensitivity analysis in hydrologic modelling. *Journal of Hydrology*, 18: 37-53.

Minns, A.W. and Hall, M.J., 1996. Artificial neutral networks as rainfall-runoff models. *Hydrological Sciences Journal*, 41: 399-417.

Mitscherlich, G., 1971. Wald, Wachstum und Umwelt. Band 2: Waldklima und Wasserhaushalt. Frankfurt, Sauerländer.

Monteith, J.L., 1965. Evaporation and environment. In: The State and Movement of Water in Living Organisms. G.T. Fogy(Editor). Proceedings of the 19th Symposium, Society of Experimental Biology, Cambridge University Press, London, 205-234

Mulvany, T. J., 1851. On the use of self-registering rain and flood gauges in making observations of the relations of rain fall and flood discharges in a given catchment. Transactions and Minutes of the Proceedings of the Institute of Civil Engineers of Ireland, Session 1850-1, v.IV, pt. II, Dublin, Ireland.

Münch, A., 1993. AKWA-M - Programmdokumentation. Dresden.

Nash, J.E. and Sutcliffe, J.V., 1970. River flow forecasting through conceptual models. Part I. A discussion of principles. *Journal of Hydrology*, 10: 280-290.

Nathan, R.J., and McMahon, T.A., 1992. Estimating low flow characteristics in ungauged catchments. *Water Resources Management*, 6: 85-100.

Niehoff, D., Fritsch, U., Bronstert, A., 2002. Land-use impacts on storm-runoff generation: scenarios of land-use change and simulation of hydrological response in a meso-scale catchment in SW-Germany. *Journal of Hydrology*, 267(1-2): 80-93.

Parkin, G., O'Donnell, G., Ewen, J., Bathurst, J.C., O'Connell, P.E. and Lavabre, J., 1996. Validation of catchment models for predicting land-use and climate change impacts. 1. Case study for a Mediterranean catchment. *Journal of Hydrology,* 175: 595-613.

Post, D.A., and Jakeman, A.J., 1999. Predicting the daily streamflow of ungauged catchmentsin S.E. Australia by regionalizing the parameters of a lumped conceptual rainfall-runoff model. *Ecological Modelling*, 123: 91-104.

Ranzi, R., Bochicchio, M. and Bacchi, B. 2002. Effects on floods of recent afforestation and urbanisation in the Mella River (Italian Alps). *Hydrol. and earth system Sci.,* 6(2): 239-253.

Refsgaard, J.C., and Kundsen, J., 1996. Operational validation and intercomparison of different types of hydrological models. *Water Resources Research*, 32(7): 2189-2202.

Richards, B.D., 1944. Flood Estimation and Control. Chapman and Hall, London.

Rutter, A.J., 1963. Studies in the water balance of *Pinus sylvestris* in plantation conditions, I. Measurements of rainfall and interception. *J. Ecol.,* 51: 191-203.

Samaniego, L.E., 2003. Hydrological consequences of land use/cover and climatic changes in mesoscale catchments. Institut für Wasserbau, Universität Stuttgart. Heft 118.

Schreider, S. Yu., Jakeman, A.J., Letcher, R.A., Nathan, R.J., Neal, B.P., and Beavis, S.G., 2002. Detecting changes in streamflow response to changes in non-climatic catchment conditions: farm dam development in the Murray-Darling basin, Australia. *Journal of Hydrology*, 262: 84-98

Sefton, C.E.M., and Howarth, S.M., 1998. Relationships between dynamic response characteristics and physical descriptors of catchmants in England and Wales. *Journal of Hydrology*, 211: 1-16.

Seibert, J., 1999. Regionalization of parameters for a conceptual rainfall-runoff model. *Agricultural and Forest Meteorology*, 98-99: 279-293.

Sherman, L.K., 1932.Streamflow from rainfall by unit-graph method. *Engineering News record,* 108: 501-505.

Singh, V.P.(Ed.), 1995. Computer Models of Watershed Hydrology. Water Resource Publications, Littleton, Colorado, USA.

Smith, J., and Eli, R.N., 1995. Neural-network models of rainfall-runoff process. *Journal of Water Resources Planning and Management,* 121: 499- 509.

Stephenson, G.R. and Freeze, R.A., 1974. Mathematical simulation of subsurface flow contributions to snowmelt runoff, Reynolds Creek, Idaho. *Water Resources Research,* 10(2): 284-298.

Stewart, J.B., 1977. Evaporation from the wet canopy of a pine forest. *Water Resources Research,* 13: 915-921.

Thomas, H.A.,1981. Improved methods for national water assessment. Report, Contract WR 15249270, US Water Resources Council, Washington, DC, USA.

Turc, L., 1961. Évaluation des besoins en eau irrigation, l'évapotranspiration potentielle. *Ann. Agron*., 12: 13-49

Waylen, P.R., and Woo, M., 1984. Regionalization and prediction of floods in the Fraser river catchment , British Colombia. *Water Resources Bulletin*, 20(6): 941-949.

Weeks, W.D. and Ashkanasy, N.M., 1985. Regional parameters for the Sacramento model: a case study. Civ. Eng. Trans., Inst. Eng., Aust., CE 27: 305-313

Wood, E.F., Lettenmaier, D.P., and Zartarian, V.G., 1992. A landsurface hydrology parameterization with subgrid variability for general circulation models. *Journal of Geophysical Research,* 97(D3): 2717-2728.

Wooldridge, S., Kalma, J., and Kuczera, G., 2001. Parameterisation of a simple semi-distributed model for assessing the impact of land-use on hydrologic response. *Journal of Hydrology*, 254: 16-32.

Xu, C.-Y., and Singh, V.P., 1998. A review of monthly water balance models for water resources investigations. *Water Resources Management*, 12: 31-50.

Yapo, P.O., Gupta, H.V., and Sorooshian, S., 1996. Automatic calibration of conceptual rainfall-runoff models: sensitivity to calibration data. *Journal of Hydrology*, 181: 23-48.

Institut für Wasserbau
Universität Stuttgart

Pfaffenwaldring 61
70569 Stuttgart (Vaihingen)
Telefon (0711) 685 - 4717/41/52 o. - 4679
Telefax (0711) 685 - 7020 o. 4746 o. 4681
email: iws@iws.uni-stuttgart.de
http://www.iws.uni-stuttgart.de

Verzeichnis der Mitteilungshefte

1 Röhnisch, Arthur: *Die Bemühungen um eine Wasserbauliche Versuchsanstalt an der Technischen Hochschule Stuttgart*, und
Fattah Abouleid, Abdel: *Beitrag zur Berechnung einer in lockeren Sand gerammten, zweifach verankerten Spundwand*, 1963

2 Marotz, Günter: *Beitrag zur Frage der Standfestigkeit von dichten Asphaltbelägen im Großwasserbau*, 1964

3 Gurr, Siegfried: *Beitrag zur Berechnung zusammengesetzter ebener Flächentragwerke unter besonderer Berücksichtigung ebener Stauwände, mit Hilfe von Randwert- und Lastwertmatrizen*, 1965

4 Plica, Peter: *Ein Beitrag zur Anwendung von Schalenkonstruktionen im Stahlwasserbau*, und Petrikat, Kurt: *Möglichkeiten und Grenzen des wasserbaulichen Versuchswesens*, 1966

5 Plate, Erich: *Beitrag zur Bestimmung der Windgeschwindigkeitsverteilung in der durch eine Wand gestörten bodennahen Luftschicht*, und
Röhnisch, Arthur; Marotz, Günter: *Neue Baustoffe und Bauausführungen für den Schutz der Böschungen und der Sohle von Kanälen, Flüssen und Häfen; Gestehungskosten und jeweilige Vorteile*, sowie Unny, T.E.: *Schwingungsuntersuchungen am Kegelstrahlschieber*, 1967

6 Seiler, Erich: *Die Ermittlung des Anlagenwertes der bundeseigenen Binnenschiffahrtsstraßen und Talsperren und des Anteils der Binnenschiffahrt an diesem Wert*, 1967

7 *Sonderheft anläßlich des 65. Geburtstages von Prof. Arthur Röhnisch mit Beiträgen von* Benk, Dieter; Breitling, J.; Gurr, Siegfried; Haberhauer, Robert; Honekamp, Hermann; Kuz, Klaus Dieter; Marotz, Günter; Mayer-Vorfelder, Hans-Jörg; Miller, Rudolf; Plate, Erich J.; Radomski, Helge; Schwarz, Helmut; Vollmer, Ernst; Wildenhahn, Eberhard; 1967

8 Jumikis, Alfred: *Beitrag zur experimentellen Untersuchung des Wassernachschubs in einem gefrierenden Boden und die Beurteilung der Ergebnisse*, 1968

9 Marotz, Günter: *Technische Grundlagen einer Wasserspeicherung im natürlichen Untergrund*, 1968

10 Radomski, Helge: *Untersuchungen über den Einfluß der Querschnittsform wellenförmiger Spundwände auf die statischen und rammtechnischen Eigenschaften*, 1968

11 Schwarz, Helmut: *Die Grenztragfähigkeit des Baugrundes bei Einwirkung vertikal gezogener Ankerplatten als zweidimensionales Bruchproblem*, 1969

12 Erbel, Klaus: *Ein Beitrag zur Untersuchung der Metamorphose von Mittelgebirgsschneedecken unter besonderer Berücksichtigung eines Verfahrens zur Bestimmung der thermischen Schneequalität*, 1969

13 Westhaus, Karl-Heinz: *Der Strukturwandel in der Binnenschiffahrt und sein Einfluß auf den Ausbau der Binnenschiffskanäle*, 1969

14 Mayer-Vorfelder, Hans-Jörg: *Ein Beitrag zur Berechnung des Erdwiderstandes unter Ansatz der logarithmischen Spirale als Gleitflächenfunktion*, 1970

15 Schulz, Manfred: *Berechnung des räumlichen Erddruckes auf die Wandung kreiszylindrischer Körper*, 1970

16 Mobasseri, Manoutschehr: *Die Rippenstützmauer. Konstruktion und Grenzen ihrer Standsicherheit*, 1970

17 Benk, Dieter: *Ein Beitrag zum Betrieb und zur Bemessung von Hochwasserrückhaltebecken*, 1970

18 Gàl, Attila: *Bestimmung der mitschwingenden Wassermasse bei überströmten Fischbauchklappen mit kreiszylindrischem Staublech*, 1971, vergriffen

19 Kuz, Klaus Dieter: *Ein Beitrag zur Frage des Einsetzens von Kavitationserscheinungen in einer Düsenströmung bei Berücksichtigung der im Wasser gelösten Gase*, 1971, vergriffen

20 Schaak, Hartmut: *Verteilleitungen von Wasserkraftanlagen*, 1971

21 *Sonderheft zur Eröffnung der neuen Versuchsanstalt des Instituts für Wasserbau der Universität Stuttgart mit Beiträgen von*
Brombach, Hansjörg; Dirksen, Wolfram; Gàl, Attila; Gerlach, Reinhard; Giesecke, Jürgen; Holthoff, Franz-Josef; Kuz, Klaus Dieter; Marotz, Günter; Minor, Hans-Erwin; Petrikat, Kurt; Röhnisch, Arthur; Rueff, Helge; Schwarz, Helmut; Vollmer, Ernst; Wildenhahn, Eberhard; 1972

22 Wang, Chung-su: *Ein Beitrag zur Berechnung der Schwingungen an Kegelstrahlschiebern*, 1972

23 Mayer-Vorfelder, Hans-Jörg: *Erdwiderstandsbeiwerte nach dem Ohde-Variationsverfahren*, 1972

24 Minor, Hans-Erwin: *Beitrag zur Bestimmung der Schwingungsanfachungsfunktionen überströmter Stauklappen*, 1972, vergriffen

25 Brombach, Hansjörg: *Untersuchung strömungsmechanischer Elemente (Fluidik) und die Möglichkeit der Anwendung von Wirbelkammerelementen im Wasserbau*, 1972, vergriffen

26 Wildenhahn, Eberhard: *Beitrag zur Berechnung von Horizontalfilterbrunnen*, 1972

27 Steinlein, Helmut: *Die Eliminierung der Schwebstoffe aus Flußwasser zum Zweck der unterirdischen Wasserspeicherung, gezeigt am Beispiel der Iller*, 1972

28 Holthoff, Franz Josef: *Die Überwindung großer Hubhöhen in der Binnenschiffahrt durch Schwimmerhebewerke*, 1973

29 Röder, Karl: *Einwirkungen aus Baugrundbewegungen auf trog- und kastenförmige Konstruktionen des Wasser- und Tunnelbaues*, 1973

30 Kretschmer, Heinz: *Die Bemessung von Bogenstaumauern in Abhängigkeit von der Talform*, 1973

31 Honekamp, Hermann: *Beitrag zur Berechnung der Montage von Unterwasserpipelines*, 1973

32 Giesecke, Jürgen: *Die Wirbelkammertriode als neuartiges Steuerorgan im Wasserbau*, und
Brombach, Hansjörg: *Entwicklung, Bauformen, Wirkungsweise und Steuereigenschaften von Wirbelkammerverstärkern*, 1974

33 Rueff, Helge: *Untersuchung der schwingungserregenden Kräfte an zwei hintereinander angeordneten Tiefschützen unter besonderer Berücksichtigung von Kavitation*, 1974

34 Röhnisch, Arthur: *Einpreßversuche mit Zementmörtel für Spannbeton - Vergleich der Ergebnisse von Modellversuchen mit Ausführungen in Hüllwellrohren*, 1975

35 *Sonderheft anläßlich des 65. Geburtstages von Prof. Dr.-Ing. Kurt Petrikat mit Beiträgen von*: Brombach, Hansjörg; Erbel, Klaus; Flinspach, Dieter; Fischer jr., Richard; Gàl, Attila; Gerlach, Reinhard; Giesecke, Jürgen; Haberhauer, Robert; Hafner Edzard; Hausenblas, Bernhard; Horlacher, Hans-Burkhard; Hutarew, Andreas; Knoll, Manfred; Krummet, Ralph; Marotz, Günter; Merkle, Theodor; Miller, Christoph; Minor, Hans-Erwin; Neumayer, Hans; Rao, Syamala; Rath, Paul; Rueff, Helge; Ruppert, Jürgen; Schwarz, Wolfgang; Topal-Gökceli, Mehmet; Vollmer, Ernst; Wang, Chung-su; Weber, Hans-Georg; 1975

36 Berger, Jochum: *Beitrag zur Berechnung des Spannungszustandes in rotationssymmetrisch belasteten Kugelschalen veränderlicher Wandstärke unter Gas- und Flüssigkeitsdruck durch Integration schwach singulärer Differentialgleichungen*, 1975

37 Dirksen, Wolfram: *Berechnung instationärer Abflußvorgänge in gestauten Gerinnen mittels Differenzenverfahren und die Anwendung auf Hochwasserrückhaltebecken*, 1976

38 Horlacher, Hans-Burkhard: *Berechnung instationärer Temperatur- und Wärmespannungsfelder in langen mehrschichtigen Hohlzylindern*, 1976

39 Hafner, Edzard: *Untersuchung der hydrodynamischen Kräfte auf Baukörper im Tiefwasserbereich des Meeres*, 1977, ISBN 3-921694-39-6

40 Ruppert, Jürgen: *Über den Axialwirbelkammerverstärker für den Einsatz im Wasserbau*, 1977, ISBN 3-921694-40-X

41 Hutarew, Andreas: *Beitrag zur Beeinflußbarkeit des Sauerstoffgehalts in Fließgewässern an Abstürzen und Wehren*, 1977, ISBN 3-921694-41-8, vergriffen

42 Miller, Christoph: *Ein Beitrag zur Bestimmung der schwingungserregenden Kräfte an unterströmten Wehren*, 1977, ISBN 3-921694-42-6

43 Schwarz, Wolfgang: *Druckstoßberechnung unter Berücksichtigung der Radial- und Längsverschiebungen der Rohrwandung*, 1978, ISBN 3-921694-43-4

44 Kinzelbach, Wolfgang: *Numerische Untersuchungen über den optimalen Einsatz variabler Kühlsysteme einer Kraftwerkskette am Beispiel Oberrhein*, 1978, ISBN 3-921694-44-2

45 Barczewski, Baldur: *Neue Meßmethoden für Wasser-Luftgemische und deren Anwendung auf zweiphasige Auftriebsstrahlen*, 1979, ISBN 3-921694-45-0

46 Neumayer, Hans: *Untersuchung der Strömungsvorgänge in radialen Wirbelkammerverstärkern*, 1979, ISBN 3-921694-46-9

47 Elalfy, Youssef-Elhassan: *Untersuchung der Strömungsvorgänge in Wirbelkammerdioden und -drosseln*, 1979, ISBN 3-921694-47-7

48 Brombach, Hansjörg: *Automatisierung der Bewirtschaftung von Wasserspeichern*, 1981, ISBN 3-921694-48-5

49 Geldner, Peter: *Deterministische und stochastische Methoden zur Bestimmung der Selbstdichtung von Gewässern*, 1981, ISBN 3-921694-49-3, vergriffen

50 Mehlhorn, Hans: *Temperaturveränderungen im Grundwasser durch Brauchwassereinleitungen*, 1982, ISBN 3-921694-50-7, vergriffen

51 Hafner, Edzard: *Rohrleitungen und Behälter im Meer*, 1983, ISBN 3-921694-51-5

52 Rinnert, Bernd: *Hydrodynamische Dispersion in porösen Medien: Einfluß von Dichteunterschieden auf die Vertikalvermischung in horizontaler Strömung*, 1983, ISBN 3-921694-52-3, vergriffen

53 Lindner, Wulf: *Steuerung von Grundwasserentnahmen unter Einhaltung ökologischer Kriterien*, 1983, ISBN 3-921694-53-1, vergriffen

54 Herr, Michael; Herzer, Jörg; Kinzelbach, Wolfgang; Kobus, Helmut; Rinnert, Bernd: *Methoden zur rechnerischen Erfassung und hydraulischen Sanierung von Grundwasserkontaminationen*, 1983, ISBN 3-921694-54-X

55 Schmitt, Paul: *Wege zur Automatisierung der Niederschlagsermittlung*, 1984, ISBN 3-921694-55-8, vergriffen

56 Müller, Peter: *Transport und selektive Sedimentation von Schwebstoffen bei gestau tem Abfluß*, 1985, ISBN 3-921694-56-6

57 El-Qawasmeh, Fuad: *Möglichkeiten und Grenzen der Tropfbewässerung unter besonderer Berücksichtigung der Verstopfungsanfälligkeit der Tropfelemente*, 1985, ISBN 3-921694-57-4, vergriffen

58 Kirchenbaur, Klaus: *Mikroprozessorgesteuerte Erfassung instationärer Druckfelder am Beispiel seegangsbelasteter Baukörper*, 1985, ISBN 3-921694-58-2

59 Kobus, Helmut (Hrsg.): *Modellierung des großräumigen Wärme- und Schadstofftransports im Grundwasser*, Tätigkeitsbericht 1984/85 (DFG-Forschergruppe an den Universitäten Hohenheim, Karlsruhe und Stuttgart), 1985, ISBN 3-921694-59-0, vergriffen

60 Spitz, Karlheinz: *Dispersion in porösen Medien: Einfluß von Inhomogenitäten und Dichteunterschieden*, 1985, ISBN 3-921694-60-4, vergriffen

61 Kobus, Helmut: *An Introduction to Air-Water Flows in Hydraulics*, 1985, ISBN 3-921694-61-2

62 Kaleris, Vassilios: *Erfassung des Austausches von Oberflächen- und Grundwasser in horizontalebenen Grundwassermodellen*, 1986, ISBN 3-921694-62-0

63 Herr, Michael: *Grundlagen der hydraulischen Sanierung verunreinigter Porengrundwasserleiter*, 1987, ISBN 3-921694-63-9

64 Marx, Walter: *Berechnung von Temperatur und Spannung in Massenbeton infolge Hydratation*, 1987, ISBN 3-921694-64-7

65 Koschitzky, Hans-Peter: *Dimensionierungskonzept für Sohlbelüfter in Schußrinnen zur Vermeidung von Kavitationsschäden*, 1987, ISBN 3-921694-65-5

66 Kobus, Helmut (Hrsg.): *Modellierung des großräumigen Wärme- und Schadstofftransports im Grundwasser*, Tätigkeitsbericht 1986/87 (DFG-Forschergruppe an den Universitäten Hohenheim, Karlsruhe und Stuttgart) 1987, ISBN 3-921694-66-3

67 Söll, Thomas: *Berechnungsverfahren zur Abschätzung anthropogener Temperaturanomalien im Grundwasser*, 1988, ISBN 3-921694-67-1

68 Dittrich, Andreas; Westrich, Bernd: *Bodenseeufererosion, Bestandsaufnahme und Bewertung*, 1988, ISBN 3-921694-68-X, vergriffen

69 Huwe, Bernd; van der Ploeg, Rienk R.: *Modelle zur Simulation des Stickstoffhaushaltes von Standorten mit unterschiedlicher landwirtschaftlicher Nutzung*, 1988, ISBN 3-921694-69-8, vergriffen

70 Stephan, Karl: *Integration elliptischer Funktionen*, 1988, ISBN 3-921694-70-1

71 Kobus, Helmut; Zilliox, Lothaire (Hrsg.): *Nitratbelastung des Grundwassers, Auswirkungen der Landwirtschaft auf die Grundwasser- und Rohwasserbeschaffenheit und Maßnahmen zum Schutz des Grundwassers*. Vorträge des deutsch-französischen Kolloquiums am 6. Oktober 1988, Universitäten Stuttgart und Louis Pasteur Strasbourg (Vorträge in deutsch oder französisch, Kurzfassungen zweisprachig), 1988, ISBN 3-921694-71-X

72 Soyeaux, Renald: *Unterströmung von Stauanlagen auf klüftigem Untergrund unter Berücksichtigung laminarer und turbulenter Fließzustände*,1991,ISBN 3-921694-72-8

73 Kohane, Roberto: *Berechnungsmethoden für Hochwasserabfluß in Fließgewässern mit überströmten Vorländern*, 1991, ISBN 3-921694-73-6

74 Hassinger, Reinhard: *Beitrag zur Hydraulik und Bemessung von Blocksteinrampen in flexibler Bauweise*, 1991, ISBN 3-921694-74-4, vergriffen

75 Schäfer, Gerhard: *Einfluß von Schichtenstrukturen und lokalen Einlagerungen auf die Längsdispersion in Porengrundwasserleitern*, 1991, ISBN 3-921694-75-2

76 Giesecke, Jürgen: *Vorträge, Wasserwirtschaft in stark besiedelten Regionen; Umweltforschung mit Schwerpunkt Wasserwirtschaft,* 1991, ISBN 3-921694-76-0

77 Huwe, Bernd: *Deterministische und stochastische Ansätze zur Modellierung des Stickstoffhaushalts landwirtschaftlich genutzter Flächen auf unterschiedlichem Skalenniveau,* 1992, ISBN 3-921694-77-9, vergriffen

78 Rommel, Michael: *Verwendung von Kluftdaten zur realitätsnahen Generierung von Kluftnetzen mit anschließender laminar-turbulenter Strömungsberechnung,* 1993, ISBN 3-92 1694-78-7

79 Marschall, Paul: *Die Ermittlung lokaler Stofffrachten im Grundwasser mit Hilfe von Einbohrloch-Meßverfahren,* 1993, ISBN 3-921694-79-5, vergriffen

80 Ptak, Thomas: *Stofftransport in heterogenen Porenaquiferen: Felduntersuchungen und stochastische Modellierung,* 1993, ISBN 3-921694-80-9, vergriffen

81 Haakh, Frieder: *Transientes Strömungsverhalten in Wirbelkammern,* 1993, ISBN 3-921694-81-7

82 Kobus, Helmut; Cirpka, Olaf; Barczewski, Baldur; Koschitzky, Hans-Peter: *Versuchseinrichtung zur Grundwasser und Altlastensanierung VEGAS, Konzeption und Programmrahmen,* 1993, ISBN 3-921694-82-5

83 Zang, Weidong: *Optimaler Echtzeit-Betrieb eines Speichers mit aktueller Abflußregenerierung,* 1994, ISBN 3-921694-83-3, vergriffen

84 Franke, Hans-Jörg: *Stochastische Modellierung eines flächenhaften Stoffeintrages und Transports in Grundwasser am Beispiel der Pflanzenschutzmittelproblematik,* 1995, ISBN 3-921694-84-1

85 Lang, Ulrich: *Simulation regionaler Strömungs- und Transportvorgänge in Karstaquiferen mit Hilfe des Doppelkontinuum-Ansatzes: Methodenentwicklung und Parameteridentifikation,* 1995, ISBN 3-921694-85-X, vergriffen

86 Helmig, Rainer: *Einführung in die Numerischen Methoden der Hydromechanik,* 1996, ISBN 3-921694-86-8, vergriffen

87 Cirpka, Olaf: *CONTRACT: A Numerical Tool for Contaminant Transport and Chemical Transformations - Theory and Program Documentation* -, 1996, ISBN 3-921694-87-6

88 Haberlandt, Uwe: *Stochastische Synthese und Regionalisierung des Niederschlages für Schmutzfrachtberechnungen,* 1996, ISBN 3-921694-88-4

89 Croisé, Jean: *Extraktion von flüchtigen Chemikalien aus natürlichen Lockergesteinen mittels erzwungener Luftströmung,* 1996, ISBN 3-921694-89-2, vergriffen

90 Jorde, Klaus: *Ökologisch begründete, dynamische Mindestwasserregelungen bei Ausleitungskraftwerken,* 1997, ISBN 3-921694-90-6, vergriffen

91 Helmig, Rainer: *Gekoppelte Strömungs- und Transportprozesse im Untergrund - Ein Beitrag zur Hydrosystemmodellierung-*, 1998, ISBN 3-921694-91-4

92 Emmert, Martin: *Numerische Modellierung nichtisothermer Gas-Wasser Systeme in porösen Medien*, 1997, ISBN 3-921694-92-2

93 Kern, Ulrich: *Transport von Schweb- und Schadstoffen in staugeregelten Fließgewässern am Beispiel des Neckars*, 1997, ISBN 3-921694-93-0, vergriffen

94 Förster, Georg: *Druckstoßdämpfung durch große Luftblasen in Hochpunkten von Rohrleitungen 1997*, ISBN 3-921694-94-9

95 Cirpka, Olaf: *Numerische Methoden zur Simulation des reaktiven Mehrkomponenten-transports im Grundwasser*, 1997, ISBN 3-921694-95-7, vergriffen

96 Färber, Arne: *Wärmetransport in der ungesättigten Bodenzone: Entwicklung einer thermischen In-situ-Sanierungstechnologie*, 1997, ISBN 3-921694-96-5

97 Betz, Christoph: *Wasserdampfdestillation von Schadstoffen im porösen Medium: Entwicklung einer thermischen In-situ-Sanierungstechnologie*, 1998, ISBN 3-921694-97-3

98 Xu, Yichun: *Numerical Modeling of Suspended Sediment Transport in Rivers*, 1998, ISBN 3-921694-98-1, vergriffen

99 Wüst, Wolfgang: *Geochemische Untersuchungen zur Sanierung CKW-kontaminierter Aquifere mit Fe(0)-Reaktionswänden,* 2000, ISBN 3-933761-02-2

100 Sheta, Hussam: *Simulation von Mehrphasenvorgängen in porösen Medien unter Einbeziehung von Hysterese-Effekten,* 2000, ISBN 3-933761-03-4

101 Ayros, Edwin: *Regionalisierung extremer Abflüsse auf der Grundlage statistischer Verfahren*, 2000, ISBN 3-933761-04-2, vergriffen

102 Huber, Ralf: *Compositional Multiphase Flow and Transport in Heterogeneous Porous Media*, 2000, ISBN 3-933761-05-0

103 Braun, Christopherus: *Ein Upscaling-Verfahren für Mehrphasenströmungen in porösen Medien,* 2000, ISBN 3-933761-06-9

104 Hofmann, Bernd: *Entwicklung eines rechnergestützten Managementsystems zur Beurteilung von Grundwasserschadensfällen,* 2000, ISBN 3-933761-07-7

105 Class, Holger: *Theorie und numerische Modellierung nichtisothermer Mehrphasen-prozesse in NAPL-kontaminierten porösen Medien,* 2001, ISBN 3-933761-08-5

106 Schmidt, Reinhard: *Wasserdampf- und Heißluftinjektion zur thermischen Sanierung kontaminierter Standorte*, 2001, ISBN 3-933761-09-3

107 Reinhold Josef:, *Schadstoffextraktion mit hydraulischen Sanierungsverfahren unter Anwendung von grenzflächenaktiven Stoffen*, 2001, ISBN 3-933761-10-7

108 Schneider, Matthias: *Habitat- und Abflussmodellierung für Fließgewässer mit unscharfen Berechnungsansätzen*, 2001, ISBN 3-933761-11-5

109 Rathgeb, Andreas: *Hydrodynamische Bemessungsgrundlagen für Lockerdeckwerke an überströmbaren Erddämmen*, 2001, ISBN 3-933761-12-3

110 Lang, Stefan: *Parallele numerische Simulation instätionärer Probleme mit adaptiven Methoden auf unstrukturierten Gittern*, 2001, ISBN 3-933761-13-1

111 Appt, Jochen; Stumpp Simone: *Die Bodensee-Messkampagne 2001, IWS/CWR Lake Constance Measurement Program 2001*, 2002, ISBN 3-933761-14-X

112 Heimerl, Stephan: *Systematische Beurteilung von Wasserkraftprojekten*, 2002, ISBN 3-933761-15-8

113 Iqbal, Amin: *On the Management and Salinity Control of Drip Irrigation*, 2002, ISBN 3-933761-16-6

114 Silberhorn-Hemminger, Annette: *Modellierung von Kluftaquifersystemen: Geostatistische Analyse und deterministisch-stochastische Kluftgenerierung*, 2002, ISBN 3-933761-17-4

115 Winkler, Angela: *Prozesse des Wärme- und Stofftransports bei der In-situ-Sanierung mit festen Wärmequellen*, 2003, ISBN 3-933761-18-2

116 Marx, Walter: *Wasserkraft, Bewässerung, Umwelt - Planungs- und Bewertungsschwerpunkte der Wasserbewirtschaftung*, 2003, ISBN 3-933761-19-0

117 Hinkelmann, Reinhard: *Efficient Numerical Methods and Information-Processing Techniques in Environment Water*, 2003, ISBN 3-933761-20-4

118 Samaniego-Eguiguren, Luis Eduardo: *Hydrological Consequences of Land Use / Land Cover and Climatic Changes in Mesoscale Catchments*, 2003, ISBN 3-933761-21-2

119 Neunhäuserer, Lina: *Diskretisierungsansätze zur Modellierung von Strömungs- und Transportprozessen in geklüftet-porösen Medien*, 2003, ISBN 3-933761-22-0

120 Paul, Maren: *Simulation of Two-Phase Flow in Heterogeneous Poros Media with Adaptive Methods*, 2003, ISBN 3-933761-23-9

121 Ehret, Uwe: *Rainfall and Flood Nowcasting in Small Catchments using Weather Radar*, 2003, ISBN 3-933761-24-7

122 Haag, Ingo: *Der Sauerstoffhaushalt staugeregelter Flüsse am Beispiel des Neckars - Analysen, Experimente, Simulationen -,* 2003, ISBN 3-933761-25-5

123 Appt, Jochen: *Analysis of Basin-Scale Internal Waves in Upper Lake Constance,* 2003, ISBN 3-933761-26-3

124 Hrsg.: Schrenk, Volker; Batereau, Katrin; Barczewski, Baldur; Weber, Karolin und Koschitzky, Hans-Peter: *Symposium Ressource Fläche und VEGAS - Statuskolloquium 2003, 30. September und 1. Oktober 2003,* 2003, ISBN 3-933761-27-1

125 Omar Khalil Ouda: *Optimisation of Agricultural Water Use: A Decision Support System for the Gaza Strip,* 2003, ISBN 3-933761-28-0

126 Batereau, Katrin: *Sensorbasierte Bodenluftmessung zur Vor-Ort-Erkundung von Schadensherden im Untergrund*, 2004, ISBN 3-933761-29-8

127 Witt, Oliver: *Erosionsstabilität von Gewässersedimenten mit Auswirkung auf den Stofftransport bei Hochwasser am Beispiel ausgewählter Stauhaltungen des Oberrheins*, 2004, ISBN 3-933761-30-1

128 Jakobs, Hartmut: *Simulation nicht-isothermer Gas-Wasser-Prozesse in komplexen Kluft-Matrix-Systemen*, 2004, ISBN 3-933761-31-X

129 Li, Chen-Chien: *Deterministisch-stochastisches Berechnungskonzept zur Beurteilung der Auswirkungen erosiver Hochwasserereignisse in Flussstauhaltungen,* 2004, ISBN 3-933761-32-8

130 Reichenberger, Volker; Helmig, Rainer; Jakobs, Hartmut; Bastian, Peter; Niessner, Jennifer: *Complex Gas-Water Processes in Discrete Fracture-Matrix Systems: Upscaling, Mass-Conservative Discretization and Efficient Multilevel Solution,* 2004, ISBN 3-933761-33-6

131 Hrsg.: Barczewski, Baldur; Koschitzky, Hans-Peter; Weber, Karolin; Wege, Ralf: *VEGAS - Statuskolloquium 2004,* 5. Oktober 2004, 2004, ISBN 3-933761-34-4

132 Asie, Kemal Jabir: *Finite Volume Models for Multiphase Multicomponent Flow through Porous Media*. 2005, ISBN 3-933761-35-2

133 Jacoub, George: *Development of a 2-D Numerical Module for Particulate Contaminant Transport in Flood Retention Reservoirs and Impounded Rivers,* 2004, ISBN 3-933761-36-0

134 Nowak, Wolfgang: *Geostatistical Methods for the Identification of Flow and Transport Parameters in the Subsurface,* 2005, ISBN 3-933761-37-9

135 Süß, Mia: *Analysis of the influence of structures and boundaries on flow and transport processes in fractured porous media*, 2005, ISBN 3-933761-38-7

136 Jose, Surabhin Chackiath: *Experimental Investigations on Longitudinal Dispersive Mixing in Heterogeneous Aquifers*, 2005, ISBN: 3-933761-39-5

137 Filiz, Fulya: *Linking Large-Scale Meteorological Conditions to Floods in Mesoscale Catchments*, 2005, ISBN 3-933761-40-9

138 Qin, Minghao: *Wirklichkeitsnahe und recheneffiziente Ermittlung von Temperatur und Spannungen bei großen RCC-Staumauern*, 2005, ISBN 3-933761-41-7

139 Kobayashi, Kenichiro: *Optimization Methods for Multiphase Systems in the Subsurface - Application to Methane Migration in Coal Mining Areas*, 2005, ISBN 3-933761-42-5

140 Rahman, Md. Arifur: *Experimental Investigations on Transverse Dispersive Mixing in Heterogeneous Porous Media*, 2005, ISBN 3-933761-43-3

141 Schrenk, Volker: *Ökobilanzen zur Bewertung von Altlastensanierungsmaßnahmen*, 2005, ISBN 3-933761-44-1

142 Hundecha Hirpa, Yeshewatesfa: *Regionalization of Parameters of a Conceptual Rainfall-Runoff Model*, 2005, ISBN: 3-933761-45-X